INFORMATION TO USERS

This dissertation was produced from a microfilm copy of the original document. While the most advanced technological means to photograph and reproduce this document have been used, the quality is heavily dependent upon the quality of the original submitted.

The following explanation of techniques is provided to help you understand markings or patterns which may appear on this reproduction.

1. The sign or "target" for pages apparently lacking from the document photographed is "Missing Page(s)". If it was possible to obtain the missing page(s) or section, they are spliced into the film along with adjacent pages. This may have necessitated cutting thru an image and duplicating adjacent pages to insure you complete continuity.

2. When an image on the film is obliterated with a large round black mark, it is an indication that the photographer suspected that the copy may have moved during exposure and thus cause a blurred image. You will find a good image of the page in the adjacent frame.

3. When a map, drawing or chart, etc., was part of the material being photographed the photographer followed a definite method in "sectioning" the material. It is customary to begin photoing at the upper left hand corner of a large sheet and to continue photoing from left to right in equal sections with a small overlap. If necessary, sectioning is continued again — beginning below the first row and continuing on until complete.

4. The majority of users indicate that the textual content is of greatest value, however, a somewhat higher quality reproduction could be made from "photographs" if essential to the understanding of the dissertation. Silver prints of "photographs" may be ordered at additional charge by writing the Order Department, giving the catalog number, title, author and specific pages you wish reproduced.

University Microfilms

300 North Zeeb Road
Ann Arbor, Michigan 48106

A Xerox Education Company

72-29,162

OLSEN, Edward Tait, 1942-
VARIATIONS IN THE 8 GHz FLUX DENSITY AND LINEAR POLARIZATION OF EXTRAGALACTIC RADIO SOURCES.

The University of Michigan, Ph.D., 1972
Astronomy

University Microfilms, A XEROX Company, Ann Arbor, Michigan

THIS DISSERTATION HAS BEEN MICROFILMED EXACTLY AS RECEIVED

VARIATIONS IN THE 8 GHz FLUX DENSITY AND LINEAR POLARIZATION OF EXTRAGALACTIC RADIO SOURCES

by

Edward Tait Olsen

A dissertation submitted in partial fulfillment
of the requirements for the degree of
Doctor of Philosophy
(Astronomy)
in The University of Michigan
1972

Doctoral Committee:

Professor Fred T. Haddock, Chairman
Assistant Professor Hugh D. Aller
Associate Professor Charles R. Cowley
Professor Herschel Weil

PLEASE NOTE:

Some pages may have

indistinct print.

Filmed as received.

University Microfilms, A Xerox Education Company

ACKNOWLEDGEMENTS

I am deeply indebted to Professor Fred T. Haddock for his guidance and invaluable advice, and the unstinting encouragement that he has given me in the pursuit of my research. I thank him for making readily available the facilities of the Radio Astronomy Observatory and granting me the necessary extensive telescope time.

I especially thank Professor Hugh D. Aller for giving generous counsel and suggestions on my work, sharing with me so much of his time and observations, and allowing me usage of his own data reduction programs.

I am grateful to Dr. T.V. Seling, and Messrs. G.E. Latimer, K.G. Holmes, J.L. Talen, and S. Taras for their development and maintenance of the technical equipment without which this study would not have been feasible.

Finally, I thank the members of my doctoral committee for their advice, patience, and cooperation; Mr. G.W. Brandie for the many hours of fruitful discussion I shared with him; and my wife, Cheryl, for her support and the typing of this manuscript.

TABLE OF CONTENTS

ACKNOWLEDGEMENTS			ii
LIST OF TABLES			v
LIST OF ILLUSTRATIONS			vi
CHAPTER I.		INTRODUCTION	1
	I-1.	Radio Studies of the Variable Sources	1
	I-2.	Optical, Infrared, and X-ray Studies of the Variable Sources	10
	I-3.	The Present Study	14
CHAPTER II.		INSTRUMENTATION AND CALIBRATION	16
	II-1.	The Apex Assembly	17
	II-2.	The Vertex Calibrator	19
	II-3.	The Instrumental Polarization	23
	II-4.	The Observing Technique	29
	II-5.	Total Flux Density Determination	31
CHAPTER III.		THE OBSERVATIONS	44
	III-1.	The Presentation of the Observations	44
	III-2.	Discussion of the Results for Individual Sources	54
		3C84	54
		NRAO 150	55
		3C120	56

	4C39.25	57
	3C273	58
	3C279	59
	3C345	60
	NRAO 530	61
	BL Lacertae	61
	3C446	62
	3C454.3	63
III-3.	Summary of Observations	64
CHAPTER IV.	ANALYSIS AND INTERPRETATION	77
IV-1.	3C279	77
IV-2.	4C39.25	85
IV-3	3C273	89
IV-4.	BL Lacertae	96
IV-5.	3C120	102
CHAPTER V.	CONCLUSIONS	107
V-1.	Summary of Results	107
V-2.	Suggestions for Future Study	110
APPENDIX I.	EXPONENTIAL CORRECTION TO THE OBSERVED ANTENNA TEMPERATURE FOR A POINT SOURCE	112
AI-1.	Observationally Determined Quantities	112
AI-2.	Probable Observed Response	113
AI-3.	The Exponential Correction Factor	115
SELECTED BIBLIOGRAPHY		117

LIST OF TABLES

Table		Page
1	Surveys of Linear Polarization of Discrete Radio Sources	4
2	Secondary Flux Density Standards	32
3	Radio Sources Which are Variable or Probably Variable in Polarization	45
4	Radio Sources Which Have Exhibited Variations in Flux Density at 8 GHz but not in Polarization	48
5	Radio Sources Which Have not Exhibited Variations	51
6	Comparison of the Polarization Position Angle, Position Angle of the Line of Separation of the Compact Double Source, and Intrinsic Position Angle	108

LIST OF ILLUSTRATIONS

Figure		Page
2.1	The Observed Polarization Position Angle of the Vertex Calibrator versus Date	22
2.2	The Standard Deviation of the Stokes Parameter Q and U for a Single Observation Sequence versus Integrated Flux Density	28
2.3	Observational Results for 3C144 versus Time	37
2.4	Observational Results for 3C145 versus Time	38
2.5	Observational Results for 3C274 versus Time	39
2.6	Observational Results for M17 versus Time	40
2.7	Observational Results for 3C405 versus Time	41
2.8	Observational Results for PD 21 versus Time	42
2.9	Observational Results for 3C461 versus Time	43
3.1	Observational Results for 3C84 versus Time	66
3.2	Observational Results for NRAO 150 versus Time	67
3.3	Observational Results for 3C120 versus Time	68
3.4	Observational Results for 4C39.25 versus Time	69
3.5	Observational Results for 3C273 versus Time	70
3.6	Observational Results for 3C279 versus Time	71
3.7	Observational Results for 3C345 versus Time	72
3.8	Observational Results for NRAO 530 versus Time	73

3.9	Observational Results for BL Lacertae versus Time	74
3.10	Observational Results for 3C446 versus Time	75
3.11	Observational Results for 3C454.3 versus Time	76
4.1	Observational Results for the Variable Component of 3C279 Averaged by Calendar-Months	80
4.2	Observational Results for 4C39.25 Averaged by Calendar-Months	86
4.3	Observational Results for 3C273 Averaged by Calendar-Months	92
4.4	Observational Results for 3C120 Averaged by Calendar-Months	103

CHAPTER I

INTRODUCTION

I-1. Radio Studies of the Variable Sources

Flux density variations have been reliably detected in more than fifty extragalactic radio sources since Dent (1965) discovered that the quasi-stellar radio sources 3C273, 3C279, and 3C345 were variable at 8 GHz. These variations have been observed throughout the range $1 \text{ mm} \leq \lambda \leq 40 \text{ cm}$ (Maltby and Moffet, 1965; Low, 1965; Medd, Locke, Andrew, and van den Bergh, 1968; Kellermann and Pauliny-Toth, 1968b; Lipovka, 1969; Hobbs, Corbett, and Santini, 1969; Witzel, 1971; Fogarty, Epstein, Montgomery, and Dworetsky, 1971). Pronounced variations have taken place on time scales extending from a week (MacLeod, Andrew, Medd, and Olsen, 1971 ; Stull, 1971) to a few years. The detection of small variations on time scales of days and even hours has been reported (Andrew, Harvey, and Medd, 1971; Wills, 1971).

In all cases, it has been found that an outburst first appears at the shortest wavelength observed. As it is followed to longer wavelengths, it becomes smaller in amplitude and longer in duration (e.g., Pauliny-Toth and Kellermann, 1966). In addition to this variable component,

many sources posses one or more non-varying radio components. Interferometric studies reveal these components to be larger than the variable components, which may be extremely compact (e.g., Fomalont, 1968; Clark, Kellermann, Bare, Cohen, and Jauncey, 1968; Gubbay, Legg, Robertson, Moffet, and Seidel, 1969; Kellermann, Clark, Jauncey, Cohen, Shaffer, Moffet, and Gulkis, 1970; Cohen, Cannon, Purcell, Shaffer, Broderick, Kellermann, and Jauncey, 1971).

Many mechanisms may be responsible for variations in total flux density. These include changes in rate of production or acceleration of relativistic particles; loss of particle energy by synchrotron emission, inverse Compton scattering, or adiabatic expansion; and changes in the strength, structure, or orientation of the magnetic field; or changes in the source size.

Prior to Dent's discovery, Shklovskii (1960, 1965a; 1965b) developed a theory completely describing the general form of the observed variations in flux density. His model assumed that the source is not a stationary formation. It consisted of an expanding cloud of relativistic particles with constant magnetic flux and has remained the most successful and widely accepted theory to date. Van der Laan (1966) gave a mathematical development to Shklovskii's model, putting it into the currently accepted form. Rees (1966; 1967) generalized the theory to the case of clouds expanding at relativistic velocity, and Ozernoi and Sazonov (1968; 1969) have treated the problem of the ejection of two clouds

in opposite directions at relativistic velocities.

An important test of the emission mechanisms in cosmic sources is the measurement of the state of polarization and its dependence upon wavelength, resolution, and epoch. Linearly polarized radiation from an extragalactic source was first detected by Mayer, McCullough, and Sloanaker at $\lambda 3.15$ cm (1962). There have since been surveys of the linear polarization of galactic and extragalactic radio sources in the wavelength range 9.5 mm $\leq\lambda\leq$74 cm. These appear in Table 1. These surveys indicate: (1) the optically thin, low-frequency spectral components are generally less highly polarized at longer wavelengths, as is expected to result from Faraday depolarization, and the observed plane of polarization of its radiation usually changes with wavelength as expected from Faraday rotation; and (2) once the opaque high-frequency components predominate the polarization may be greater or less than at lower frequencies and the variation in position angle of the observed plane of polarization generally does not follow the trend indicated by the low-frequency data. The net degree of polarization[1] rarely exceeds 10 per cent in either component.

---

[1]The "degree of polarization" is the fraction of the total intensity which is linearly polarized.

Table 1

Surveys of Linear Polarization of Discrete Radio Sources

(cm)	Reference
0.95	Hobbs (1968)
0.95	Wardle (1971)
1.55	McCullough and Waak (1969)
1.95	Mezger and Schrami (1966)
2.07	Boland, Hollinger, Mayer, and McCullough (1966)
2.07	Hobbs, Hollinger, and Marandino (1968)
3.12	Berge and Seielstad (1969)
3.15 to 11.5	Mayer, McCullough and Sloanaker (1964)
3.6	Hollinger and Hobbs (1968)
3.75	Hobbs and Haddock (1967)
3.75	Aller (1970b)
5.0	Hollinger, Mater, and Menella (1964)
6.0	Sastry, Pauliny-Toth, and Kellermann (1967)
6.0	Morris and Whiteoak (1968)
6.6	Gol'nev and Soboleva (1965)
10.3 to 21.6	Morris and Berge (1964)
10.6	Seielstad, Morris, and Radhakrishnan (1963)
10.6	Maltby and Seielstad (1966)
11.3 to 74.3	Gardner and Davies (1966)
11.3 to 21.2	Gardner, Morris, and Whiteoak (1969)
18.0	Morris, Radhakrishnan, and Seielstad (1964)
18.0	Berge and Seielstad (1967)
20.0	Gardner and Whiteoak (1962)
21.2	Bologna, McClain, Rose, and Sloanaker (1965)
21.2	Bologna, McClain, and Sloanaker (1969)
21.6	Morris and Radhakrushnan (1963)
49.2	Kronberg and Conway (1970)

Variations in the linear polarization of 3C273, 3C279, and 3C345 with time at 8 GHz were discovered by Aller and Haddock (1967). Since then, variations in the linear polarization of extragalactic sources have been detected throughout the range 1.55 cm $\leq \lambda \leq$ 6 cm (Hobbs, Hollinger, and Marandino, 1968; McCullough and Waak, 1969; Gardner, Whiteoak, and Morris, 1969; Olsen, 1970; Aller, 1970b; Aller, 1970c; Olsen and Aller, 1971; Aller and Olsen, 1971).

To date, three mechanisms have been advanced to explain the observed variations in linear polarization: the first two assume an unmodified Shklovskii model and are important only when the optical depth of the radio source is greater than or equal to unity. In the first, it is noted that the ratio of the absorption coefficients for radiation whose planes of polarization are parallel or perpendicular to the magnetic field is different from the ratio of the emissivity coefficients. Thus, as the expanding source changes from opaque to optically thin, the plane of its polarized emission should be seen to rotate by 90° and the degree of polarization should increase (Aller, 1968; Kellermann and Pauliny-Toth, 1968b; Aller, 1970a; Aller, 1970c; Tokarada, 1970a). For a homogeneous ensemble of relativistic electrons with an isotropic velocity distribution and with an electron density as a function of energy of the form:

$$N(E)\,dE = K \cdot E^{-\gamma}\,dE \qquad (1)$$

the maximum degree of linear polarization which may be obtained in either limiting case is:

$$\gamma \gg 1 : \quad P_{max} = \frac{3}{6\gamma + 13}, \quad \text{polarization parallel to magnetic field}$$

$$\gamma \ll 1 : \quad P_{max} = \frac{\gamma + 3}{\gamma + 7}, \quad \text{polarization perpendicular to magnetic field} \qquad (2)$$

(e.g., Aller, 1968).

The second mechanism arises from the possibility that the magnetic field may not be homogeneous throughout the source, so that as the source becomes optically thin, a change in the integrated polarization will take place due to averaging of the contributions from differently polarized regions as they become visible (Aller, 1970a).

The third mechanism is evolution in the structure of the magnetic field contained within the emitting region (Gardener and Whiteoak, 1966; Aller and Olsen, 1971). This effect is practically independent of optical depth.

Soon after the detection of variable linear polarization, the possibility that circularly polarized radiation might be observed in compact radio sources was raised (Legg and Westfold, 1967; Sciama and Rees, 1967; Legg and Westfold, 1968). The degree of such polarization expected from the Shklovskii model is small (less than 0.1 per cent for fields of 10^{-5} gauss at a frequency of 100 MHz) and varies with wavelength as $\lambda^{\frac{1}{2}}$. Several unsuccessful

attempts have been made to detect this quantity in the wavelength range 3.12 cm $\leqslant\lambda\leqslant$69 cm (Mayer, Hollinger, and Allen, 1963; Seielstad, 1967; Komesaroff, Gardner, Morris, Roberts, and Whiteoak, 1968; Seielstad and Weiler, 1968; Seielstad and Yip, 1969; Berge and Seielstad, 1969; Seielstad, 1969). There have been a few reports of detection of circular polarization, as well as of variation in this quantity (Biraud and Veron, 1968; Biraud, 1969; Gilbert and Conway, 1970; Seaquist, 1970; Conway, Gilbert, Raimond, and Weiler, 1971; Seaquist, 1971).

The observations, although relatively inaccurate at this time, clearly show that the expected variation of circular polarization with frequency has not materialized. Pacholczyk and Swihart (1971a; 1971b) and Melrose (1971) have shown that even though the same $\lambda^{\frac{1}{2}}$ wavelength dependence is to be expected in sources of high and low absorption depth, a reversal in the sense of polarization is expected upon change from the first case to the latter. Referring to the data published by Conway, et al (1971), Pacholczyk and Swihart call attention to the fact that the presence or absence of a reversal is statistically related to the appearance of the spectrum of the radio source. Those sources which exhibit straight spectra more often than not exhibit no reversal, whereas the majority of those with complex, multi-component and variable spectra do exhibit a reversal.

Recently, precision measurements of the circular polarization of extragalactic sources have been made at 1.4 and 5 GHz (Roberts, Ribes, Murray, and Cook, 1972). Citing a private communication from Weiler that the data published by Conway, et al. (1971), has a sign error, Roberts, et al. (1972), find that the combined data indicate that for radio sources consisting of a single component, the circular polarization is greatest in the inverted spectrum region. The circular polarization decreases towards higher frequencies, but there is no reversal of the sense of polarization near the peak. Roberts, et al. (1972) point out that the observed pattern is consistent with the predictions of Melrose (1971) for the case where the spectral inversion of the total flux density is caused by the Razin-Tsytovich effect, but that synchrotron self-absorption should not be rejected until its predictions for non-uniform models have been calculated.

Very-long-baseline interferometry has recently provided very important data on variable radio sources. Resolutions as high as 0.0004 second of arc have been achieved (Broderick, Vitkevich, Jauncey, Efanov, Kellermann, Clark, Kogan, Kostenko, Cohen, Matveenko, Moiseev, Payne, and Hansson, 1970), but it is difficult to determine the small-scale structure in detail as the available interferometric observations are insufficient to allow a full synthesis of the brightness distributions. However, these

data combined with measurements of interplanetary scintillations (e.g., Little and Hewish, 1968; Harris and Hardebeck, 1970) indicate a continuous scale of dimensions from one second of arc to less than 0.001 second of arc. Sources may show as many as four separate components differing in angular extent by up to 2000:1. It is not yet clear whether the individual components are spatially separated or concentric. At this stage, the structures are being interpreted in terms of the simplest models, i.e., disks, rings, core-halo and double-point sources.

Variations in the small-scale structure of variable radio sources have been detected by several groups of experimenters (Gubbay, Legg, Robertson, Moffet, Ekers, and Seidel, 1969; Knight, Robertson, Rogers, Shapiro, Whitney, Clark, Goldstein, Marandino, Vandenberg, 1971; Whitney, Shapiro, Rogers, Robertson, Knight, Clark, Goldstein, Marandino, Vandenberg, 1971; Kellermann, Jauncey, Cohen, Shaffer, Clark, Broderick, Ronnang, Rydbeck, Matveyenko, Moiseyev, Vitkevitch, Cooper, and Batchelor, 1971; Cohen, Cannon, Purcell, Shaffer, Broderick, Kellermann, and Jauncey, 1971). In particular, changes in the structure of 3C84, 3C273, and 3C279 have been reported. The observed variations in the structure of 3C273 and 3C279 imply that faster-than-light velocities of expansion are occurring. Current data suggest that 3C120 is also undergoing faster-than-light expansion (Kellermann, 1971b).

The possibility of such rapid apparent expansion was suggested before it was detected through observation (Rees, 1967; Rees and Simon, 1968). Cavaliere, Morrison, and Sartori (1971) have recently reviewed several models in which apparent faster-than-light expansion velocities may be observed.

I-2. Optical, Infrared, and X-ray Studies of the Variable Sources

Significant variability was discovered in the optical emissions of quasi-stellar objects even before the magnitude of their redshifts was realized (Matthews and Sandage, 1963). Extensive studies have been carried out which demonstrate that all identified radio variables are also optically variable, and many of the other identified compact radio sources are optically variable (Kinman, 1968; Lü and Hunter, 1969; Penston and Cannon, 1970; Cannon, Penston, and Brett, 1971; Tritton and Selmes, 1971; Angione, 1971). Variations with time scales as short as 2 minutes have been reported (Racine, 1970) and violent flaring has occurred over the period of a few days (Folsom, Smith, and Hackney, 1970). Recently, observations suggesting a correlation of radio and optical variations on a day-to-day basis have been reported (Kinman and Conklin, 1971; Andrew, Harvey, and Medd, 1971).

Optical polarization variations were first discovered

in the quasi-stellar radio source 3C446 (Kinman, Lamla, and Wirtanen, 1966). Since this time, it has been found that radio sources 3C279, 3C345, 3C454.3, BL Lac, OJ 287, and NGC 4151 are optical polarization variables (Kinman, 1967; Kinman, Lamla, Ciuria, Harlan, and Wirtanen, 1968; Visvanathan, 1969; Dyck, Kinman, Lockwood, and Landolt, 1971; Kruszewski, 1971; Kinman and Conklin, 1971). In general, there is a strong correlation between the existence of radio variability and the presence of large optical polarizations. The variations in this polarization are often rapid and large, and as yet no observing program has been undertaken which is of intensity necessary to resolve these variations. The relatively well-observed radio source 3C345 has been seen to vary its degree of polarization from 3 to 11 per cent, while its polarization position angle[1] has changed by more than 100 degrees (e.g., Kinman, Lamla, Ciuria, Harlan, and Wirtanen, 1968). The radio source OJ 287 has been found to change its degree of polarization from 15 to 9 per cent in only 24 hours, while its polarization position angle changed by 13 degrees (Kinman and Conklin, 1971). The radio source 3C273 has been found to be weakly polarized, and there is at present

---

[1]The term "polarization position angle" (or, χ) has been used throughout this thesis in place of the more correct term: "position angle of the electric vector of the polarized radiation", measured from the North point through East.

some question as to the possibility of its variability (Appenzeller and Hiltner, 1967; Appenzeller, 1968; Visnavathan, 1968; Liller, 1969). A possible detection of circular polarization in 3C273 and the nuclei of the Seyfert galaxies NGC 4151 and NGC 1068 has been reported (Nikulin, Kuvshinov, and Severny, 1971).

A flux of infrared radiation which is much greater than that radiated in the radio or optical region of the spectrum has been detected in some compact objects out to 60 microns wavelength (Pacholczyk and Wisniewski, 1967; Low and Kleinman, 1968; Kleinman and Low, 1970; Low, 1970). Variations in this flux have also been reported (Pacholczyk and Weymann, 1968; Stein and Gillett, 1969; Kleinman and Low, 1970). In particular, the flux of NGC 4151 has varied by a factor of nearly 50. The emission has a maximum around a wavelength of 60 microns and falls off quite steeply on either side of this wavelength. The emission mechanism of this infrared radiation is not yet clear, and it has been proposed by several authors that it is due to synchrotron or thermal processes (Low, 1970; Burbidge and Stein, 1970; Krishnaswamy, 1971). A study of the absolute spectral energy distribution from 0.32 to 2.2 microns shows that the continuum over this restricted wavelength range does not sensibly change slope during large variations in visual magnitude of the optical object (Oke, Neugebauer, and Becklin, 1970). Because the infrared and

visual continua of 3C279 and 3C345 follow each other during variations, Oke, et al. (1970), conclude that the same mechanism is probably responsible for the production of the radiation from the violet to the infrared. Takarada (1970b) has shown that the shape of the nearly flat optical continuum of 3C273, for example, can be explained by the inverse Compton effect. This interpretation requires that γ of the energetic particle distribution be unity and that the synchrotron radiation arising from these particles cut off in the infrared wavelength region.

Bowyer, Lampton, Mack, and de Mendonca (1970) discovered X-ray emission from 3C273, 3C274, and NGC 5128. These observations were confirmed, but the source which had been identified with 3C274 was found to be more than one degree in extent (Kellogg, Gursky, Leong, Schreier, Tananbaum, and Giacconi, 1971). X-rays have also been detected in NGC 1275 and NGC 4151, but not in NGC 1068 (Gursky, Kellogg, Leong, Tananbaum, and Giacconi, 1971). The spectrum of the X-ray photons is roughly proportional to λ^{a}. In galaxies, the X-ray luminosities are comparable to the luminosities at optical wavelengths.

A wealth of data is available on the absorption and emission spectra of quasi-stellar ojects and Seyfert galaxies (e.g., Burbidge and Burbidge, 1967; Burbidge, 1967; Burbidge, 1970). Highly excited, broad permitted and forbidden emission lines are visible in both classes of

objects. Some quasi-stellar objects exhibit emission and absorption lines of different redshift, and there exist objects in which absorption lines indicate the presence of several redshifts. No generally acceptable explanation has been advanced as to the nature of these lines. The emission lines detected in Seyfert galaxies often indicate bulk motions of the order of 1000 km/sec. In the case of NGC 1275, a startling H_α interference-filter photograph obtained by Lynds (1971) shows filamentary structure which is very similar to the Crab Nebula, but on a much grander scale.

I-3. The Present Study

This investigation is a continuation of the study initiated by Aller (Thesis, 1968) and with his kind permission, his data has been included. The primary goal was to establish the nature and general characteristics of the variations in polarization and their relationship, if any, to the variations in total flux density.

The advent of very-long-baseline interferometry at short wavelengths and the detection of changes in the structure of radio sources with time have made this monitoring program particularly important, for the evolution of the polarized emission of the sources may now be compared with the changes in their physical structure. This in turn leads to an evaluation of the structure and development

with time of the magnetic fields which are present.

Chapter II describes the instrumentation, observational techniques, and the procedure by which the observations were calibrated. Chapter III presents the observation results, describing briefly the form of the variations which have been observed and summarizing their general characteristics. Chapter IV analyses the evolution of the polarized emission of selected radio sources in terms of the structure observed in their compact components, and a consistent relationship is found between the two sets of data. Chapter V summarizes the results which have been obtained.

CHAPTER II

INSTRUMENTATION AND CALIBRATION

The observations were carried out using the 85-foot equatorially mounted paraboloid of the University of Michigan Radio Observatory at Stinchfield Woods. At 8 GHz, the half-power circular beam width of the antenna was 5.9 minutes of arc; the Dicke-type radiometer used had a band-width of 1 GHz.

Prior to October 1966, the radiometer consisted of two tunnel-diode preamplifiers followed by two wide-band travelling-wave tubes. From that time until May 1968, the system consisted of four tunnel-diode amplifiers and the standard deviation of the noise fluctuations in a ten-second integration period was 0.025 K. In May 1968 a second channel consisting of four tunnel-diode amplifiers was installed, converting the system to a dual-channel radiometer. For this configuration, the standard deviation of the noise fluctuation in a ten-second integration period was 0.17 K. The radiometer gain was determined prior to each series of source observations by the injection of noise from an argon discharge tube.

The telescope position and radiometer output was recorded digitally each integration period. All but the

earliest observations were recorded on magnetic tape and most of the data taken after late 1967 were reduced on an SDS 930 computer applying the Fourier analysis technique of H.D. Aller (1968) to obtain the position angle and amplitude of the linear polarization.

II-1. The Apex Assembly.

The polarimeter was comprised of two linearly polarized feed horns which rotated synchronously. These horns were coupled to the radiometer input by a wave-guide rotary joint and were driven by a synchronous motor which was controlled by the same oscillator used to control the digital recording equipment. The timing of the digital recording cycle was controlled by a microswitch (see page 21). In October 1968 the rotation period of the horns was reduced to a half-minute.

The polarimeter was periodically disassembled for maintenance and repair, but the electric vectors of the primary and reference horns were carefully realigned after each dissembly so that cancellation of background polarized emission would be maximized.(Aller, 1968). A vertex calibrator (see Section II-2) provided a source of known polarized emission which was used to determine the angle between the electric vectors of the horns after one such disassembly. As the feed horns rotated continuously, the radiometer output first of the primary horn and then of the primary

and reference horns was digitally recorded. Fourier analysis of the two sets of data revealed the angle between the electric vectors of the two horns to be 0.90 ± 0.04 degrees.

The vertex calibrator, further, was used to search for rotation of the entire feed support due to change in gravity loading as the orientation of the telescope altered. Once again, the horns were rotated continuously and the reference signal provided by a resistive load. The telescope was pointed at -3^h, 0^h, and $+3^h$ at each of the declinations +60, +15, and -30 degrees. The peak-to-peak variation in position angle of the polarized radiation from the vertex calibrator for these orientations was 0.2 degree. No systematic variation was detected.

In March 1970, the position of the reference horn relative to the primary horn and the responses of the two horns were determined using scans through 3C273 at twice the sidereal rate and an integration time constant of 0.4 second. The data were reduced using a program which fit two gaussians of variable amplitudes, half-widths, and separation by the method of least-squares. The reference horn was found to be 15.25 ± 0.17 minutes of arc to the east and 0.60 ± 0.13 minute of arc to the south of the primary horn. The ratio of the peak response of the reference horn to that of the primary horn was 0.86 ± 0.01; the

half-widths of the responses of the reference and primary horns were, respectively, 5.95 ± 0.06 and 5.78 ± 0.04 minutes of arc. Both responses were circularly symmetric within the measurement uncertainties.

II-2. The Vertex Calibrator

In April 1969 a new linearly polarized radiator was installed at the vertex of the parabolic reflector. This radiator consists of a "sugar-scoop" microwave horn fed by a broad-band noise source. Its aperture is a 12-inch square and its half-power circular beam width is $8.^{\circ}5$. The degree of linear polarization of the emitted radiation is very nearly 100 per cent on axis.

The plane of polarization of the vertex calibrator could not be determined using single-frequency measurements because of mode mixing in the aperture of the horn. A wide-band noise source was used to determine this plane after the calibrator had been installed at the vertex in late June 1970. A length of waveguide which had been accurately surveyed was substituted for the primary horn in the polarimeter assembly. An 18-inch aluminum bar was permanently attached to this waveguide orthogonal to its length and at an angle of $90.^{\circ}185 \pm 0.^{\circ}002$ to the plane of the electric vector for the TE_{10} mode of propagation. An avalanche diode noise source installed in the vertex calibrator provided a signal level of approximately 80 K.

The polarimeter rotation speed was reduced to 1.0 rpm, and the integration period of the digital system was $0^{s}.4$. After switching the noise diode on, the polarimeter assembly was rotated continuously and the output of the radiometer recorded digitally on magnetic tape. The polarimeter was halted after approximately 306° of rotation using a digital counter. The radiometer output was recorded for several minutes thereafter in order to determine the exact angle at which the horn rotation had stopped. Finally, the azimuth of the aluminum bar and the star Polaris were determined with a theodolite.

Should the polarimeter have ceased rotating instantaneously upon shutting off its motor, it would merely have been necessary to Fourier analyze several "on-off" records and to measure the bar azimuth after the stopping of rotation at a predetermined angle of rotation. However, subsequent analysis of the recorded data revealed that the polarimeter assembly coasted approximately one degree after the power was turned off. Second-order least-squares fits to the signals recorded during the last 50° of rotation and during the polarimeter's stationary period provided a best determination of the amount of coasting. An analysis of four independent observations produces a value of $172^{\circ}.414 \pm 0^{\circ}.130$ for the position angle of the electric vector of the linearly polarized signal from the vertex calibrator. Its agreement with the position angle of the

axis of symmetry of the "sugar-scoop" horn radiator is within the error estimates, and this is the value which has been used in all data analyses.

The vertex calibrator has been used to calibrate the position angle of the polarimeter since July 1969. Between this time and June 1970 the noise source was an argon discharge tube, and the rms error in determining the polarimeter's position angle during an observation sequence was $0.^{\circ}27$. In June 1970 the discharge tube was replaced by an avalanche diode. The equivalent antenna temperature of the vertex calibrator signal was increased from 4 K to a nominal 50 K. This reduced the rms error in determining the polarimeter position angle to $0.^{\circ}05$.

The new vertex calibrator was used to redetermine the polarization position angle of emission from Cygnus A (3C405). The value obtained indicates that a correction amounting to an increase of $3.^{\circ}43$ should be applied to all Aller's data (1968). This correction has been applied to all his data included in this study.

Figure 2.1 is a plot of observed polarization position angle of the vertex calibrator versus date. The digital recording system is triggered by a microswitch attached to the polarimeter assembly and the observed polarization position angle is the angle through which the polarimeter must rotate after the microswitch closes before the electric vector of the main horn is parallel to

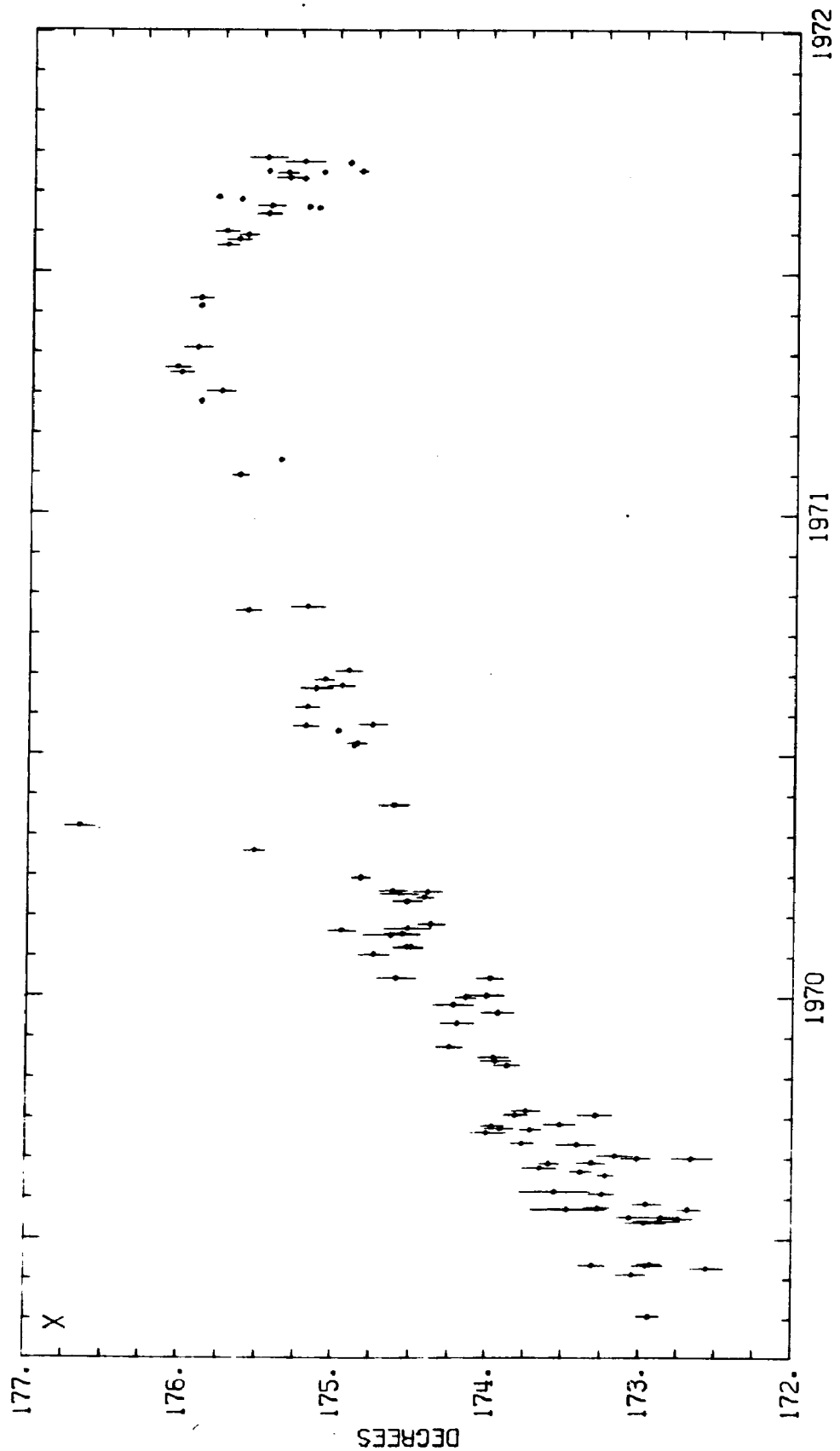


Figure 2.1: The observed polarization position angle of the vertex calibrator versus date.

the plane of polarization of the vertex calibrator . The data points are daily averages of all sets of observations of the polarization position angle of the vertex calibrator. The error bars are the rms scatter in the position angle determinations for each day and are a measure of the repeatability of the angle of rotation at which the microswitch closes. The average value of the rms scatter is $0.^{\circ}35$. It is seen that the scatter of the daily average values over a month may be as great as 1°. Thus Figure 2.1 demonstrates the unreliability of the microswitch as a position angle reference and the necessity of utilizing the vertex calibrator during every set of observations of a source.

II-3. The Instrumental Polarization

The overall gain of the radio telescope is not invariant under a rotation of the position angle of the plane of polarization of the feed. Hence a radio source can appear to be partially linearly polarized even though it's emission is completely randomly polarized. This instrumental effect must be determined and removed from the observations. It has been done on the assumption that radiation from galactic HII regions is unpolarized.

Using 3C145, M17, NGC 6857, and PD 21, Aller (1968) found that the instrumental polarization varied with position as the cosine of the zenith distance and did

not change with time through April 1968. Observations since show that the instrumental polarization has been monotonically changing since the beginning of 1968.

Commonly, polarization data is expressed in terms of a position angle and by a polarized intensity or degree of polarization. It is mathematically more convenient to use the Stokes parameters representation (Chandrasekar, 1950). For linearly polarized radiation from radio sources, these parameters are defined as follows:

$$
\begin{aligned}
S &= \text{total flux density (polarized and unpolarized)} \\
Q &= S_p \cdot \cos(2\chi), \qquad (1) \\
U &= S_p \cdot \sin(2\chi), \\
V &\equiv 0,
\end{aligned}
$$

where S_p is the polarized flux density and χ is the polarization position angle.

The quantities $Q' = Q/S$ and $U' = U/S$ were used to analyze the instrumental polarization. The advantage of using these normalized Stokes parameters is that errors in determining the total flux density of a radio source do not enter into the determination of the degree of polarization.

After the data were calibrated with respect to the position angle standard, each normalized Stokes parameter for the strong sources 3C145, M17, and 3C461 was subjected to a linear least-squares analysis in order to determine variation with time. It was found that dQ'/dt and dU'/dt

did not exhibit significant correlation with zenith distance: that is, the rate of change in instrumental polarization has been the same and is independent of zenith distance. The data from 1968.0 to 1971.5 for these three sources yield the following rates of change for the instrumental polarization:

$$dQ_I'/dt = 0.0678 \pm 0.0083, \quad \%/\text{yr}. \qquad (2)$$

$$dU_I'/dt = 0.0003 \pm 0.0097, \quad \%/\text{yr}.$$

The rms error in instrumental polarization beyond that which can be accounted for by uncertainty in individual measurements of the standards was obtained from the daily scatter of Stokes parameters for 3C145, M17, 3C405 (U' only), and 3C461 about the linear fits just previously described. The scatter of Q_I' and U_I' about the fits was the same and equal to 0.093 per cent, which is slightly larger than the values 0.072 per cent in Q_I' and 0.076 per cent in U_I' determined by Aller (1968).

The dependence of instrumental polarization on zenith distance along the meridian was reevaluated using a least-squares fit to the calculated values of Q_I' and U_I' for 3C145, M17, and PD 21 at 1970.0:

$$P_I = A_I + B_I \cdot [\cos(42\overset{\circ}{.}4-\delta) - \cos(42\overset{\circ}{.}4)]. \qquad (3)$$

This form was chosen so that the constant term is equal to the instrumental polarization at $\delta = 0^\circ$.

Data presented in this study have been corrected for instrumental polarization and its uncertainty, according to these expressions:

$$
\begin{aligned}
q' \text{ (source)} &= q' \text{(observed)} - q'_I \text{ , } \% \\
u' \text{ (source)} &= u' \text{(observed)} - u'_I \text{ , } \% \\
\sigma_{q'} \text{ (source)} &= (\sigma^2_{q'} \text{(obs.)} + \sigma^2_{q'_I})^{\frac{1}{2}} \text{ , } \% \\
\sigma_{u'} \text{ (source)} &= (\sigma^2_{u'} \text{(obs.)} + \sigma^2_{u'_I})^{\frac{1}{2}} \text{ , } \%
\end{aligned}
\qquad (4)
$$

Prior to 1968.0, instrumental polarization was represented as follows (Aller, 1968):

$$
\begin{aligned}
q'_I(z) &= -0.788 + 1.497 \cdot \cos(z) \text{ , } \% \\
u'_I(z) &= +0.304 - 0.329 \cdot \cos(z) \text{ , } \% \\
\sigma_{q'_I} &= 0.072 \text{ , } \% \\
\sigma_{u'_I} &= 0.076 \text{ , } \%
\end{aligned}
\qquad (5)
$$

After 1968.0, instrumental polarization was represented thus:

$$
\begin{aligned}
q'_I(z,T) &= 0.4735 + 0.0678(T - 1970.0) + \\
&\quad 1.4825[\cos(z) - 0.75] \text{ , } \% \\
u'_I(z,T) &= -0.663 - 0.0003(T - 1970.0) - \\
&\quad 0.3674[\cos(z) - 0.75] \text{ , } \% \\
\sigma_{q'_I} &= \sigma_{u'_I} = 0.093 \text{ , } \%
\end{aligned}
\qquad (6)
$$

The major part of the variations of instrumental polarization with time has occurred in the Stokes parameter Q_I'. A likely origin of this variation is a change in the transmission losses through the rotary joint. For example, an increase with time in the amplitude of the variation in the VSWR of the rotary joint with rotation of the polarimeter would cause the observed variation in instrumental polarization if the VSWR were greater at a position angle of 90 degrees than at a position angle of zero degree. A change in the VSWR of less than 10 per cent would be adequate to account for the variation of the instrumental polarization which has been observed over the last three years. Another possible origin of the change in instrumental polarization is a progressive deformation of the parabolic reflector as a result of gravity loading. The fact that Q_I' increased with time while U_I' remained nearly constant indicates that the gain of the reflector in the north-south plane of polarization has steadily become greater than the gain in the orthogonal plane. If the radii of curvature of the reflector in these two planes became different, the resulting astigmatism could produce the observed variation in instrumental polarization.

A further empirical study of the random errors associated with instrumental polarization is demonstrated in Figure 2.2. The standard deviation of Q and U for a single observation sequence is plotted against the integrated flux density for twelve sources which are unpolarized

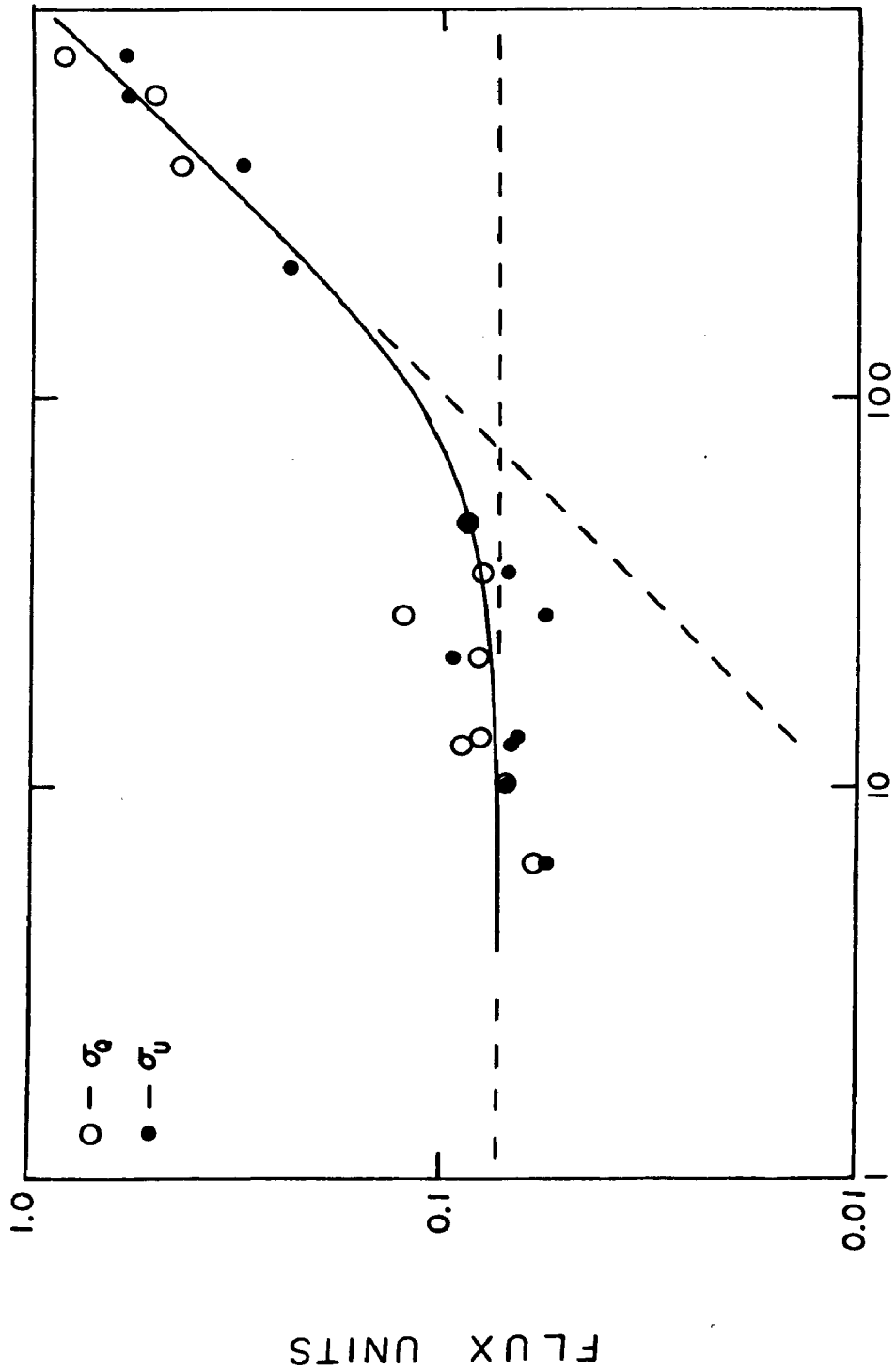


Figure 2.2: The standard deviation of the Stokes parameters Q and U for single observation sequence versus integrated flux density.

or only weakly polarized (except for 3C405, whose Q value has been eliminated because it is sensitive to small errors in the position angle calibration). The expected theoretical relationship between σ and S for the two Stokes parameters is:

$$\sigma^2 = (\sigma_o^2 + \sigma_I^2 \cdot S^2)^{\frac{1}{2}} , \qquad (7)$$

where σ equals the standard deviation per observation sequence; σ_o equals a sensitivity limit imposed by radiometer noise and fluctuations in the background radiation during the time it takes to make the observation; σ_I equals the rms fluctuation in the instrumental polarization; and S is the total flux density of the source. By previous analysis, σ_I = 0.093 per cent; the smooth heavy curve in the figure is the result of choosing this value of σ_I and setting σ_o = 0.074 flux units, the average σ of the sources for which S<3 flux units.

II-4. The Observing Technique

Prior to each series of "off-on-off" measurements on a source, the radiometer gain was determined by injecting 10 K of noise from an argon discharge tube into the radiometer input. The apparent source position was determined by making scans at a sidereal rate across it in right ascension and in declination.

A series of "off-on-off" measurements was then made with the horns rotating continuously. The total on-source and off-source integration times were each equal to sixteen minutes; the total time spent moving between on-source and off-source positions equalled eight minutes. The polarimeter completed one revolution at each off-source position and two revolutions on-source. Off-source measurements were made alternately 20 minutes of arc to the north and then to the south of the source position.

After completing each measurement series, the antenna was pointed at an off-source position while the polarimeter continued rotating. The reference signal was switched to a resistive load and the vertex calibrator used to calibrate the position angle of the polarimeter. It was important that the polarimeter rotate continuously throughout the entire series of "off-on-off" and vertex calibration measurements. If this were not done, an error of undetermined magnitude would be introduced into the position angle calibration by retriggering the digital system with the microswitch, and the benefit of the vertex calibrator would be lost.

An entire observing sequence required one hour and was usually repeated to complete the day's observations of a variable source. Each calibration source was observed once during a day's observations.

The automatic antenna control was installed in July 1968, making more rapid observations possible. The 2-rpm motor supplanted the 1-rpm motor on the polarimeter in October 1968; the integration time was then changed from 2^s to 1^s. By February 1969 automatic antenna control had been modified to permit rapid movement between off-source and on-source positions, and the time involved in a single "off-on-off" measurement was reduced from 5 minutes to $2\frac{1}{2}$ minutes. This improved the quality of flux density measurements, especially during the summer. The standard deviation of a flux density measurement for a daytime observation in summer 1969 compared to that from the summer of 1968 gave an average value of the ratio $(\sigma_{1969}/\sigma_{1968})$ for six sources equal to 0.6. The polarization determination showed a slight improvement over this same period of time for weak, slightly polarized sources.

II-5. Total Flux Density Determination

The flux density calibration was based upon the spectrum of 3C461 (Cas A) given in the review article by Scheuer and Williams (1968). This scale is 7.2 per cent higher than that used by Aller (1968). The flux density of Cas A at 8 GHz is assumed in this work to be 629.6 flux units[1] (epoch 1964.4) and to have a secular decline

[1] One flux unit equals 10^{-26} W m^{-2} Hz^{-1}.

of 1.1 per cent per year. The source size correction factor determined by Dent (1965) is $C_s = 1.16 \pm 0.03$. This is the factor by which observed antenna temperature must be multiplied to correct for the decrease in the response of the antenna pattern over the finite extent of the source.

The secondary source standards utilized are tabulated in Table 2. The flux density given is that which results after applying source size correction factor to the observed peak antenna temperature. Those correction factors for which an error is quoted have been taken from Dent (1965) whereas the others have been calculated from response widths of the scans in right ascension and in declination assuming the source brightness distribution to be gaussian shaped.

TABLE 2

Secondary Flux Density Standards

Name	S(flux units)	C_s
3C123	10.2 ±0.6	1.00±0.00
3C144 (Tau A)	578.0 ±2.5	1.23±0.03
3C145 (M 42)	394.5 ±1.5	1.46
3C274 (Vir A)	47.75±0.20	1.04±0.02
M 17	757.8 ±2.1	2.82
3C405 (Cyg A)	214.40±0.01	1.05±0.02

These sources were usually observed within one hour of transit, except for Virgo A. This source was generally observed twice during each day, two hours before and two hours after transit.

Dent (1965) found that the antenna gain varies with zenith distance according to the empirical relation

$$G(z) = G_o[1 - A(1 - \cos(z))]. \qquad (8)$$

Klein (1968) redetermined the constant A along the meridian and found it to be 0.15 ± 0.03.

Aller (1968) determined that the gain of the antenna varies asymmetrically about the meridian and may be represented by

$$G(HA) = G(0)[1 + B \cdot HA] \qquad (9)$$

where HA is the hour angle in hours and $B = -0.0072 \pm 0.0012$ (m.e.) $hour^{-1}$. It has since been found that this variation of the gain holds true for all declinations.

The asymmetrical variation of the antenna gain about the meridian is now understood qualitatively in terms of the relative position of the main horn and the electrical axis of the telescope. Observations with the triple horn feed system indicate that the electrical axis is not coincident with the polarimeter main horn (Brandie, 1971). The accuracy of the zenith distance correction factor is not precisely known at this time. This does not affect the accuracy with which variations in flux density and

polarization can be determined. It does mean that there may be present a systematic error in flux density calibration amounting to as much as 3 per cent in some sources at large zenith distances.

Beginning in late 1967 scans across sources used to determine pointing on the analog recorder were also recorded on magnetic tape for later computer determination of the source positions. A least-squares fit of a parabola about the peak of the response yields a position with an error of 0.2 seconds of arc for the strongest source and and error of 5.0 seconds of arc for a 10 flux unit source. Since 1967 the errors in the measured antenna temperatures due to missing the source have been determined and an exponential correction applied to T_A(obs.):

$$C_{exp} = \left[1+ \frac{\sigma_{\alpha_o}^2 + \sigma_{D_\alpha}^2}{\sigma_\alpha^2}\right]^{\frac{1}{2}} \left[1+ \frac{\sigma_{\delta_o}^2 + \sigma_{D_\delta}^2}{\sigma_\delta^2}\right]^{\frac{1}{2}} \qquad (10)$$

$$e^{\overline{D}_\alpha^2/2(\sigma_\alpha^2 + \sigma_{\alpha_o}^2 + \sigma_{D_\alpha}^2)} \cdot e^{\overline{D}_\delta^2/2(\sigma_\delta^2 + \sigma_{\delta_o}^2 + \sigma_{D_\delta}^2)}$$

where $(\overline{D}_\alpha , \overline{D}_\delta)$ are the average offsets of the antenna from the true source position during the on-source measurements; $(\sigma_{D_\alpha} , \sigma_{D_\delta})$ are the standard deviations of this offset; $(\sigma_{\alpha_o} , \sigma_{\delta_o})$ are the errors in determining the true position of the source from scans in each coordinate; and $(\sigma_\alpha , \sigma_\delta)$ are the standard deviations of the gaussian response of the main beam (see Appendix I).

The antenna temperature of each source is then corrected to the zenith according to

$$T_A = \frac{C_s C_{exp}}{G(z)G(HA)} \cdot T_A(obs.). \qquad (11)$$

Flux density standards were observed every three or four hours during a day's observations to monitor the gain of the antenna-radiometer system. It was not feasible to do this at more closely spaced intervals because of the necessity for observing each variable source for one to two hours to accurately determine its polarization. Each time a standard source was observed, its corrected antenna temperature and absolute total flux density were used to find the factor ξ, defined by

$$\xi = S/T_A . \qquad (12)$$

The value of this flux density calibration factor typically ranged from 11.0 to 12.0 flux units per K. This factor changed slowly during a day because of variations in the overall gain of the system. Least-square analyses up to second order were made to determine the time dependence of ξ utilizing the observations of the flux density standards. Gauss' criterion was applied to decide which $\xi(t)$ would be used to compute the total flux densities of the non-standard sources. The estimated mean uncertainty in the determination of the total flux density for sources stronger than 10 flux units is 2.5 per cent.

Plots of the individual observations of flux density and polarization standards are presented in Figures 2.3 through 2.9.

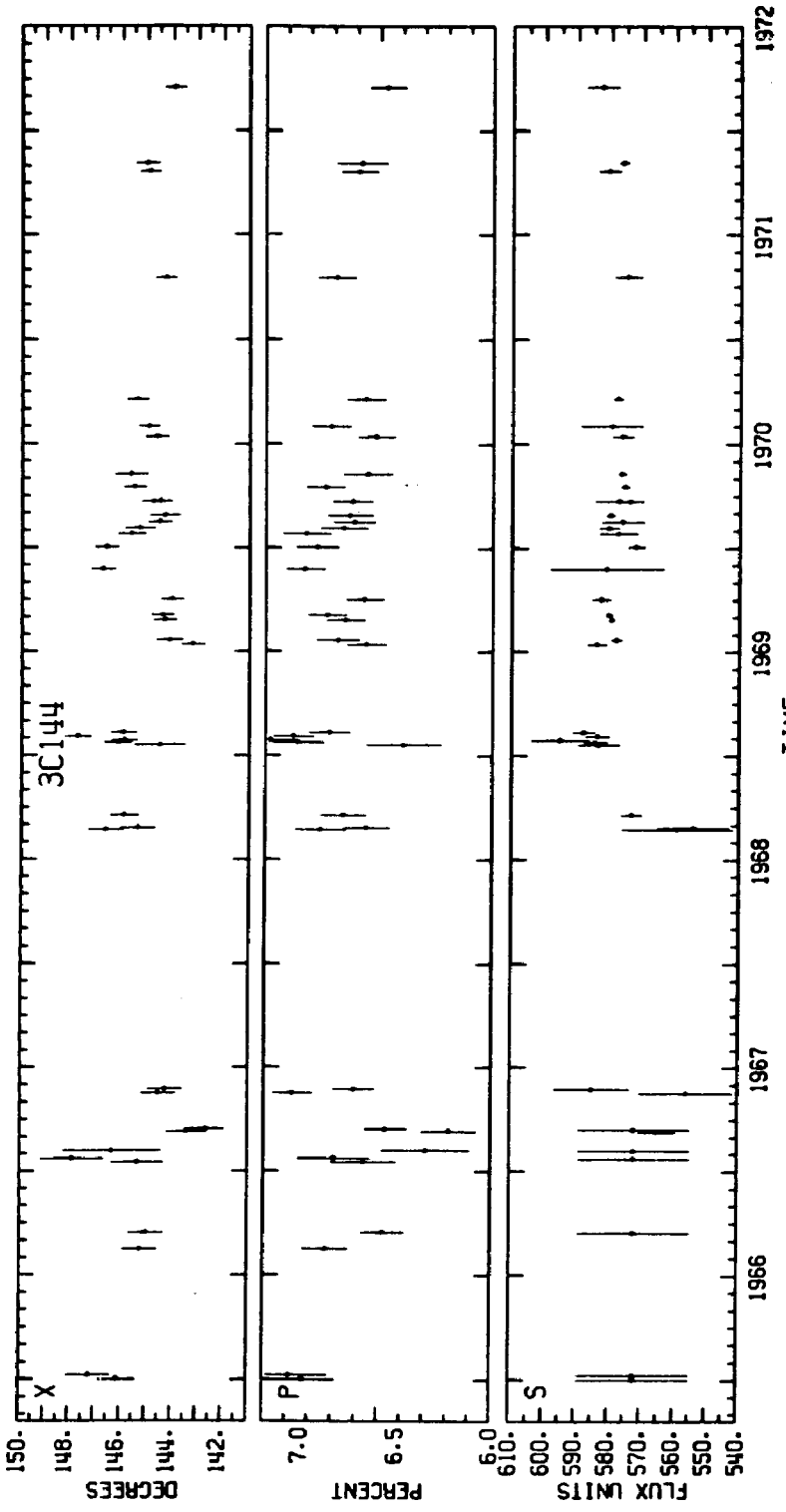


Figure 2.3: The polarization position angle, degree of polarization, and total flux density of 3C144 versus time.

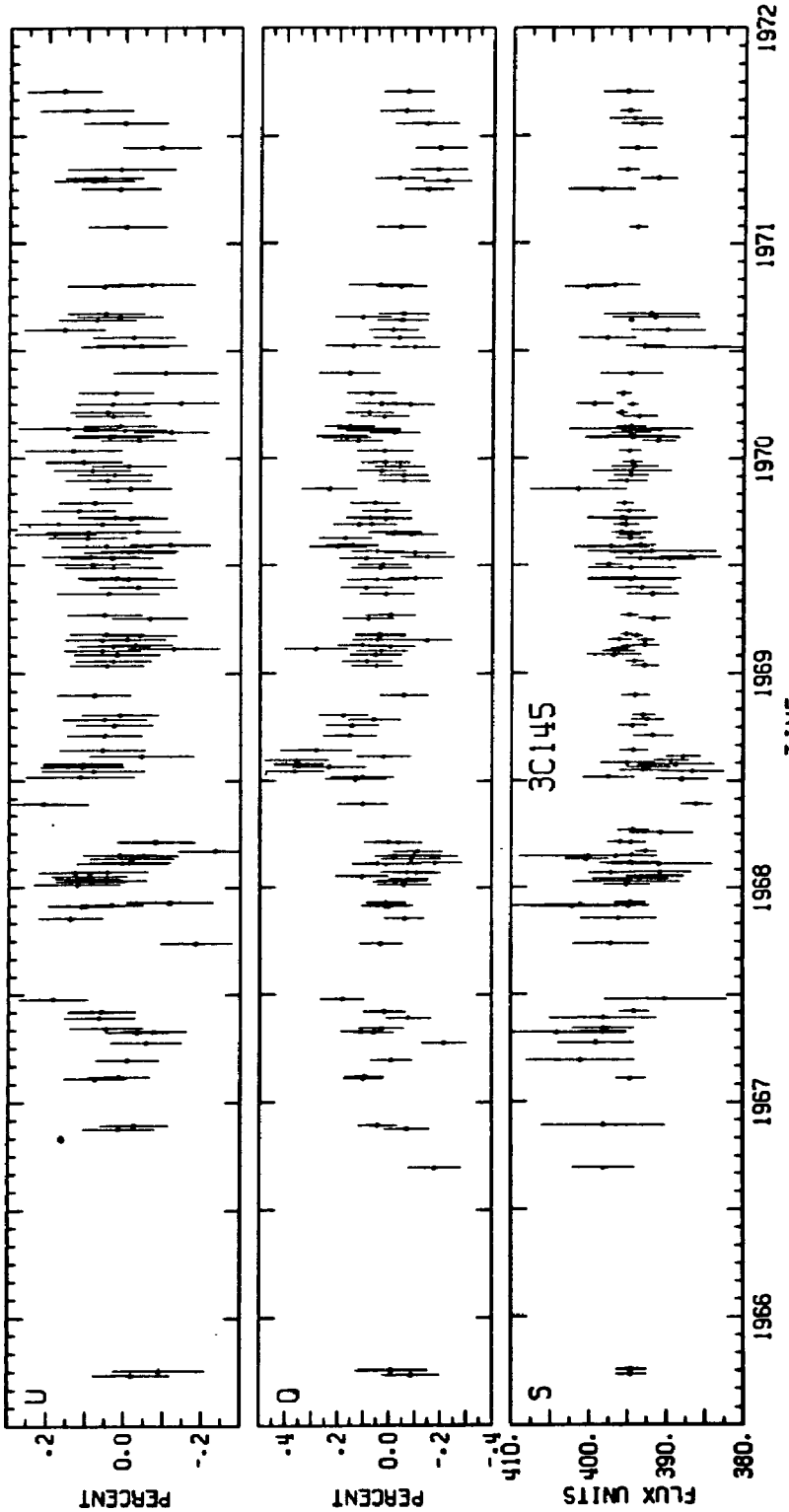


Figure 2.4: The normalized Stokes parameters U' and Q' and the total flux density of 3C145 versus time.

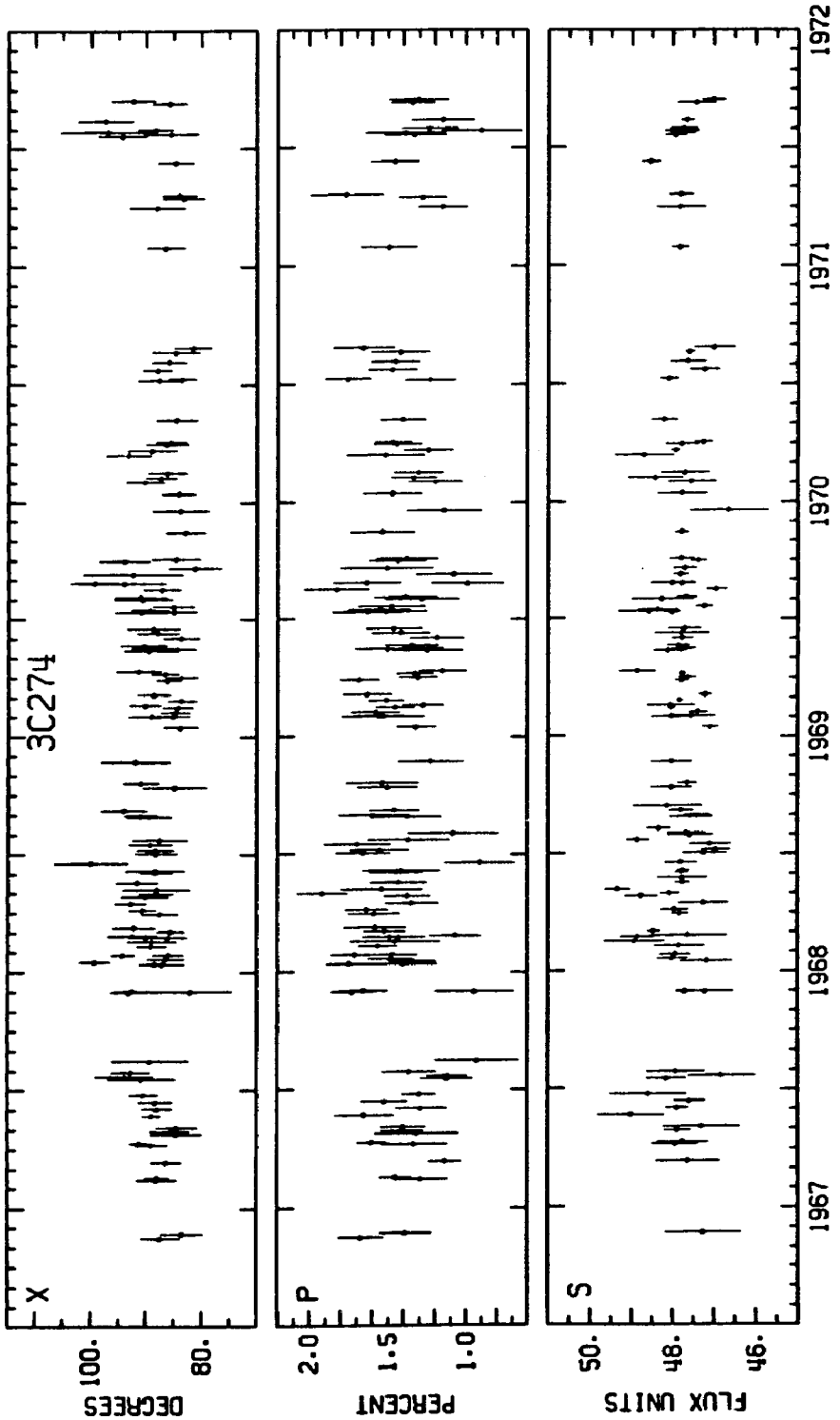


Figure 2.5: The polarization position angle, degree of polarization, and total flux density of 3C274 versus time.

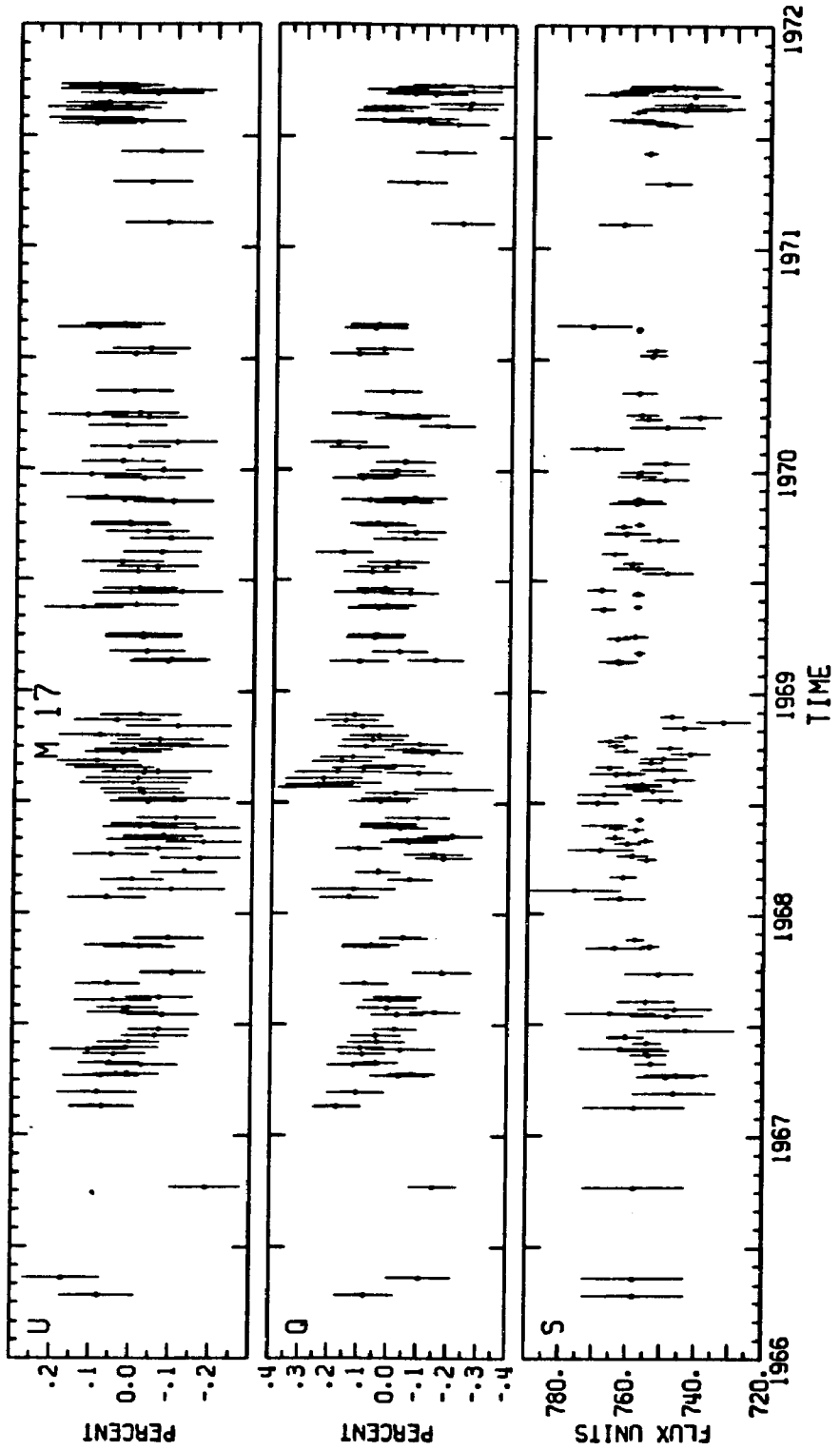


Figure 2.6: The normalized Stokes parameters U' and Q' and the total flux density of M17 versus time.

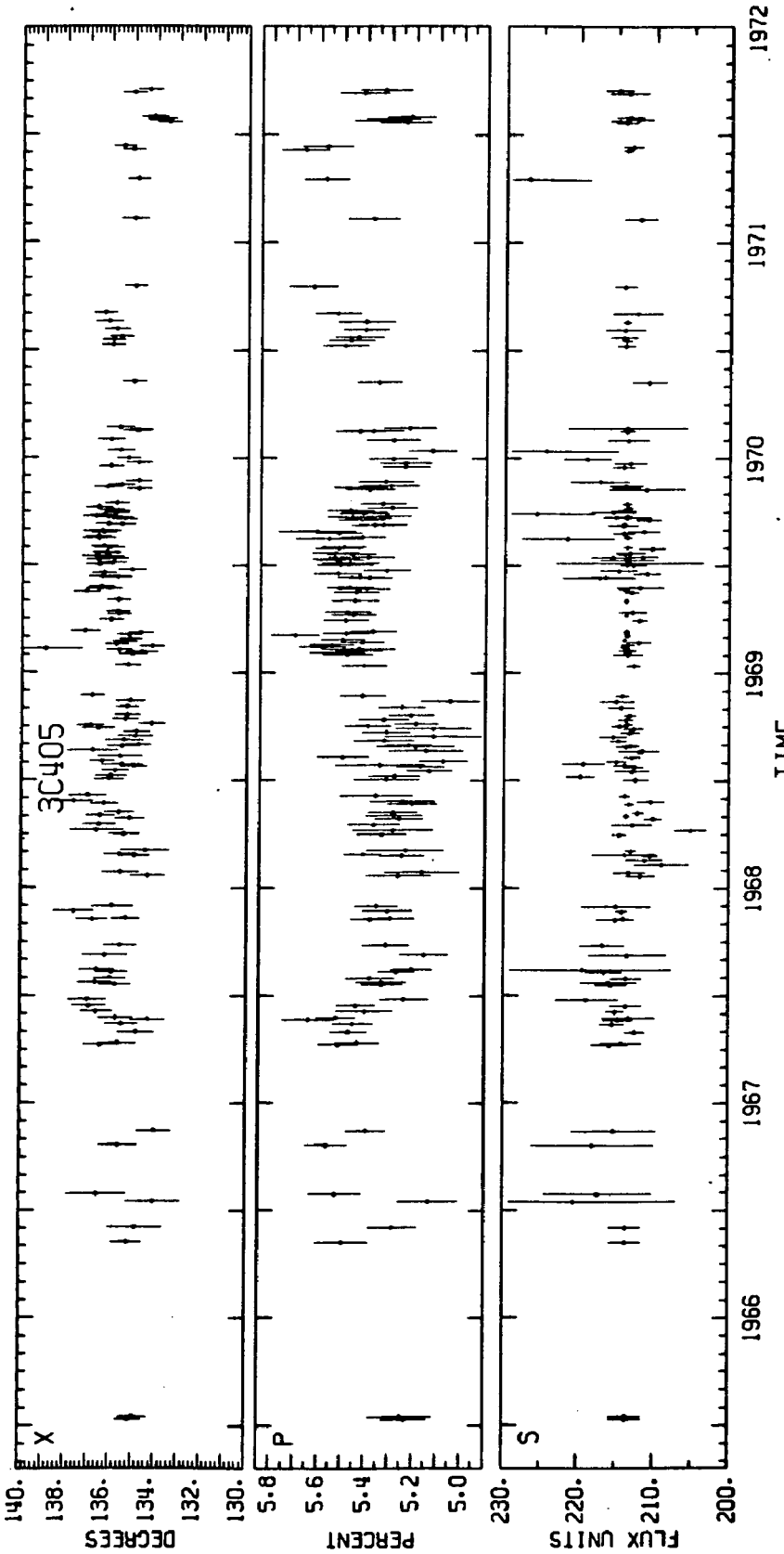


Figure 2.7: The polarization position angle, degree of polarization, and total flux density of 3C405 versus time.

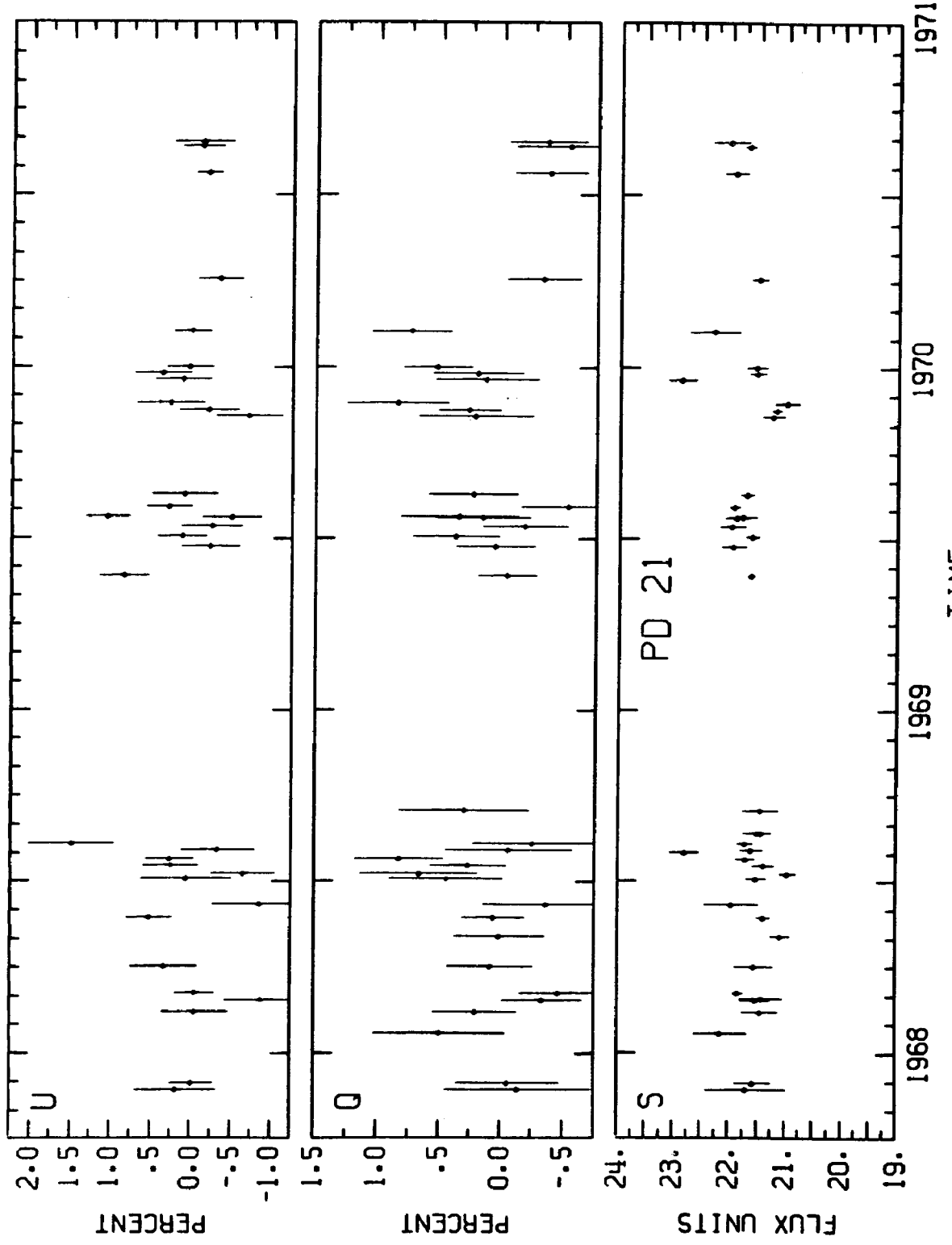


Figure 2.8: The normalized Stokes parameters U' and Q' and the total flux density of PD 21 versus time.

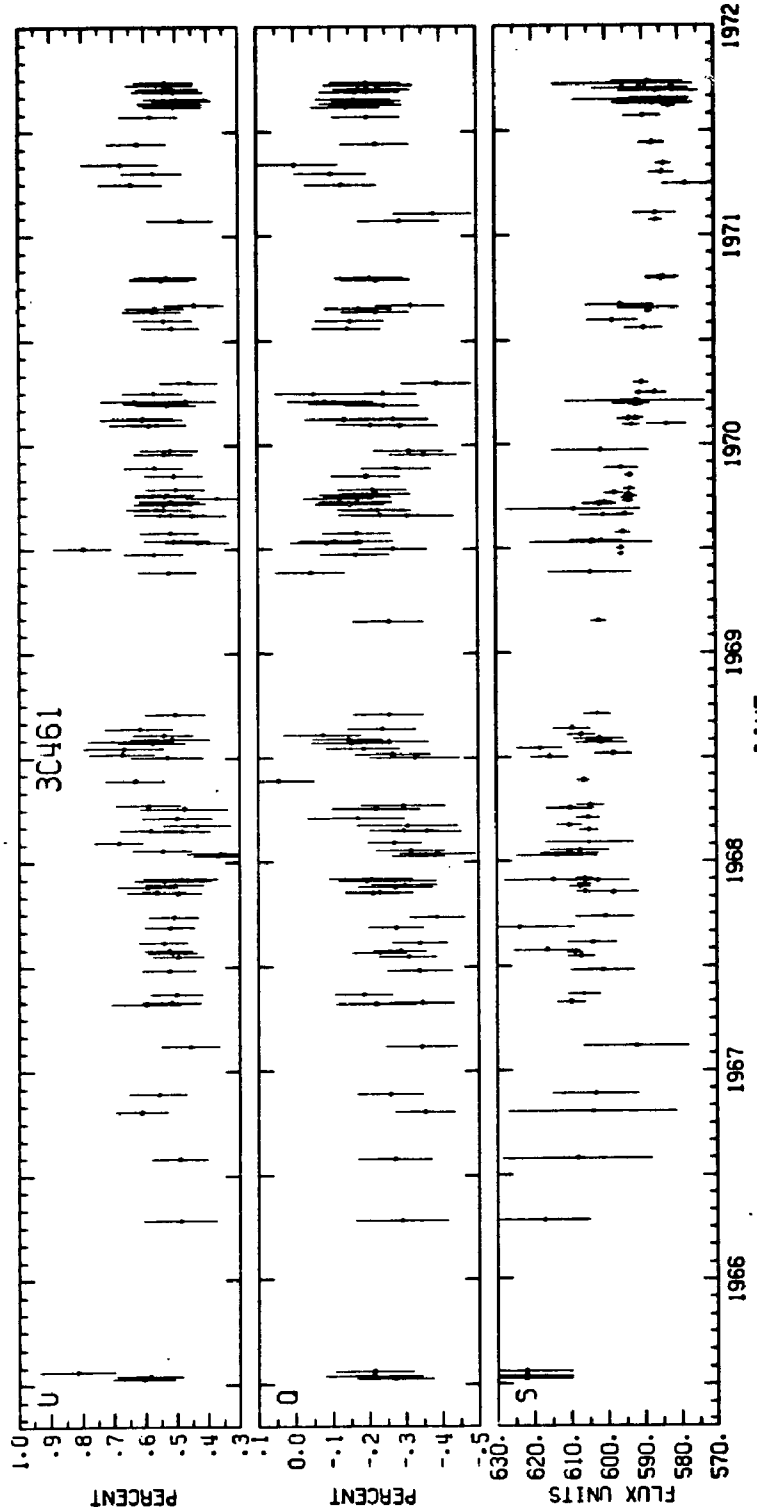


Figure 2.9: The normalized Stokes parameters Q' and U' and the total flux density of 3C461 versus time.

CHAPTER III

THE OBSERVATIONS

Flux density and polarization measurements of fifty radio sources were made at 8 GHz; of these, sixteen were observed on more than thirty occasions and nine observed between ten to thirty times. Total flux density variations were detected in twenty-one sources (other than Cas A); polarization variations were definitely detected in seven of these sources and probably observed in another four. Some characteristics for these eleven sources are listed in Table 3.

III-1. The Presentation of the Observations

The measured flux densities and polarizations of eleven intensively monitored variable radio sources are shown in Figures 3.1 through 3.11 in order of increasing righ ascension. Figure 3.1 shows the total flux density and normalized Stokes parameters Q' and U' for 3C84 versus time. Figures 3.2 through 3.4 show the total flux density and Stoke's parameters for NRAO 150, 3C120, and 4C39.25 versus time. Figures 3.5 through 3.11 present the total flux densities and polarized flux densities and position angles versus time for 3C273, 3C279, 3C345,

TABLE 3

Radio Sources Which are Variable or Probably Variable in Polarization

Source	Optical Ident.	m_V	z	Comments
3C84 †	Seyfert Galaxy	12.8	0.018	NGC 1275; expansion detected by VLBI*
NRAO 150 †	Unidentified			
3C120	Seyfert Galaxy	14.2	0.034	Expansion detected by VLBI
4C39.25	Quasar	17.3	0.699	Radio structure ≤0.0004 second of arc
3C273	Quasar	12.8	0.158	Low optical polarization; expansion detected by VLBI
3C279	Quasar	17.8	0.536	Expansion detected by VLBI
3C345	Quasar	16.0	0.594	Optical variable
NRAO 530 †	Unidentified			Probably polarization variable
BL LAC	Unclassified	16.0		Rapid variable
3C446 †	Quasar	18.4	1.404	Optical polarization variable
3C454.3	Quasar	16.1	0.860	Optical variable

*Very-long-baseline interferometry

† Probably Variable

NRAO 530, BL Lac, 3C446, and 3C454.3.

The polarization measurements have been corrected for instrumental polarization as discussed in section II-3. Standard errors shown in the figures include the internal uncertainty of each day's measurements, the rms error in estimating the daily instrumental polarization, and the uncertainty in position angle calibration for the measurement.

Individual measurements for the ten sources (other than Cas A) which exhibited variations in total flux density but in which no evidence for polarization variability exists are listed in Table 4. Column 1 lists the name of the source and optical identification (when known); column 2, date of observation; column 3, measured total flux density and its standard error; column 4, average polarized flux density and its standard error; and column 5, average polarization position angle.

The measurement results for the remaining twenty-nine sources which have not exhibited a detectable variation (except for Cas A) are listed in Table 5. Column 1 lists the source name; column 2, total flux density and its standard error; column 3, average degree of polarization and its standard error; column 4, average polarization position angle and its standard error; column 5, number of days the source was observed; column 6, mean epoch of the observations; and column 7, optical identification, if any.

Sources marked by asterisks are those that were used as flux density standards.

The polarization values quoted in Tables 4 and 5 were determined from weighted averages of daily measurements of the normalized Stokes parameters. Weights were calculated from daily measurement uncertainties. The polarized flux density was then calculated by multiplying the average degree of polarization by average flux density. If a source had been observed ten or more days, mean errors of the average values were computed from standard deviations of the daily measurements; otherwise, they were computed from the sum of the internal mean uncertainties and the rms error in the estimation of the daily instrumental polarization. For those sources in which average polarization is less than the mean error, an upper limit equal to twice the mean error is quoted, and no polarization position angle is quoted.

TABLE 4

Radio Sources which have Exhibited Variations in Flux Density at 8 GHz but not in Polarization

(1) Name/Opt. Ident.	(2) Date	(3) S(f.u.)	(4) P(f.u.)	(5) χ(°)
P0048-09/ Quasar	9/18/69	1.68±0.10	0.056±0.048	8±21
	2/16/70	2.39±0.18		
DW0727-11	4/14/71	4.10±0.16	0.076±0.049	136±14
	7/29/71	4.55±0.18		
P0736+01 Quasar	12/ 2/69	2.24±0.47	0.247±0.101	53±9
	9/14/71	10.58±0.12		
P0834-20	11/29/67	3.89±0.12	0.016±0.011	96±24
	12/17/67	3.74±0.13		
	2/25/68	3.69±0.12		
	3/16/68	3.50±0.10		
	7/ 6/68	3.14±0.18		
	2/14/69	2.40±0.07		
	8/15/69	2.44±0.56		
	8/22/69	2.21±0.13		
	12/17/69	2.14±0.15		
	1/13/70	2.60±0.22		
	2/ 5/70	2.30±0.15		
	2/ 6/70	2.21±0.12		
	2/23/70	2.28±0.09		
	4/19/71	2.35±0.10		
OJ287/ Unclas-sified	1/27/71	4.50±0.08	<0.060	
	4/19/71	3.90±0.05		
	5/ 3/71	3.92±0.06		
	6/ 9/71	3.94±0.24		
	7/20/71	4.02±0.09		
	9/14/71	4.90±0.10		
P1055+01/ Quasar	2/16/67	3.53±0.15	0.167±0.032	126±5
	11/30/67	3.44±0.11		
	1/12/68	3.54±0.12		
	1/16/68	3.73±0.16		
	2/23/68	3.17±0.13		
	2/17/69	3.16±0.11		
	7/ 6/70	3.40±0.15		
	7/ 7/70	3.42±0.11		

TABLE 4 -- Continued

(1)	(2)	(3)	(4)	(5)
	4/14/71	3.12±0.18		
	7/20/71	3.05±0.21		
P1127-14/ Quasar	4/10/67	6.66±0.18	0.204±0.023	134±2
	11/29/67	6.87±0.15		
	12/ 1/67	6.94±0.29		
	1/26/68	6.94±0.14		
	2/25/68	6.54±0.14		
	3/16/68	6.57±0.15		
	3/29/68	6.40±0.11		
	1/14/69	5.90±0.10		
	2/15/69	5.98±0.05		
	7/11/69	6.09±0.14		
	9/ 9/69	6.05±0.12		
	9/19/69	5.95±0.10		
	12/ 2/69	5.86±0.11		
	7/ 7/70	5.56±0.11		
	7/21/70	5.32±0.09		
	4/14/71	5.06±0.20		
	7/29/71	4.95±0.09		
	9/14/71	5.19±0.16		
3C418	7/16/66	3.67±0.19	0.08±0.021	79±6
	7/28/66	3.71±0.12		
	2/18/67	3.75±0.22		
	4/25/67	3.24±0.13		
	4/29/67	2.98±0.20		
	5/13/67	3.18±0.11		
	6/24/67	3.06±0.18		
	8/14/67	3.24±0.13		
	9/ 7/67	3.04±0.16		
	11/ 7/67	3.20±0.12		
	9/ 8/69	3.15±0.14		
	9/19/69	2.95±0.07		
	2/16/70	2.55±0.17		
P2134+00/ Quasar	8/11/67	12.38±0.30	0.437±0.025	3±1
	11/28/67	12.47±0.28		
	12/ 1/67	12.55±0.15		
	6/ 5/68	13.42±0.07		
	9/14/68	12.51±0.14		
	11/22/68	13.12±0.11		
	4/12/69	12.50±0.09		
	5/20/69	12.88±0.06		
	5/21/69	12.77±0.07		
	6/11/69	12.67±0.11		

TABLE 4 -- Continued

(1)	(2)	(3)	(4)	(5)
	6/17/69	12.84±0.08		
	3/15/70	12.01±0.08		
	4/ 1/70	12.29±0.10		
P2145+06/ Quasar	7/29/67	5.89±0.74	0.052±0.033	40±14
	11/ 9/67	5.10±0.12		
	2/21/69	4.39±0.09		

TABLE 5

Radio Sources which have not Exhibited Variations

(1) Name	(2) S(f.u.)	(3) P(%)	(4) χ(°)	(5) N	(6) Epoch	(7) Optical Ident.
3C10	14.30±0.44	<2		1	1967.86	Supernova Remnant
3C33	4.01±0.20	3.59±2.46	76 ±20	1	1969.58	DE Galaxy
DA55	2.57±2.04	5.04±2.04	162 ±12	1	1971.30	
3C48	3.40±0.15	5.99±1.39	120 ± 6	1	1969.63	Quasar
3C58	27.64±0.08	5.46±0.14	0.1± 0.3	10	1970.04	
DW0224+67	1.76±0.17	4.24±3.52	137 ±27	2	1971.33	
3C66	3.28±0.18	4.75±3.61	75 ±19	1	1971.33	ED Galaxy
CTA21	1.55±0.30	5.53±3.94		1	1971.34	
CTA26	2.22±0.08	3.77±1.17	46 ± 8	6	1967.65	Quasar
3C123*	10.2 ±0.6	3.88±0.24	169.7± 1.8	8	1969.42	Galaxy
NRA0190	2.91±0.07	1.32±1.23		1	1968.15	Quasar
3C144*	578.0 ±2.5	6.79±0.02	145 ± 0.2	41	1969.48	Supernova Remnant
3C145*	394.5 ±1.5	0.03±0.01	30.9± 9.6	132	1969.56	HII Region

TABLE 5 -- Continued

(1)	(2)	(3)	(4)	(5)	(6)	(7)
3C147	5.15±0.05	1.54±0.45	141.1± 8.4	7	1969.32	Quasar
DA193	5.27±0.10	3.17±1.58	87 ±16	1	1970.80	
3C196	2.63±0.06	1.79±0.82	136 ±14	8	1967.91	Quasar
P0859-14	1.96±0.06	2.99±1.46	105 ±14	4	1968.58	Quasar
3C274*	47.75±0.20	1.41±0.02	87.9± 0.3	120	1969.39	E Galaxy
3C295	3.67±0.41	<4		1	1969.64	Galaxy
3C348	9.45±0.98	9.06±1.30	22.4± 4.1	1	1971.58	cD Galaxy
3C353	15.31±0.18	4.59±0.63	80.9± 2.8	1	1971.57	D Galaxy
M17*	757.8 ±2.1	0.02±0.01	114 ±17	120	1969.37	HII Region
3C380	5.61±0.04	1.04±0.51	146 ±14	3	1969.04	Quasar
3C391	5.92±0.12	2.50±0.01	76 ±11	2	1970.86	
3C405*	214.4 ±0.01	5.40±0.01	135.6± 0.1	148	1969.26	cD Galaxy
NGC6857	13.48±0.06	<0.28		15	1968.90	K3-50 Included
PD21	21.60±0.05	0.08±0.06	9 ±23	40	1969.31	HII Region

TABLE 5 -- Continued

(1)	(2)	(3)	(4)	(5)	(6)	(7)
NGC7027	6.36±0.09	0.54±0.45	45 ±25	4	1967.42	Planetary Nebula
3C461*	629.6	0.57±0.01	56.7 ± 0.4	108	1969.62	Supernova Remnant

*Source used as a flux density standard.

III-2. Discussion of the Results for Individual Sources

3C84: [Figure 3.1]

The total flux density of this Seyfert galaxy has been increasing almost linearly throughout the period of observation. This increase is evidently the result of successive small outbursts; the dotted curve drawn through the data indicates the fine structure of the variation. Data at other wavelengths also demonstrate the existence of these mini-bursts (Hobbs, Corbett, and Santini, 1969; McCullough and Waak, 1969; Fogarty, Epstein, Montgomery, and Dworetsky, 1971). A linear least-squares analysis of the variation at $\lambda 3.75$ cm yields an average annual increase of 2.78 ± 0.08 flux units, which is shown by the dashed line. It is interesting that this rate of increase is almost exactly equal to that reported by Dent (1966). Extrapolation of his data spanning the period 1961-1965, after increasing it by 7.2 per cent to take into account the change in flux density scale, accurately predicts the value of the total flux density which was measured in mid-1971.

Aller (1968) reported that the polarization of this source was not significantly different from zero, except for a short period in mid-1966. The form of this variation at that time is indicated by the short-dashed curves sketched in the plots of the normalized Stokes parameters. Now that more data have become available, it is apparent

that this galaxy is only slightly polarized and has not exhibited polarization variations since that time. Application of Snedecor's F test to the ratio s/σ, in a comparison of the calculated uncertainties σ of measurements of the polarization and the standard deviations s of the daily averages, indicates that the probability that this ratio would be exceeded by random chance is greater than 25 per cent. Thus there is no evidence for polarization variations after mid-1966.

The overall weighted averages of the normalized Stokes parameters for 3C84 are:

$$Q' = 0.113 \pm 0.021 \quad , \%$$

$$U' = 0.104 \pm 0.020 \quad , \%$$

and are indicated by dashed lines in Figure 3.1. The foregoing analysis is also evidence that the calculated uncertainties of measurements of the polarizations of radio sources observed in this study have not been underestimated.

NRAO 150: [Figure 3.2]

At least four small bursts have taken place in the total flux density during the time spanned by the observations. The degree of polarization is small, and thus the Stokes representation is used to illustrate this quantity. Q has exhibited a long-term secular decrease at the rate of 0.036 flux unit per year. Two large

excursions have been recorded in the polarized emission: the first, in late April 1967 appears in Q , and the second, in mid-April 1971 appears in U.

3C120: [Figure 3.3]

Six separate outbursts have been recorded in the total flux density of this Seyfert galaxy after that which was observed in 1966 at 2 cm by Kellermann and Pauliny-Toth (1968).

The degree of polarization has ranged between zero and five per cent while the position angle of the polarized emission has fluctuated over a 75-degree range. The most rapid variations took place during the two large outbursts of 1967-1968 after total flux density had reached maximum. During the first outburst, U decreased and then increased by 0.25 flux unit in November-December 1967. It then decreased again throughout the first four months of 1968. Q decreased slightly over this entire period. These fluctuations were comparable to the magnitude of the total polarized emission. In the second outburst, Q increased slightly during the time that the total flux density increased. U likewise increased by 0.25 flux unit with the same time scale as the increase in total flux density, although delayed by more than three months. After a decline of 0.15 flux unit in early 1969, U remained nearly constant until June 1970, at which time

it rapidly decreased another 0.15 flux unit. Since this time, it has remained nearly constant. Throughout this entire period too, Q has been relatively constant. In 1971, however, Q began increasing, so that by the last observed date, it had doubled.

4C39.25: [Figure 3.4]

Before early 1968 this quasi-stellar radio source appeared to be nonvarying and was reported as such by Aller (1968). From that time onward, the total flux density increased in a manner similar to the variation exhibited by 3C84. A weighted least-squares analysis indicates that the average annual rate of increase in total flux density has been 0.67 ± 0.01 flux unit per year since mid-1968.

The variation in the polarized emission also commenced in mid-1968. Q has fluctuated about an average value of 0.028 ± 0.0009 flux unit, whereas U has increased at the average rate of 0.071 ± 0.005 flux unit per year. The variations in total flux density and U are highly correlated (correlation coefficient equals 0.74) and if the same component is responsible for their increase, it can be inferred that its net degree of polarization is 10 ± 1 per cent at a position angle of 39 ± 2 degrees.

3C273: [Figure 3.5]

Dent (1965) observed a steady increase in the total flux density from mid-1962 to early 1965 which amounted to 3.6 flux units per year, corrected to the new flux density scale. In early 1966, the flux density at centimeter wavelengths began to increase very rapidly, apparently a major outburst took place. It appears that three more outbursts superimposed on a background flux density which has been steadily increasing at an average rate of nearly 2.2 flux units per year have followed the event of 1966, although none are quite as distinct. The total flux density variations of this quasi-stellar radio source appear more like those exhibited by 3C84 than by 3C120 in that the source exhibits a long-term increase made up of several small outbursts, instead of several distinct outbursts each of which decays back to a quiescent level before the next.

Polarization measurements by Kuzmin and Dent (1966) and by Hobbs and Haddock (1967) and the data reported here indicate that the polarized flux density remained approximately equal to 0.5 flux unit from June 1963 until April 1966. Between the latter date and June 1966, the strength of the polarized emission decreased to 0.2 flux unit, and it rose during the following month to approximately 1.0 flux unit. Throughout 1967 and 1968, it remained nearly constant at this level. Beginning in 1969

the polarized flux density exhibited short-term variations which appear in general to mimic the form of the variations which occurred in the total flux density. In 1970, the peak-to-peak variation in the strength of the polarized emission was 0.6 flux unit.

The position angle has fluctuated between 140 and 155 degrees with very few excursions beyond this range, the most notable of which was during the rapid increase in total flux density in 1966. In general, the largest excursions occurred just before or during the relative peaks in the total flux density variations.

3C279: [Figure 3.6]

The total flux density of this quasi-stellar radio source increased rapidly in 1966, and remained at a nearly constant level throughout 1967. Beginning in 1968 a general decline exhibiting variations with a time scale of approximately six months appeared. These variations persisted until the source had subsided to the 1965 level of emission.

Polarized flux density rose and dipped sharply during the first six months of 1966. After total flux density had levelled off, the polarized flux density underwent a dramatic decline beginning in February 1971, which exhibited structure with time scales of the order of four months. After it reached its minimum level in

January 1968, several peaks with time scales of four to eight months (February, 1968; June, 1968; May, 1969; and March, 1970) were recorded. The one which occurred in May 1969 was particularly complex.

The polarization position angle was remarkably constant in 1967 after the sharp variation which took place in May-June 1966 during the increase in total flux density. Beginning in 1968, it too began to exhibit large variations, the most rapid ones occurring during the peaks in polarized flux density mentioned above. In the first six months of 1970, the polarization position angle varied over 100 degrees.

An analysis of these variations has already been published (Aller and Olsen, 1971).

3C345: [Figure 3.7]

The variation in the total flux density of this quasi-stellar radio source is similar to that of 3C279 before it declined. This source was quiescent in 1966, rose quickly throughout 1967, and remained steady at the elevated level for the next year-and-a-half. During December of 1969 the flux density rose through one more flux unit and has remained constant at this new level since.

Prior to 1967, the data are too sparse and scattered to identify the nature of the variations in polarized emission. While the total flux density was increasing

throughout 1967, the amount of polarized emission remained constant at 0.1 flux unit. During March-April 1967, however, the position angle of the polarized emission varied through 50 degrees. The strength of the polarized emission did not change until August 1968 when it began increasing. Since then, polarized emission has generally increased, although not uniformly. A sharp, temporary decrease of nearly 0.15 flux unit occurred in April 1969.

NRAO 530: [Figure 3.8]

As many as five maxima, counting a small one in May 1969, are apparent in the data. The peak-to-peak variation in the total flux density has been 1.0 flux unit.

Although the data is scanty, it is sufficient to conclude that this source is most likely a polarization variable. The polarized flux density has ranged between 0.1 and 0.3 flux unit, while the position angle has varied by more than 70 degrees. In particular, the stability of the polarized flux density in 1969 should be compared to the scatter which preceeded and followed this period.

BL Lacertae [Figure 3.9]

During the three years in which this source has been observed, no less than nine significant outbursts have taken place. Large outbursts occurred within the span of a single month (Andrew, MacLeod, Locke, Medd, and Purton,

1969) and recently, radio "spikes" of amplitude 1 to 2 flux units and duration 7 to 20 days have been detected (MacLeod, Andrew, Medd, and Olsen, 1971). BL Lac qualifies as one of the most active and rapid radio variables known to date.

In general, the variations in the polarized emission have been slower than those in total flux density, although polarization variations with a time scale of less than one week have been detected (Olsen, 1969). The polarized emission has varied by a factor of five, whereas the total flux density has varied by a factor of a little more than two. The position angle of polarized radiation has ranged over more than 130 degrees.

3C446: [Figure 3.10]

This quasi-stellar radio source is known to have increased in flux density during 1966 (Dent, private communication; Kellermann and Pauliny-Toth, 1968). Since 1962 it has fluctuated from 3.5 to 5.0 flux units.

The major variation in polarized flux density occurred simultaneously with a small peak after June 1968. The increase recorded at that time apparently completely faded away by June 1969. The position angle of the polarized radiation has fluctuated over a range of 90 degrees.

3C454.3: [Figure 3.11]

The variation in total flux density which this quasi-stellar radio source has exhibited is remarkable. After the initial increase to a value two-and-a-half times that of the pre-outburst level, the total flux density remained at maximum value for the nine-month period from April 1967 to December 1967. Throughout the period April 1968 to January 1970, a linear decline of 8.50 ± 0.04 flux units per year took place. The only deviation from this smooth decline is a possible increase in December 1968.

Rapid variations in the polarized flux density are apparent in April-May 1967, just after the total flux density reached a maximum, and July-August 1968 while the total flux density was declining. The peak-to-peak variations in the polarized flux density is 0.3 flux unit.

The polarization postion angle has remained remarkably constant throughout the period of observation, undergoing its greatest variation in 1966 while the total flux density was increasing rapidly.

Finally, it is interesting to note that the polarized emission has been varying throughout 1970-71, during which time the total flux density has remained stable at pre-outburst level. The variations are apparent in both the amplitude and the orientation of the polarized emission, but the major variations have been in orientation. Thus it appears that the radio source is still active even though

the total flux density is not changing.

III-3. Summary of Observations

The variations in total flux density which have been detected in this study may be divided into four general types: (1) impulsive outburst, in which there is sharp rise and fall; (2) extended outburst, in which a rapid rise is followed by a quiescent period and then slow decline; (3) sustained outburst, in which a rapid rise is followed by a period of enhanced emission of several years' duration; (4) a long-term increase of the total flux density. Examples of these four types are: (1) 3C120 and BL Lac; (2) 3C279 and 3C454.3; (3) 3C345 and 3C446; and (4) 3C84, 4C39.25 and 3C273.

The great majority of rapid polarization variations (time scales less than several months) occur while the total flux density is increasing or after it has reached its maximum value (e.g., 3C454.3; 3C279).

Generally, the variations in polarization are not closely correlated with those in the total flux density, but 4C39.25 is a noteworthy exception. In the small outburst of mid-1968, 3C446 also appears to have undergone similar variations in total flux density and the amplitude of polarized emission.

The fractional change of the polarization variations are often several times that of the average polarization

for a radio source. Thus a strongly variable source may double its total flux density during an outburst whereas the polarized flux density may change by a factor of four. Significant changes in the polarization may also occur while the total flux density is not changing, indicating that the source is still active during this time.

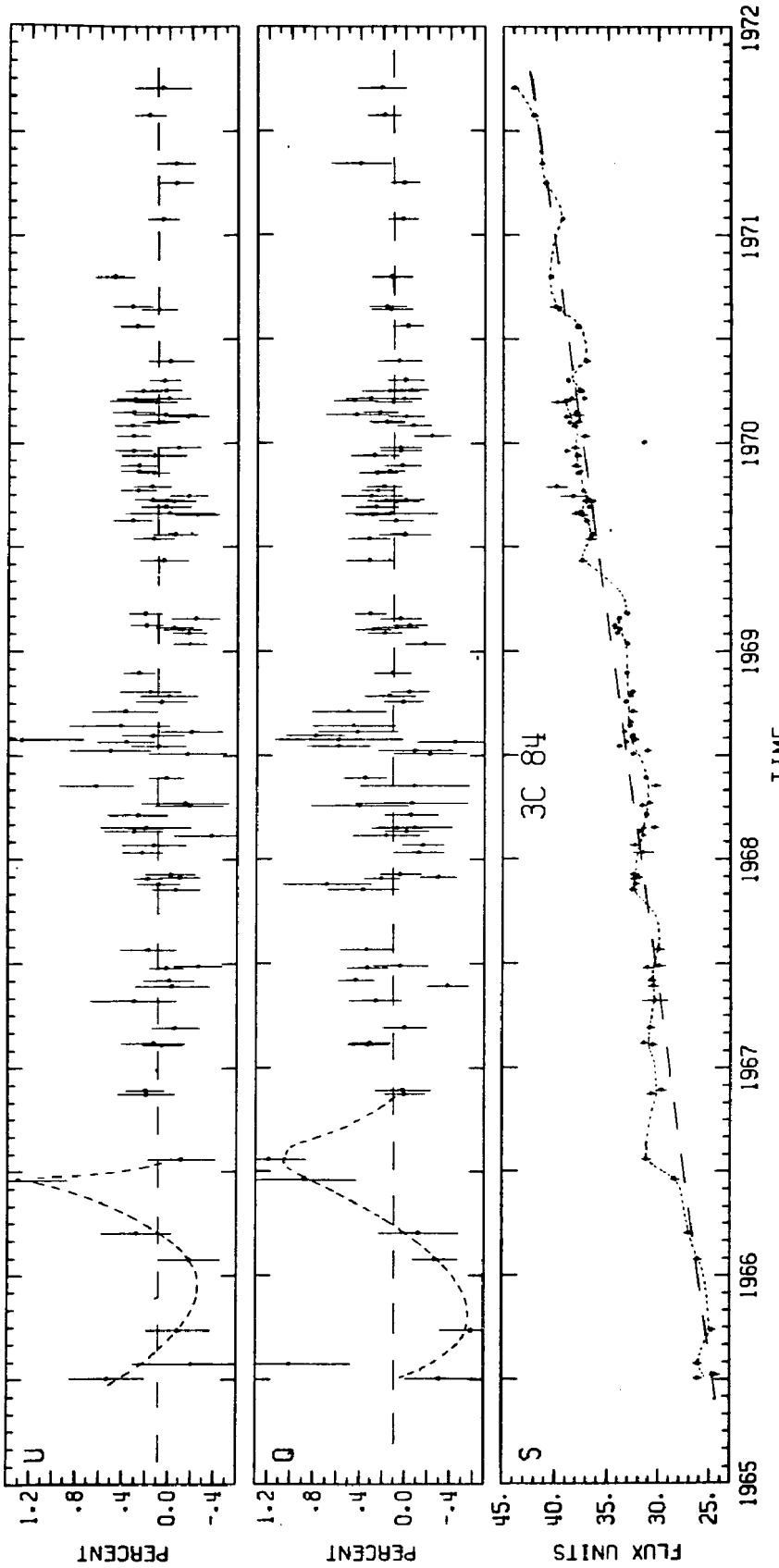


Figure 3.1: The normalized Stokes parameters U' and Q' and the total flux density of 3C84 versus time. Horizontal dashed lines are the weighted average values of the Stokes parameters, and the dashed line through the total flux density data represents the result of a weighted least-squares analysis.

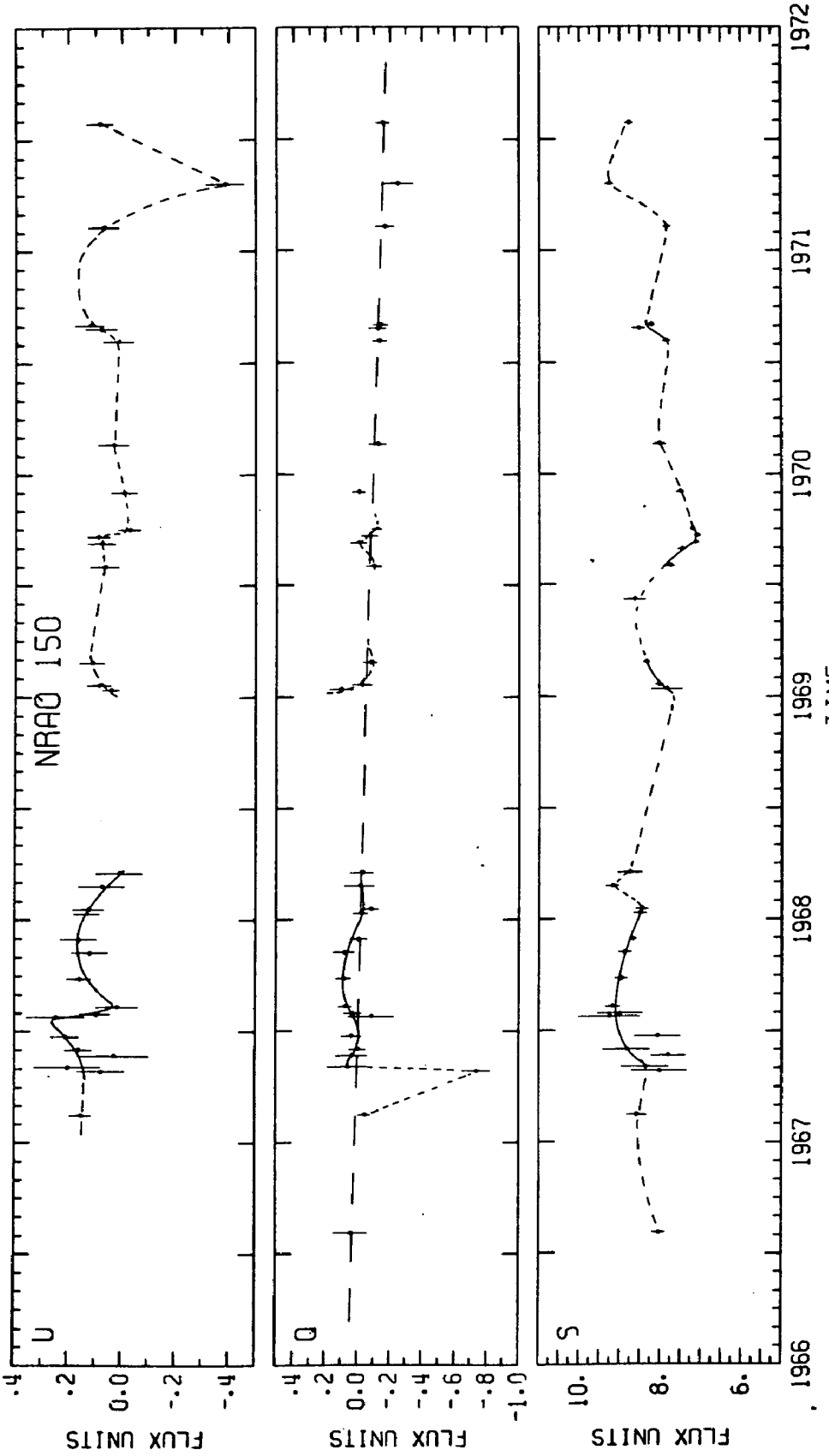


Figure 3.2: The Stokes parameters U and Q and the total flux density of NRAO 150 versus time. The dashed line through Q represents a long-term secular decrease in this parameter.

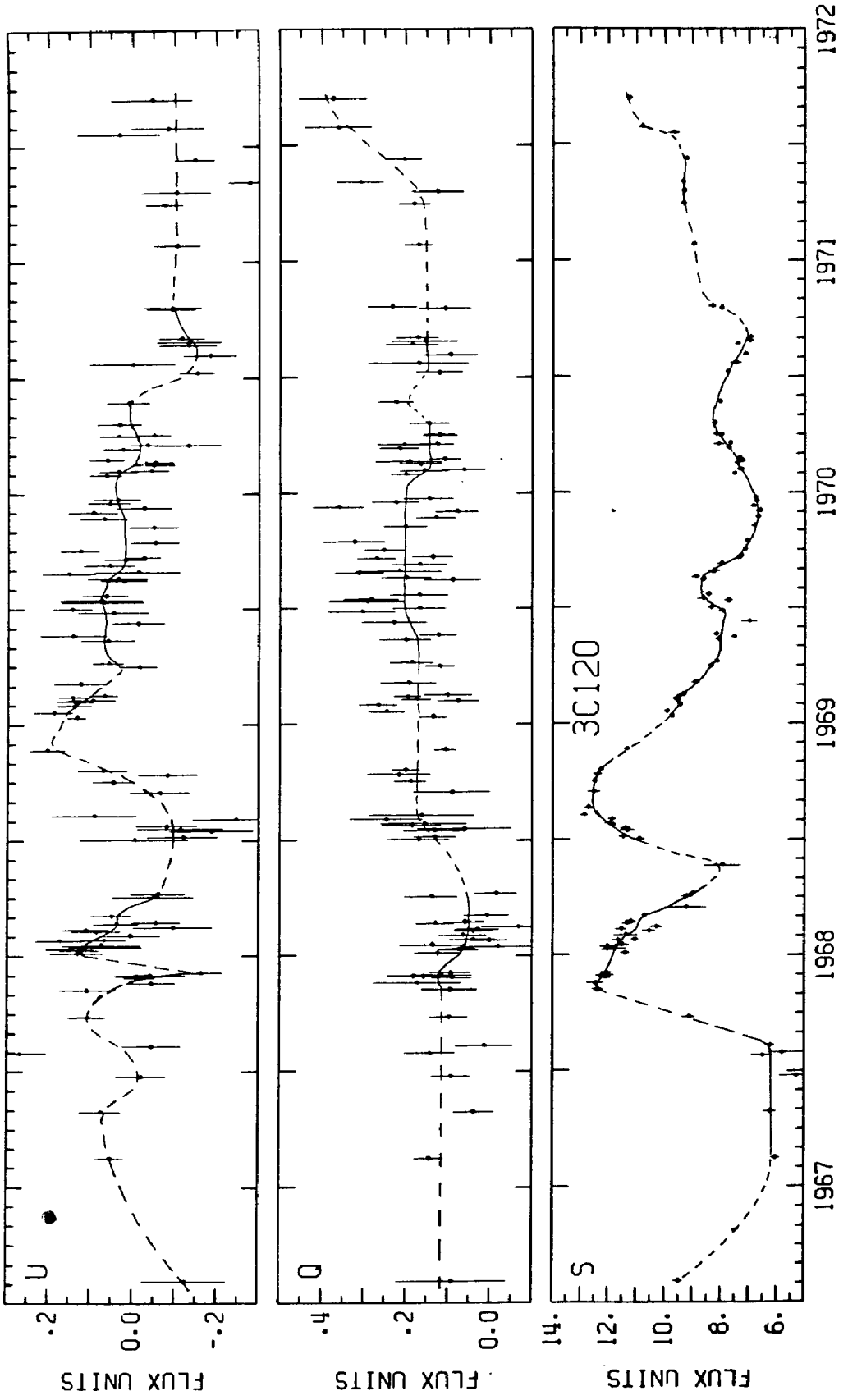


Figure 3.3: The Stokes parameters U and Q and the total flux density of 3C120 versus time.

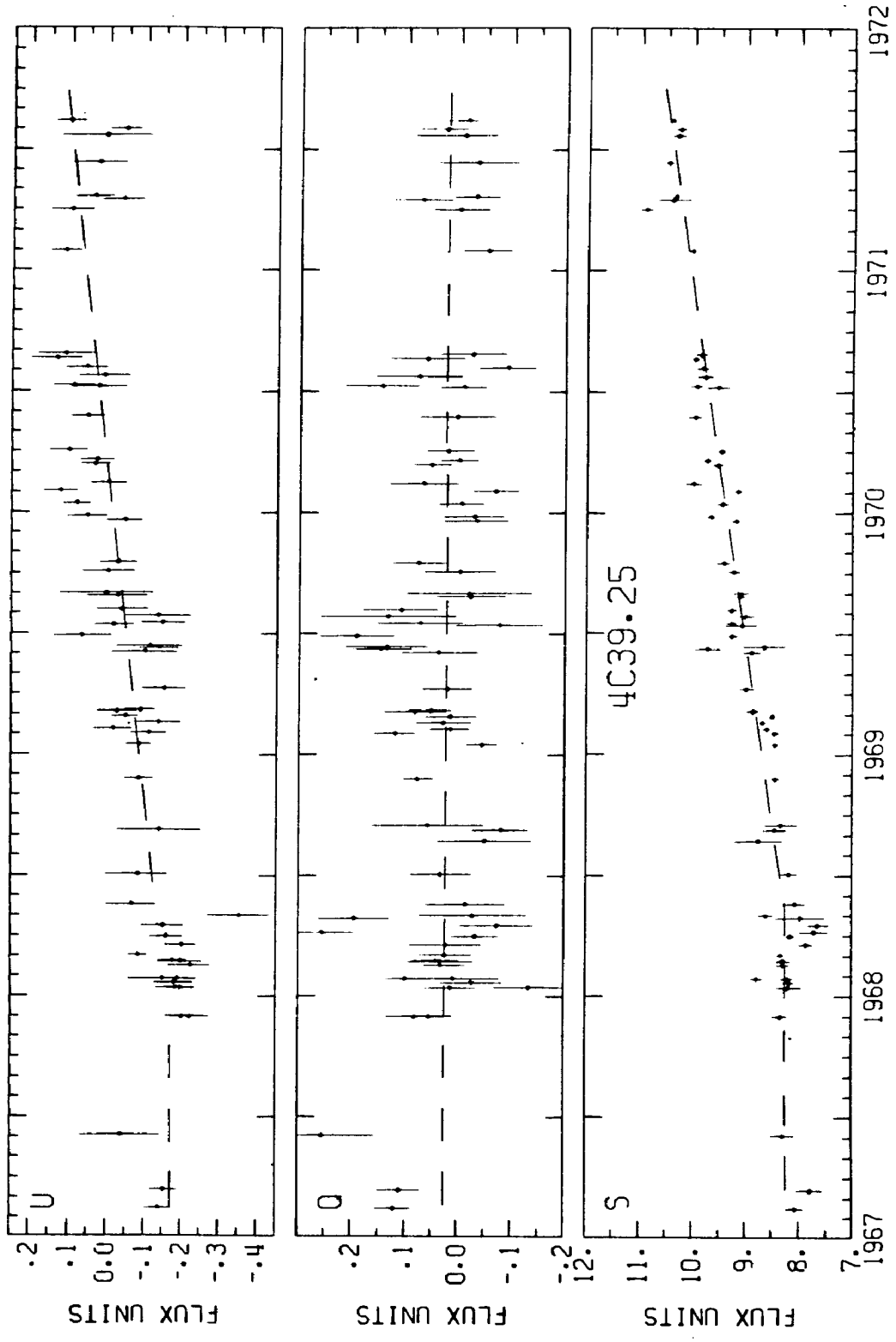


Figure 3.4: The Stokes parameters U and Q and the total flux density of 4C39.25 versus time. The dashed line through Q represents the weighted average value of this parameter. The dashed lines through U and S represent the results of weighted least-squares analyses of the variations in these quantities.

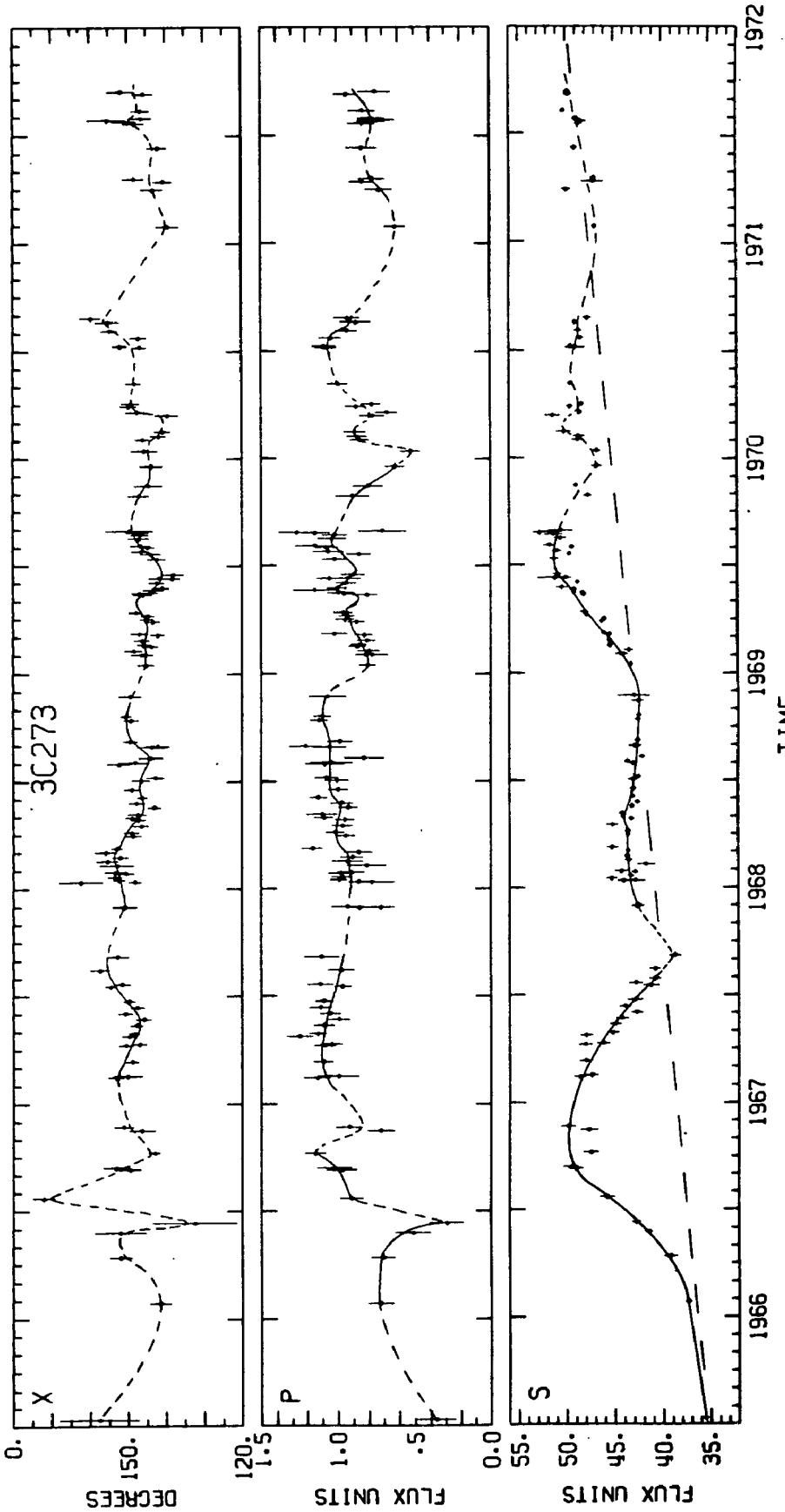


Figure 3.5: The polarization position angle, polarized flux density, and total flux density of 3C273 versus time. The dashed line represents a secular increase in the background flux density at the rate of 2.2 f.u./yr.

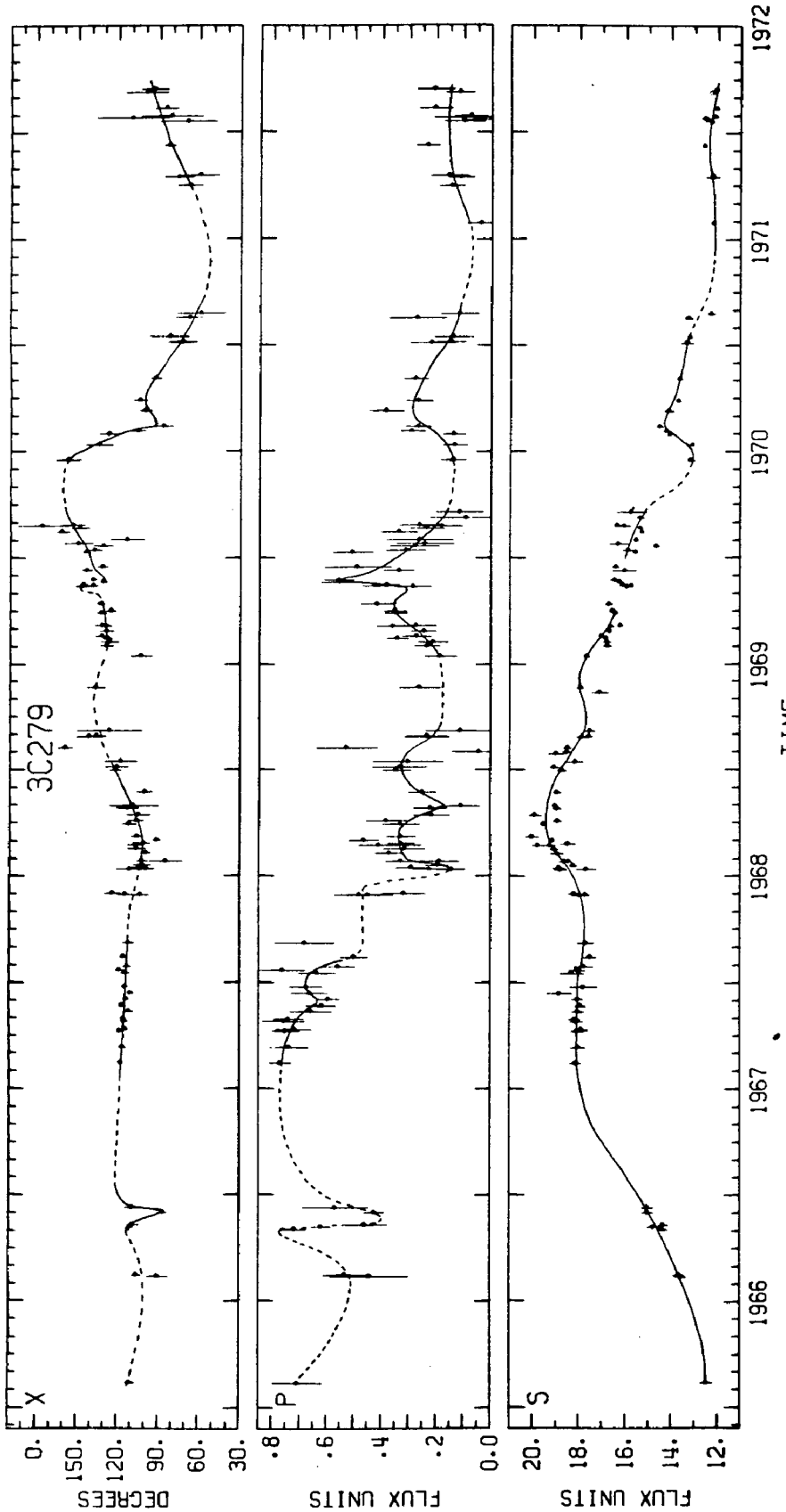


Figure 3.6: The polarization position angle, polarized flux density, and total flux density of 3C279 versus time.

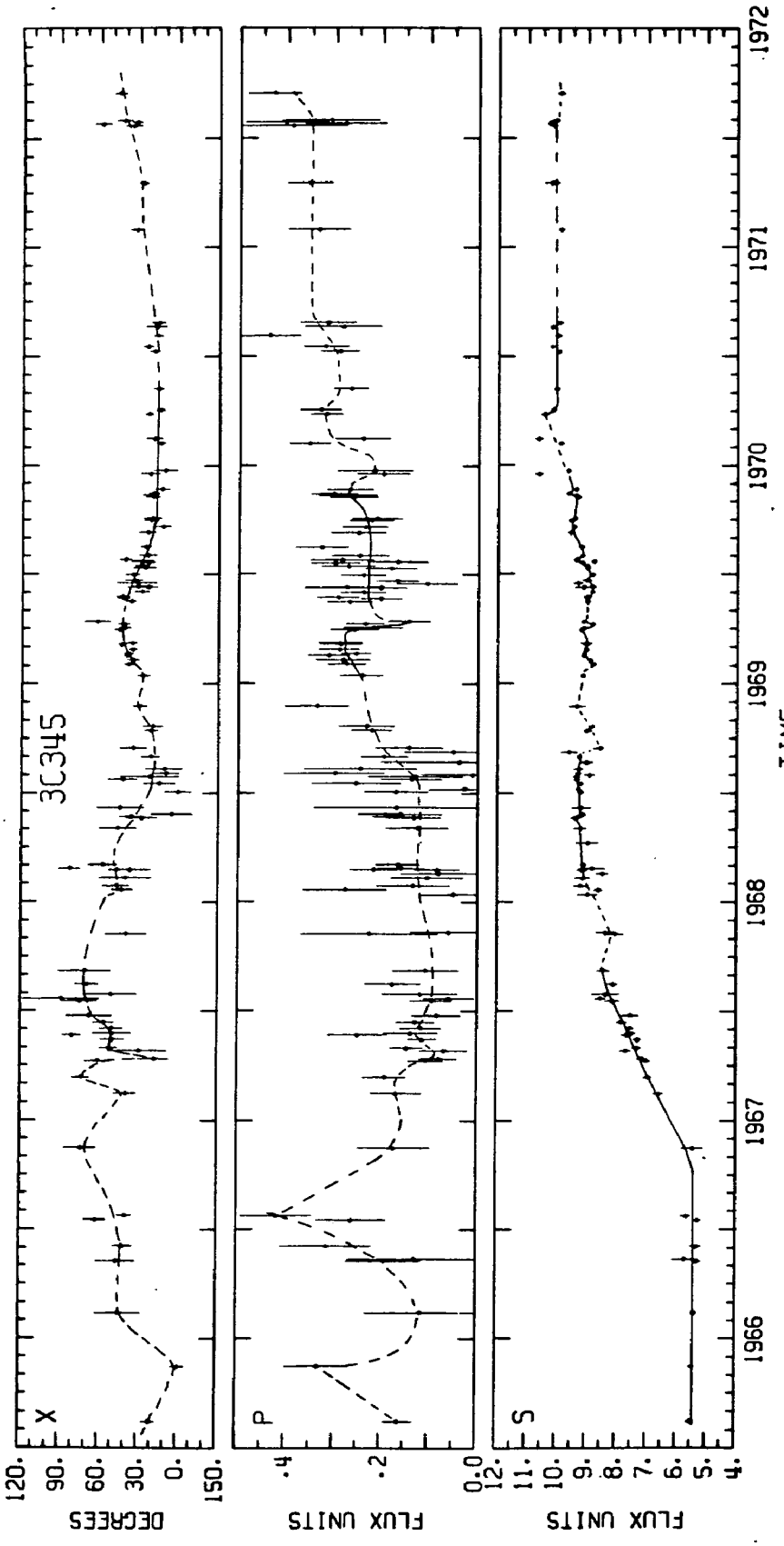


Figure 3.7: The polarization position angle, polarized flux density, and total flux density of 3C345 versus time.

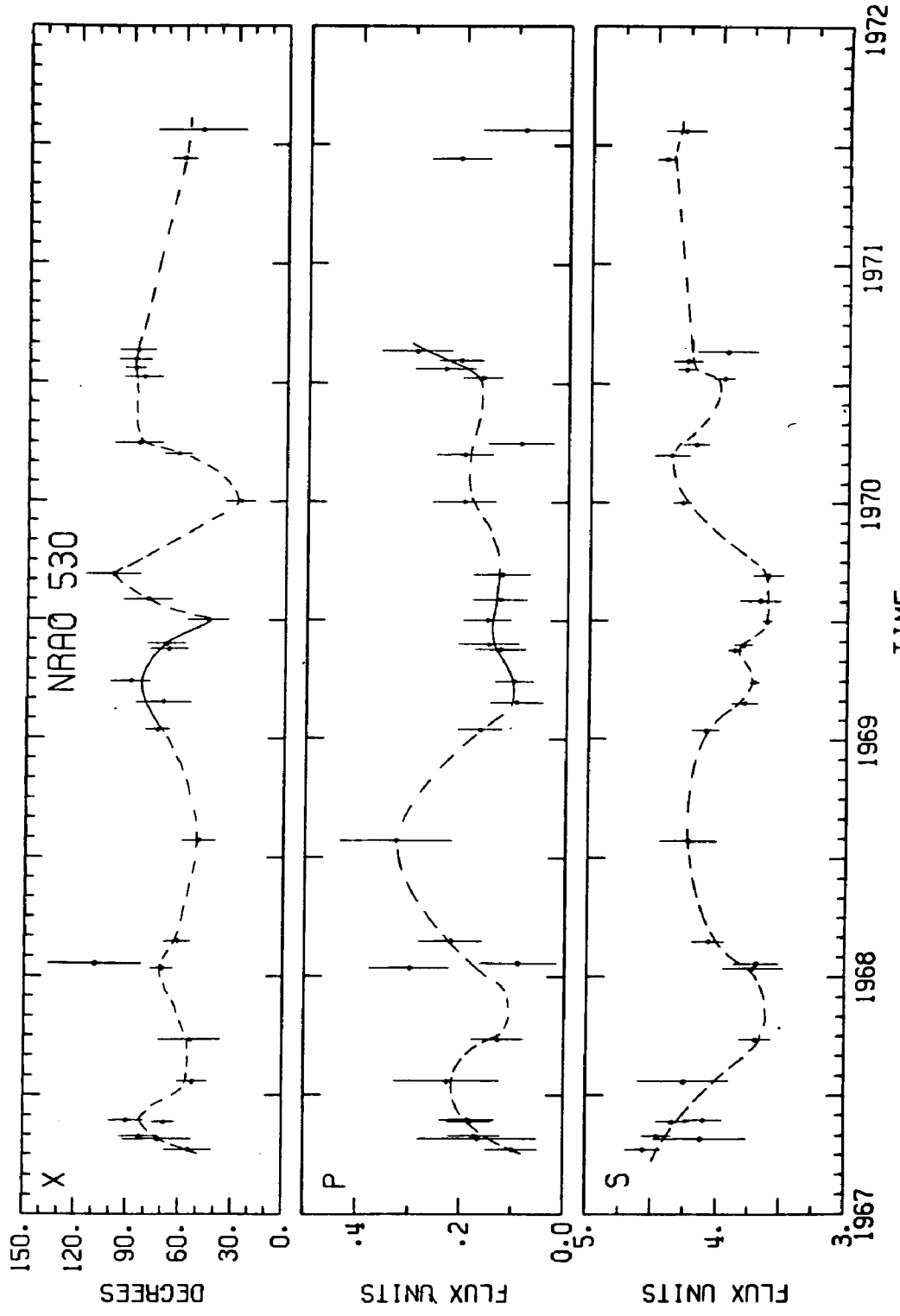


Figure 3.8: The polarization position angle, polarized flux density, and total flux density of NRAO 530 versus time.

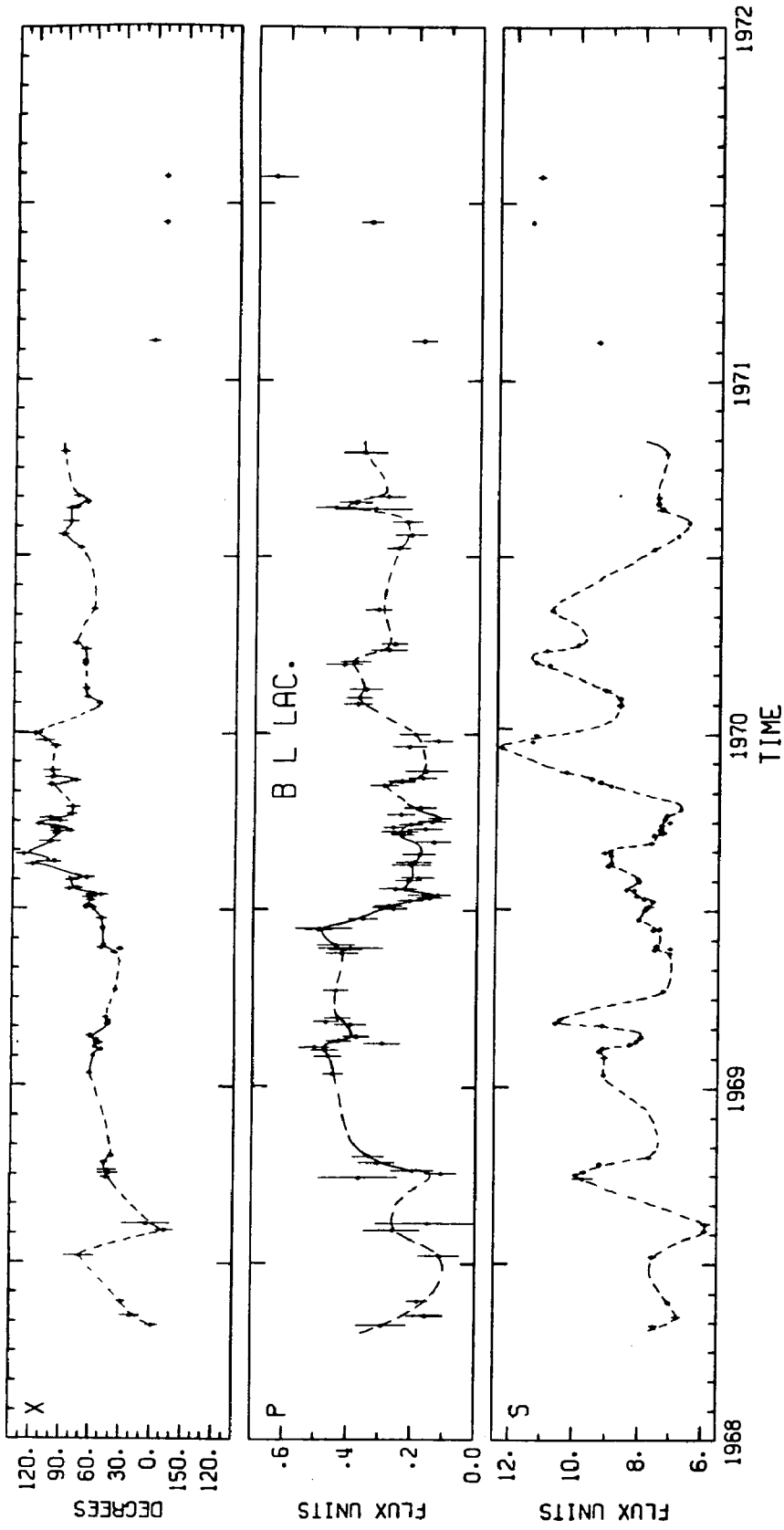


Figure 3.9: The polarization position angle, polarized flux density, and total flux density of BL Lacertae versus time.

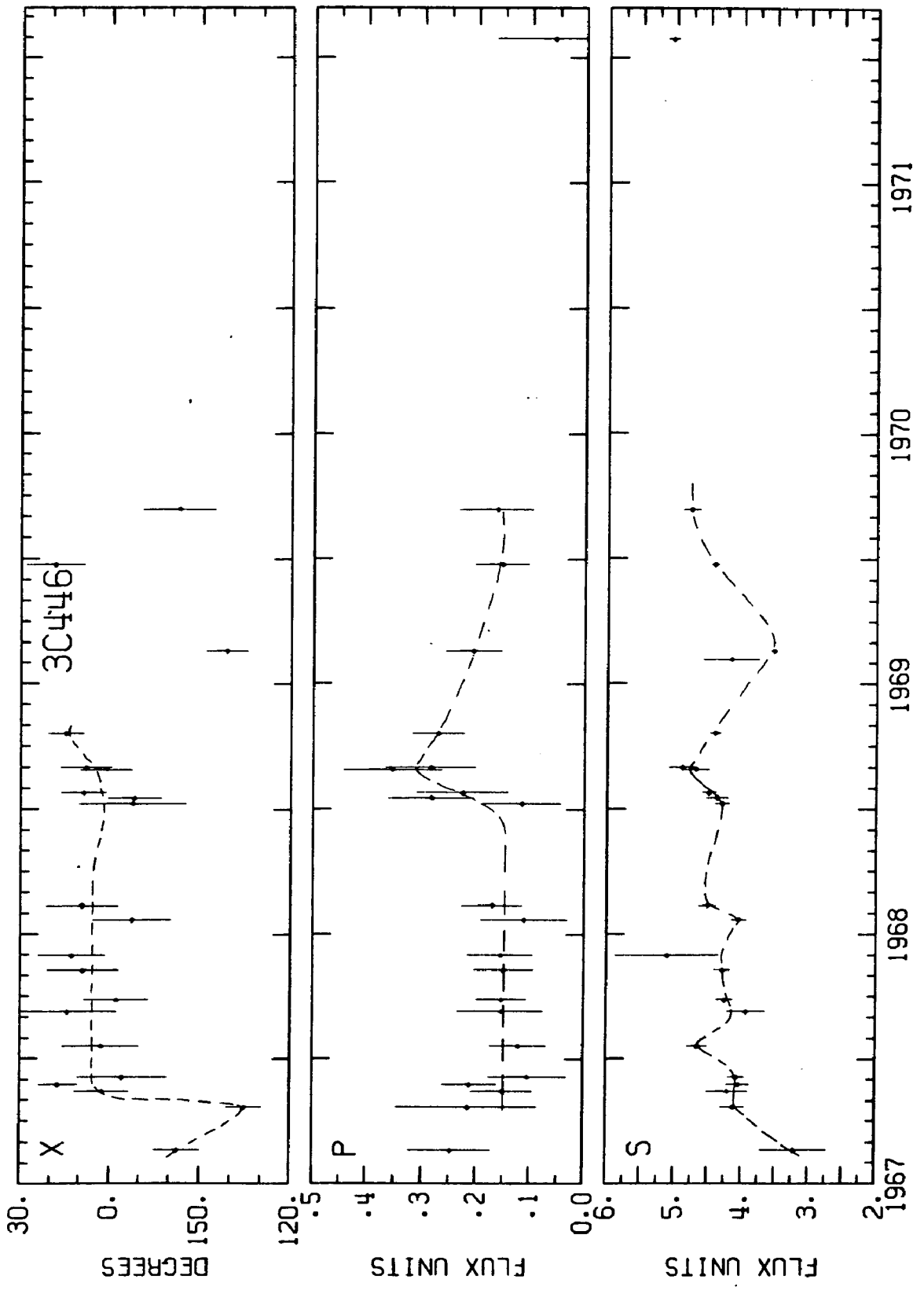


Figure 3.10: The polarization position angle, polarized flux density, and total flux density of 3C446 versus time.

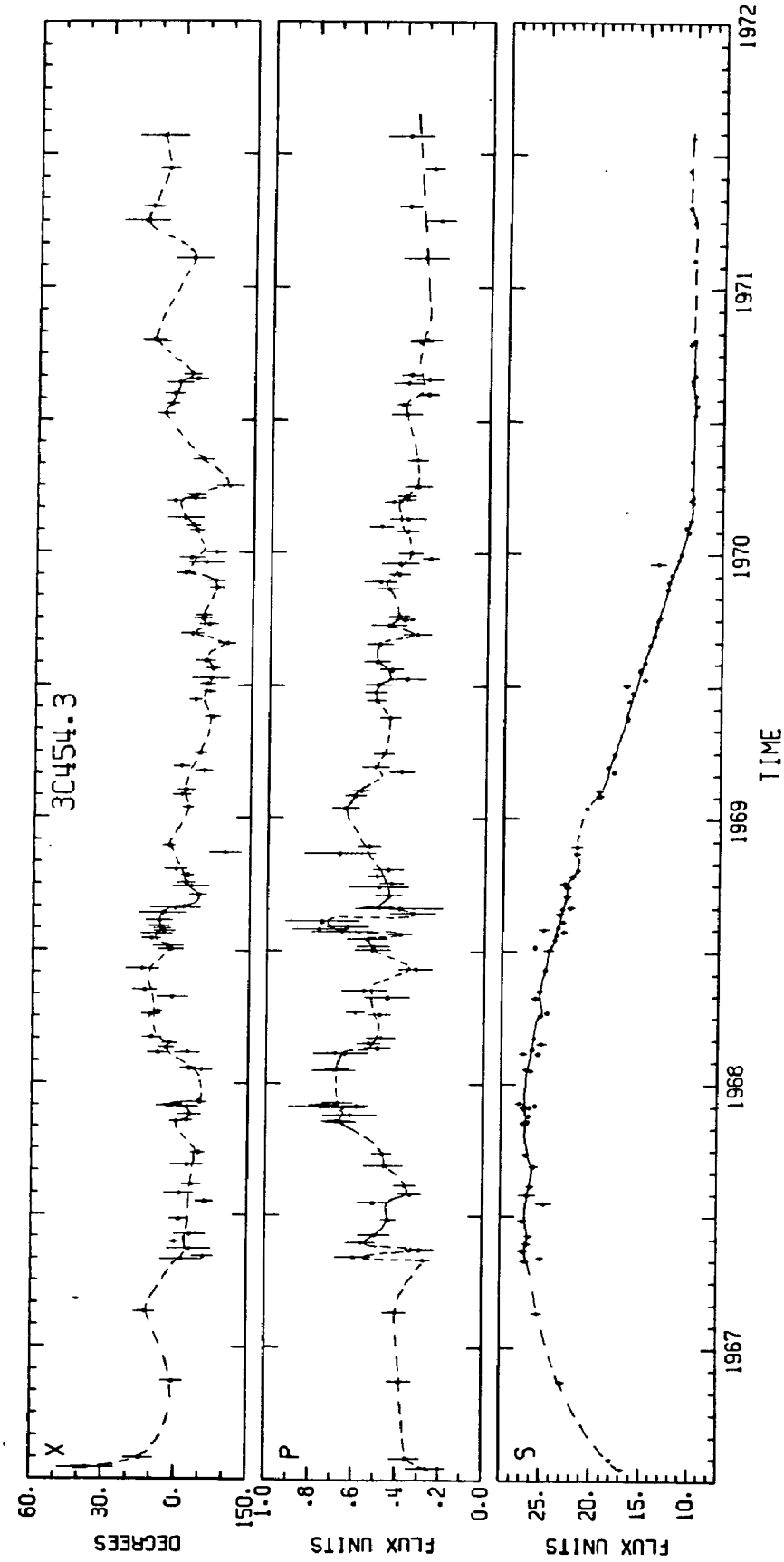


Figure 3.11: The polarization position angle, polarized flux density, and total flux density of 3C454.3 versus time.

CHAPTER IV

ANALYSIS AND INTERPRETATION

IV-1. 3C279[1]

Since 1966 the flux density at 8 GHz has exhibited a single extended outburst containing small, short-term fluctuations. At higher frequencies, several large-amplitude, short-term outbursts have been reported (e.g., Kellermann and Pauliny-Toth, 1968; Hobbs, Corbett, and Santini, 1969; McCullough and Waak, 1969). Variations in the linear polarization of this source were discovered in the early development of the outburst (Aller and Haddock, 1967) and subsequent changes in polarization have been reported in the frequency range of 5 to 20 GHz (Hobbs, Hollinger, and Marandino, 1968; Gardner, Whiteoak, and Morris, 1969; McCullough and Waak, 1969; Aller, 1970b).

Interest in this source has increased with the recent very-long-baseline interferometer measurements which indicate that a large fraction of the 8 GHz emission arises from a small double source whose components are separated at a relativistic speed (Knight, Robertson, Rogers, Shapiro,

---

[1]This analysis of the observed variations in the radio emission of quasi-stellar source 3C279 has been published (Aller and Olsen, 1971).

Whitney, Clark, Goldstein, Marandino, and Vandenberg, 1971; Whitney, Shapiro, Rogers, Robertson, Knight, Clark, Goldstein, Marandino, and Vandenberg, 1971; Cohen, Cannon, Purcell, Sheffer, Broderick, Kellermann, and Jauncey, 1971).

In order to facilitate the study of the polarization of the variable component, the contribution at 8 GHz of the non-variable, low-frequency component was removed from the data displayed in Figure 3.6. The extrapolation of the spectrum at frequencies below 1 GHz, which is attributed to an extended "halo" component, yields

$$S(\text{halo}) = 2.7 \pm 0.5 \text{ , flux units}$$

$$S_p(\text{halo}) = 0.19 \pm 0.04 \text{ , flux units.}$$

$$\chi(\text{halo}) = 2.7 \pm 2.0 \text{ , degrees}$$

where S(halo) is the contribution of the halo at 8 GHz to the observed total flux density; S_p(halo) is the contribution to the polarized flux density; and χ(halo) is the polarization position angle of the contribution (Aller, 1970c). The polarized emission of the halo was converted to the Stokes representation

$$Q(\text{halo}) = 0.189 \pm 0.040 \text{ , flux units}$$

$$U(\text{halo}) = 0.018 \pm 0.014 \text{ , flux units}$$

so that its removal from the data could be effected:

$$S_{(\text{variable component})} = S_{(\text{observed})} - S_{(\text{halo})}$$

$$Q_{(\text{variable component})} = Q_{(\text{observed})} - Q_{(\text{halo})}$$

$$U_{(\text{variable component})} = U_{(\text{observed})} - U_{(\text{halo})}$$

The results of this subtraction are shown in Figure 4.1 where the data points represent averages over calendar-month intervals and are not running averages. The uncertainties in the halo contribution to the total flux density and polarization are not included in the figure since such errors enter equally into all the determinations.

Aside from the smoothing effect of the averaging, the total flux density curve of the corrected data is shifted vertically with respect to the observations presented in Figure 3.6 due to the removal of the halo contribution. A nearly linear, long-term decrease in total flux density (indicated by the straight dashed line) following the maximum in 1968 is apparent in this data. However, the data does deviate significantly from this line, especially near 1970.0. It is suggested that these short-term fluctuations are due, at least in part, to sudden compressions of the magnetic fields in the radiating regions as the expanding source components encountered intergalactic material.

One of the most fascinating features of the polarization variability of this source has been the change of the position angle of the polarized emission with time. The removal of the halo contribution has not significantly changed the polarized flux density curve, but it does reveal the monotonic nature of the variations of χ in

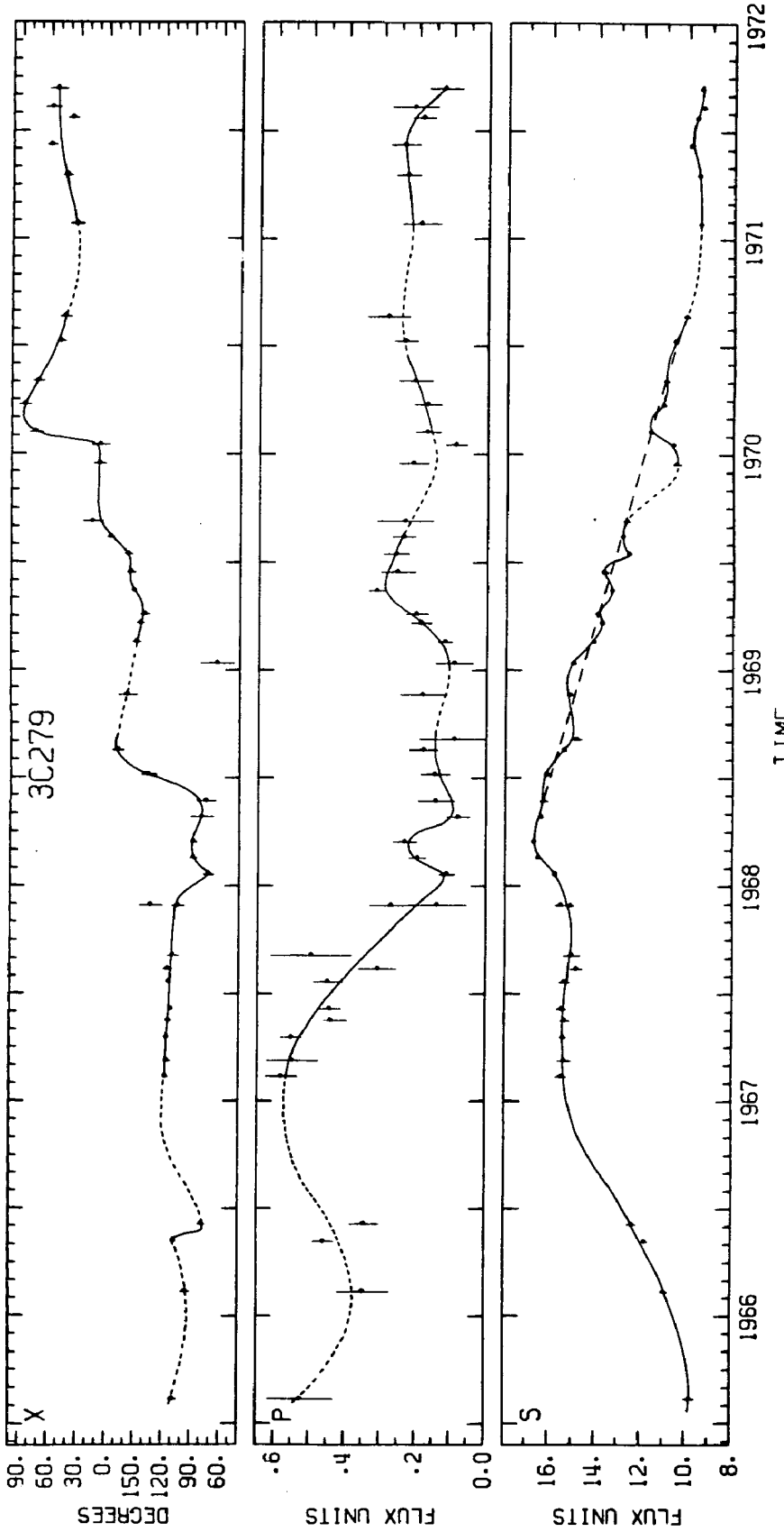


Figure 4.1: The polarization position angle, polarized flux density, and total flux density of the variable component of 3C279 versus time. These quantities have been averaged over calendar-month intervals. The dashed line indicates the average rate of decline of the total flux density.

the variable component since 1968. Before early 1968, χ = 114 ± 2 degrees, which is almost exactly the value for the intrinsic position angle of the halo component χ_o = 116 ± 2 degrees (Aller, 1970b); since that time an overall change in χ of about 100 degrees has occurred, so that an average of all data since July 1970 yields a degree of polarization of 2.4 ± 0.4 per cent at χ = 43 ± 4 degrees for the variable component at 8 GHz; these standard errors include the uncertainty in the extrapolated halo component. The intrinsic position angle of the plane of polarization of the variable component was found to be 42 ± 4 degrees by using the Faraday rotation measure of RM = 13.88 rad m^{-2} derived for the halo component (Aller, 1970b).

This intrinsic polarization position angle is very close to ϕ, the position angle of the direction of the line of separation of the two source components (36 ± 1 degree for Knight, et al., 1971; 39 degrees for the model of Cohen, et al., 1971, which is supported by the observations of Broderick, et al., 1972). If, as believed, the observed emission is produced by synchrotron radiation in regions of low absorption depth, then the magnetic fields in the emitting regions have been predominantly oriented perpendicular to the direction of the line of separation of the two components during the past year. On the other hand, before 1969, the predominant orientation of the

magnetic fields was at a position angle of $\theta_B \approx 24$ degrees. This is nearly parallel to the direction separating the two components ($\phi \approx 39$ degrees) and also to the general direction of the magnetic field in the low-frequency halo component of the source (θ_B (halo) ≈ 26 degrees).

The fact that the plane of the polarization of a double radio source tends to be either perpendicular or parallel to the direction separating the components is well known (e.g., Gardner and Whiteoak, 1963; Morris and Berge, 1964; Gardner and Whiteoak, 1966; Gardner and Davies, 1966; Seielstad and Weiler, 1971). Also, a 90-degree change in the plane of polarization from perpendicular to parallel to the direction of the line of component separation was expected to occur as a consequence of evolution in the structure of the source (e.g., Gardner and Davies, 1964; Morris and Berge, 1964; Gardner and Whiteoak, 1966). In the model described by Gardner and Whiteoak, the magnetic field is initially a loop-shaped structure with most of the radio emission originating in the inner regions where the magnetic field lines have been elongated parallel to the line separating the components. As the source components separate, they encounter stationary ambient material which compresses their outer boundaries. The increase in the particle energy and magnetic field strength resulting from this compression at the boundary increases the intensity of the emission in

the outer regions of the components where the magnetic field lines are predominantly oriented perpendicular to the line separating the two components. Evidence for this type of compression can be seen in the intensity and polarization maps of some extended double sources (e.g., Gardner and Davies, 1964; Gardner and Whiteoak, 1966; Moffet, 1966) although it is not present in all such sources (Seielstad and Weiler, 1971).

3C279 appears to have exhibited the expected variation in the source polarization which is indicative of a change in the structure of the magnetic fields within the emitting regions of the separating source components. The fact that such a change in the field structure is observed indicates that the expanding source components are encountering material in their path. In addition, it is evident from Figure 4.1 that χ does not change smoothly with time but rather in several sudden steps such as would occur if the intergalactic material were unevenly distributed in space rather than distributed as a smooth uniform medium. Since optical spectra indicate that large HII regions are associated with quasi-stellar sources, it is especially tempting to identify such regions with the material encountered by the expanding source components.

Sudden compressions of the magnetic field in the emitting region would be expected to increase the radiated flux, and it is interesting to note for example that the

sudden change in χ near 1970.0 was coincident with a sudden increase in total flux density. A series of collisions with ambient material during expansion of the double source components could produce the observed small fluctuations in the total flux density curve. Presumably in the absence of ambient gas, the total flux density would have declined more rapidly. The effect of the ambient medium is to lengthen the decay time of the outburst because of the reduced rates at which the magnetic field strength and the average particle energy decrease by adiabatic expansion. It thus appears that the deviations of the flux density variations of sources from the behavior expected from the simple expanding source model arise not only from the multiple injection of relativistic particles but also from the effects of an ambient medium surrounding the central source region.

Dent (1972) has recently proposed a model to account for the reported apparent suprarelativistic expansion. Noting that the total flux density had decreased by ~ 0.4 flux unit during the period of time between the two interferometric measurements, he argued that an apparent expansion can result if the decline in total flux density is the result of the fading of a third component. Thus he proposes a three-component model in which the source structure consists of an unresolved variable component situated midway between two static, non-varying components of equal

magnitude.

The character of the variation in the polarized emission found here is strong evidence that the interferometric observations are truly the result of the expansion of a double source and not just an illusion, as suggested by Cavaliere, et al. (1971) or the result of a third component as suggested by Dent (1972).

IV-2. 4C39.25

The spectrum of 4C39.25 contains two distinc components. The low-frequency component (hereinafter referred to as "A") is optically thin throughout the spectrum whereas the high-frequency component ("B") dominates the spectrum for $\lambda \leq 20$ cm and peaks near 4 cm (Kellermann and Pauliny-Toth, 1971). Interferometric studies indicate that the angular size of "B" is ≤ 0.0004 second of arc (Kellermann and Pauliny-Toth, 1971).

In order to demonstrate more clearly the long-term variation in the emission of this source, the data displayed in Figure 3.4 have been averaged over calendar-month intervals and the results are shown in Figure 4.2 The dashed lines indicate long-term trends of variations of total flux density and the Stokes parameter U, as well as the value of $\bar{Q} = 0.028 \pm 0.0009$ flux unit, A weighted least-squares analysis of the variations indicates that the linear change in the total flux density has an apparent

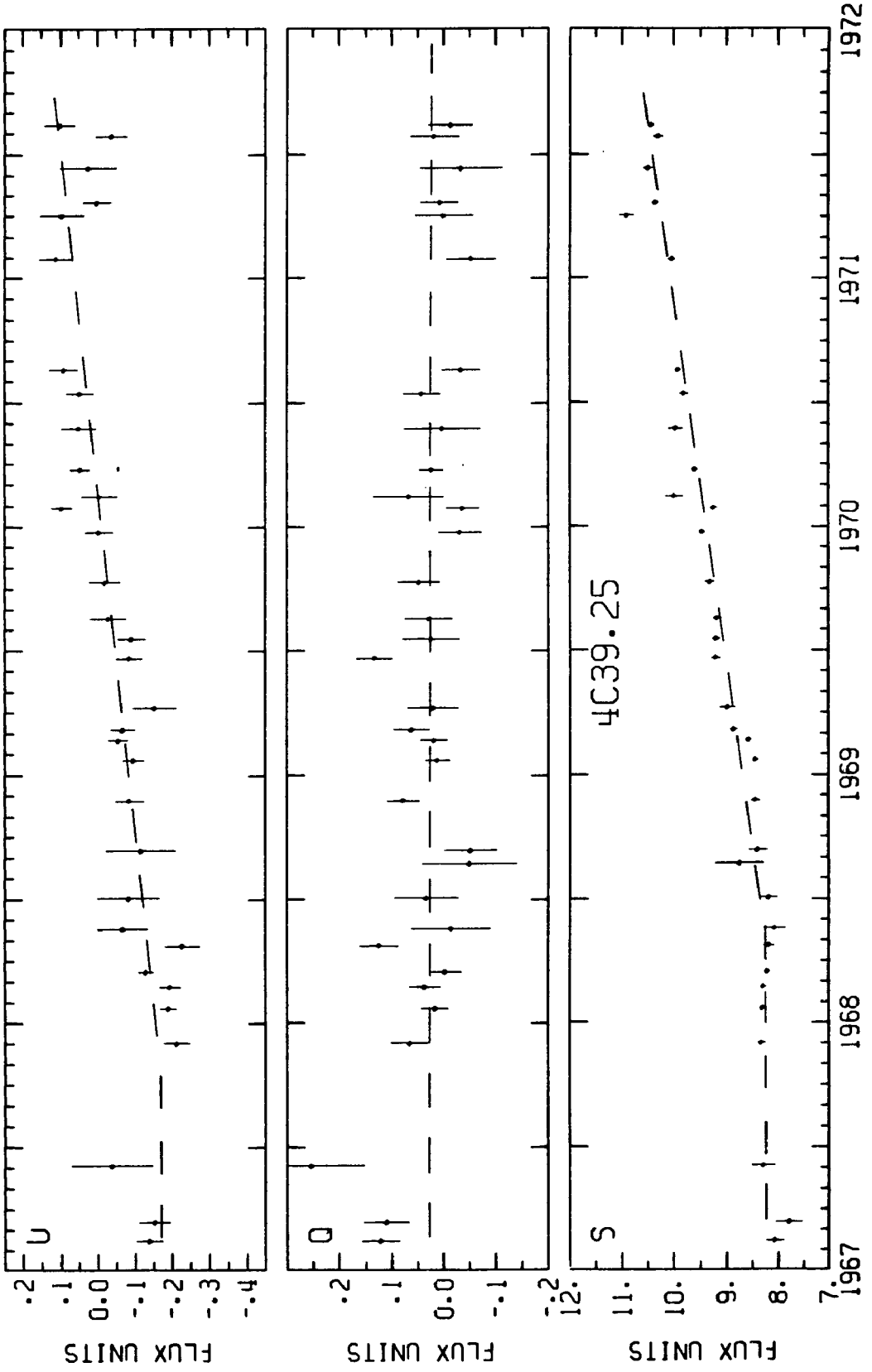


Figure 4.2: The Stokes parameters U and Q and the total flux density of 4C39.25 versus time. The data have been averaged over calendar-month intervals. The dashed lines are the same as those in Figure 3.4.

degree of polarization of 10 ± 1 per cent with χ = 39 ± 2 degrees.

A simple model assumes that the net polarization of component "B: is the same as that of the variable flux density (10 per cent). It is then possible to calculate the polarized emission of component "A". If S_i and P_i and χ_i are the total flux density, the fractional degree of polarization, and the polarization position angle, respectively, of component "i", the net polarization in terms of the Stokes paramters Q and U which will be observed is:

$$Q_{obs} = Q_A + Q_B = S_A P_A \cos(2\chi_A) + S_B P_B \cos(2\chi_B) \quad \text{f.u.}$$
$$U_{obs} = U_A + U_B = S_A P_A \sin(2\chi_A) + S_B P_B \sin(2\chi_B) \quad \text{f.u.} \qquad (1)$$

At 8 GHz, S_A = 2.3 flux units (Cohen, et al., 1971), so that these equations may be solved for P_A and χ_A throughout the period of observation. During the first six months of 1963,

$$\bar{S}_{obs} = 8.2 \text{ flux units},$$
$$\bar{U}_{obs} = -0.167 \text{ flux unit};$$

thus S_B = 5.9 flux units. Using $\bar{Q}_{obs}$ = 0.028, equations (1) above yield P_A = 0.33 and χ_A = 131 degrees. The observations taken throughout 1971 give

$$\bar{S}_{obs} = 10.4 \text{ flux units},$$
$$\bar{U}_{obs} = 0.047 \text{ flux unit}$$

thus, S_B = 8.1 flux units at that time. Equations (1)

yield P_A = 0.33 and χ_A = 130 degrees. The average degrees of polarization for component "A" is thus found to be $\bar{P} \approx$ 33 per cent at $\chi_A \approx$ 130 degrees.

This high degree of polarization is unlikely, and the almost exact cancellation of the two components would be extremely fortuitous. The largest net degree of polarization which has been measured in an unresolved source is only equal to the 10 per cent value observed here in the linearly increasing component of 4C39.25: e.g., 3C286 (Morris and Berge, 1964). Only in the case of local regions in some extended sources has a degree of polarization approaching 40 per cent been observed: e.g., Centaurus A (Gardner and Whiteoak, 1962).

A more reasonable picture is one in which the polarization of component "B" is changing with time as a result of changes in the structure of the magnetic field in the emitting regions as the component expands. The average polarized flux density in early 1968 before the variation began was 0.177 ± 0.014 flux unit at χ = 141 ± 3 degrees; since that time, it has steadily decreased to an average of 0.047 ± 0.019 flux unit at χ = 50 ± 12 degrees in 1971. It thus appears that the magnetic field was more regular in the region where the polarized emission arose in early 1968 as well as having a different average orientation.

Since the upper limit to the angular extent of component "B" corresponds to a physical diameter of less than

2 pc, it is quite possible that prior to early 1968 the polarized emission was produced in a volume of space dominated by the magnetic field of the central object. As the expansion progressed, compression would tend to scramble the magnetic field lines. In particular, if the expansion were along the magnetic axis of the object, the field lines would become tangled and then compressed in the direction of expansion. This would result in a field oriented tangent to the expanding surface and thus orthogonal to the previous field. The result would be a decrease by partial cancellation in the polarized flux density and rotation of position angle of polarization by 90 degrees, which was indeed observed here. If the contribution of component "A" could be removed from this data, an analysis similar to that of 3C279 could be performed. The present observations suggest that a variation very much like that observed in 3C279 has occurred. If the analogy holds, very-long-baseline interferometry at some future date may discern a compact double source separating along a line at position angle $\phi \approx 50$ degrees.

IV-3. 3C273

Variations in the total radio flux density of 3C273 have been observed in the wavelength range $3.3 \text{ mm} \leq \lambda \leq 22$ cm since Dent (1965a) announced his discovery that the source was a radio variable (e.g., Derossi, 1970;

Kellermann, 1971a). The observations at $\lambda < 3.75$ cm clearly show that the outburst which peaked in 1966 was much greater than the subsequent outbursts. Aller and Haddock (1967) announced the discovery of variable linear polarization, and subsequent changes in polarization have been reported at 5 GHz as well as 8 GHz (Gardner, Whiteoak, and Morris, 1969; Aller, 1970b).

Berge and Seielstad (1969) have pointed out that 3C273 exhibits "negative depolarization", meaning that the degree of polarization at low frequencies is greater than at high frequencies. This implies that the older, more evolved components have a higher degree of polarization.

Recent very-long-baseline interferometry has resulted in a fairly detailed picture of the structure of 3C273 (Kellermann, et al., 1971). Three distinct components have been detected in 3C273B (exclusive of 3C273A, the jet). The largest is a halo which is 0.022 second of arc in extent. The next smaller component is $\sim$0.002 second of arc in extent and its total flux density has been seen to decline at a frequency of 2300 MHz (Gubbay, Legg, Moffet, Ekers, and Seidel, 1969). This component has been identified with the 1966 outburst. The third component is an unequal double point source separated by 0.00155 second of arc along a line whose position angle is $\phi \approx 60$ degrees (Cohen, Cannon, Purcell, Shaffer, Broderick, Kellermann, and Jauncey, 1971). This last component is

apparently separating at suprarelativistic velocities (Cohen, et al., 1971) and spectral data indicates it is still opaque at 8 GHz (MacLeod, private communication). It is notable that the line of separation of the small double is nearly parallel to that of the optical jet (223 degrees), differing by only 17 degrees.

In order to make the long-term variations more clear, the data appearing in Figure 3.5 have been averaged over calendar-months and is presented in Figure 4.3. It is apparent that the position angle has been remarkably constant, deviating from its average value of 147.3 ± 0.4 degrees by less than 10 degrees throughout the period except during June-July 1966. Note too that the average value of the polarization position angle χ is almost exactly perpendicular to ϕ, the position angle of the line of separation of the small double source.

Measurements of the polarization position angle at various times in the wavelength interval 1.5 cm $\leq\lambda\leq$74.3 cm have shown that it is remarkably stable at a value $\chi \sim 155$ degrees, and no measurable Faraday rotation is evident (e.g., Morris and Berge, 1964; Gardner and Davies, 1966; McCullough and Waak, 1969). The observations reported here show that χ has not changed even though large variations in the total flux density have occurred. These results suggest that the magnetic field of 3C273 is regular and is ordered along a line parallel to the line

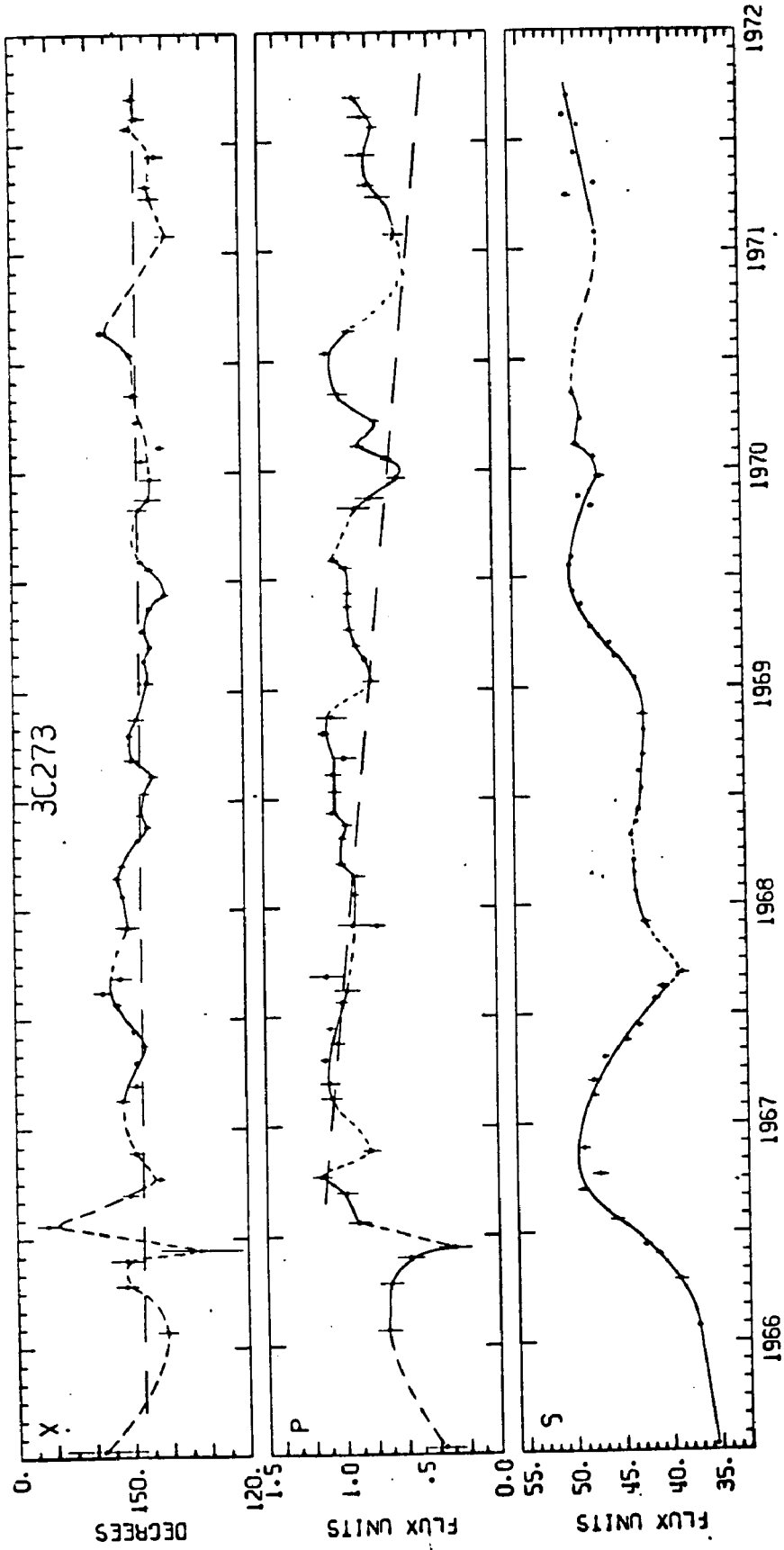


Figure 4.3: The polarization position angle, polarized flux density, and total flux density of 3C273 versus time. The data have been averaged over calendar-month intervals. The horizontal dashed line represents the weighted average value of the polarization position angle. The sloped dashed line represents the postulated long-term decline of the background polarized emission.

of separation of the small double source at $\phi \approx 60$ degrees. Further, the majority of the polarized emission at 8 GHz is apparently produced in a region of low absorption depth, for even though the optical depth of the variable component has changed with time, the polarization position angle observed at 8 GHz has remained stable and nearly parallel to that of the halo component observed at much longer wavelengths.

The polarized flux density increased rapidly during the 1966 outburst but did not resume its former value after the total flux density had subsided. Instead, it appears to have undergone the slow decline indicated by the dashed line, which was interrupted by the succeeding outbursts. The decline could be due to the loss of energy of the radiating electrons as a result of their synchrotron emission. It is well known that the rate of loss of energy of an electron due to synchrotron emission is

$$\frac{dE}{dt} = -3.8 \cdot 10^{-15} B^2 E^2 \sin^2 \psi \ , \quad \text{eV/sec.} \qquad (2)$$

and that most of the energy is radiated around the critical frequency

$$\nu_c = 1.6 \cdot 10^{-5} E^2 B \sin \psi \ , \quad \text{Hz} \qquad (3)$$

where E is the electron energy in electron volts, B is the magnetic field in gauss, and ψ is the pitch angle of the electron velocity with respect to the magnetic field (e.g., Westfold, 1959).

Equation (2) may be integrated to arrive at an expression for the electron energy as a function of time assuming the only mechanism for energy loss is synchrotron radiation:

$$E(t) = \frac{E_o}{1 + 3.8 \cdot 10^{-15} B^2 E_o \sin^2 \psi \, t} \quad (4)$$

Thus, the time required for the electron to radiate away one-half of its energy is:

$$T_{\frac{1}{2}} = \frac{10^{15}}{3.8 B^2 E \sin \psi} \text{ sec.}$$

$$= \frac{8.3 \cdot 10^6}{B^2 E \sin \psi} \text{ yr.} \quad (5)$$

Setting sin ψ equal to unity and assuming a magnetic field strength of 10^{-4} gauss, the energy of the electrons which contribute the majority of the emission at 8 GHz is $E = 2.7 \cdot 10^9$ eV. Equation (5) indicates that it would take $\sim 10^5$ years for the radiation intensity to decrease to $\frac{1}{2}$ of its initial value, assuming synchrotron losses alone. On the contrary, the apparent decline required only 5 years for the polarized emission to decrease by $\frac{1}{2}$ its peak value.

Another possible explanation of the variation in the polarized flux density employs the fact that it is a vector. If a portion of the radio source whose

polarization position angle is perpendicular to that which has been observed begins to brighten, a growing cancellation of the two polarization components will result, and the polarized flux density will be seen to decrease. This new component cannot arise in the variable source which is responsible for the increase in the total flux density because these increases are correlated with increases in the polarized flux density. This component must therefore be at some distance from the energetic core which is the source of relativistic electrons. A likely possibility is a remnant of a previous outburst. Such a remnant would very likely contain in its leading edge a volume in which the magnetic field was perpendicular to its direction of motion due to compression. Thus as the relativistic electrons responsible for the polarized emission migrated outward along the magnetic field lines, they would encounter this region. The result of more and more electrons being dumped into this volume would be a steady decrease in the net polarized flux density due to cancellation of the two polarization vectors.

Hence a relatively simple model of 3C273 can qualitatively account for the variations in the total flux density and polarized emission. It involves an energetic core embedded in a volume of space which contains a magnetic field whose gross structure is oriented at position angle $\theta_B \approx 57$ degrees. This is almost exactly

parallel to the line of expansion of the suprarelativistic double source ($\phi \approx 60$ degrees).and within 15 degrees of the line defining the optical jet. Most of the polarized emission arises in a region of low optical depth so that the observed polarization position angle is $\chi = 147$ degrees. This region was heavily populated by relativistic electrons which originated in the strong outburst of 1966; it has continued to radiate a significant amount of polarized emission long after that event ceased to be discernible in the total flux density curve. As the electrons migrated outward, they encountered remnants of one or more previous outbursts which had compressed the field, giving rise to domains whose gross structures are oriented at a position angle $\theta_B \approx 150$ degrees. The net polarized emission commenced decreasing as these domains began radiating due to the influx of particles. Meanwhile, the energetic core released several more clouds of particles into the undistorted field, keeping polarized emission enhanced.

IV-4. BL Lacertae

The unusual radio source VRO 42.22.01 has been identified with the optical variable BL Lacertae (MacLeod and Andrew, 1968; Schmitt, 1968). Optically, variations of the order of 1^m have been detected in a twenty-four hour period (DuPuy, Schmitt, McClure, van den Bergh, and

Racine, 1969; Bertaud, Dumortier, Veron, Wlerick, Adam, Bigay, Garnier, and Duruy, 1969; Tritton and Brett, 1970). The spectrum between 0.32 and 2.2 microns suggests that the optical radiation may be a continuation of the radio synchrotron emission (Oke, Neugebauer, and Becklin, 1969), a theory which is supported by the detection of strong, variable optical polarization (Visvanathan, 1969). No spectral lines have been found though a number of spectra have been taken, some near minimum brightness (DuPuy, et al., 1969); consequently, no redshift is available.

Very-long-baseline interferometry has shown that the radio source consists of a compact component which is not circularly symmetric (Cohen, et al., 1971; Broderick, Kellermann, Shaffer, and Jauncey, 1972). The simplest model which fits the data at 8 GHz is an equal point double whose position angle is 174 degrees (Cohen, et al., 1971).

The flux density and linear polarization of BL Lac have been monitored for three years at λ2.8 cm, λ3.75 cm, and λ4.5 cm.[1] The observations at λ2.8 and λ4.5 cm were carried out with the 46-m telescope of the Algonquin Radio Observatory, while the λ3.75 cm observations were made with the 26-m telescope of the University of

---

[1]This analysis of the observed variations in the radio emission of BL Lacertae has been published (MacLeod, Andrew, Medd, and Olsen, 1971).

Michigan. During this period, nine radio outbursts have occurred. The variations in the total flux density agree qualitatively with what is expected from the simple expanding source model (Shklovsky, 1965; Pauliny-Toth and Kellermann, 1966; van der Laan, 1966). Each outburst appeared first at the shortest wavelength and later at the longer wavelengths, and the shorter the wavelength, the greater was the maximum flux density of the outburst. A cross-correlation analysis indicates that the outbursts at $\lambda 2.8$ cm lead those at $\lambda 3.75$ cm by about 4 days (correlation coefficient 0.86) while the outbursts at $\lambda 4.5$ cm lag behind those at $\lambda 2.8$ cm by about 8 days (correlation coefficient 0.86).

The variations in the polarized emission exhibited no correspondence with those in the total flux density. The large-scale variations in the polarized flux density had time scales equal to or greater than those of the variations in the total flux density, but fluctuations in the polarization position angle had time scales of much shorter duration.

The variations of the polarization position angle do lend some support to the expanding source model. For example, when the source is optically thick at all wavelengths, the observed polarization is primarily determined by the orientation and regularity of the magnetic field on the near side of the cloud. As the source becomes

optically thin at $\lambda 2.8$ cm, but is still opaque at other wavelengths, the contribution to the polarization observed at $\lambda 2.8$ cm by emitting regions throughout the volume of the source will become important. Since the orientation of the magnetic field will in general vary throughout the source, the polarization may change quite rapidly during the short time when $\tau_\lambda \sim 1$ (Aller, 1970a). As the source subsequently becomes optically thin at $\lambda 3.75$ and then $\lambda 4.5$ cm, similar changes will occur in the polarization at these wavelengths, but at correspondingly later times. One would then expect the variations of the position angles at the three wavelengths to be basically similar, with the major differences occurring at times when the absorption depth is unity. A study was made of the differences between the polarization position angles observed at $\lambda 2.8$ cm and $\lambda 4.5$ cm as a function of time to see if such differences did indeed occur at the times of maximum flux density. On four occasions, this difference in polarization position angles changed by some 20 degrees from its mean value, and then returned to near the mean value each time. Each occurrence was during a maximum in the total flux density.

Assuming that the expanding source model is applicable to BL Lac, an attempt was made to determine whether the electron energy distribution was the same for each outburst. The model produces more relations between

parameters than there are parameters. Hence one can calculate the index of the electron energy distribution γ, defined by equation (1) in Chapter I in a number of independent ways. The value of γ was calcu- for each of the first eight outbursts in three different ways (e.g., van der Laan, 1966):

(i) from the relative rates of increase and decrease of the flux density during the outburst,

$$S(t) \sim (t-t_o)^{3\beta}, \text{ source optically thick,}$$
$$S(t) \sim (t-t_o)^{-2\beta\gamma}, \text{ source optically thin,} \quad (6)$$

where t_o is the time of the initiation of the outburst and β is the acceleration parameter;

(ii) from the flux density at each wavelength when the source is optically thin,

$$S \sim \lambda^{(\gamma - 1)/2} ; \quad (7)$$

(iii) from the ratios of the maximum flux densities reached by the outburst at the different wavelengths,

$$S_{max} \sim \lambda_{max}^{-(7\gamma + 3)/(4\gamma + 6)} . \quad (8)$$

The latter two methods are critically dependent on the choice of a base level (which was assumed to be 6.1 flux units at all three wavelengths). Although the values of γ obtained by the different methods were not in good agreement with each other, it was clear that γ varied

from burst to burst. For the fourth, sixth and eighth outbursts, values of γ lie in the range $1.0 < \gamma < 2.0$, whereas for the first, third, fifth, and seventh outbursts, γ is always greater than 2.0 and is sometimes greater than 4.0. These variations in γ imply that conditions differed during the generation of the relativistic electrons corresponding to the various outbursts, or that this analysis is too simplified to account for the variations quantitatively.

A last point may be made concerning the variations in the total flux density of BL Lac. A study of the form of the curve in Figure 3.9 impresses one with the basic similarity in shape and duration of the group of outbursts observed between June 1968 and April 1969 to the group of outbursts observed between August 1969 and July 1970. Although these two groups are not exactly similar, they do both show a steady decrease in the separation between the maxima, accompanied by a steady rise in the minima between. After the fourth and eighth outbursts, a deep minima occurs followed in each case by a small shoulder on the rising portion of the next outburst. It would appear that the outbursts may occur in groups of four, but it must be noted that the ninth outburst (which was not observed at $\lambda 3.75$ cm, but was extensively observed at $\lambda 2.8$ cm and $\lambda 4.5$ cm) does not fit this pattern.

IV-5. 3C120

Analyses of the total flux density variations occurring during the three outbursts in the period from 1966 to 1969 show a good agreement with the simple expanding source model (e.g., Pauliny-Toth and Kellermann, 1968; Derossi, 1970). The fact that δ does not change significantly from its value of ~ 1.0 for at least one year following the appearance of each outburst at $\lambda 2$cm indicates that energy losses are not due to radiation. The period of time between the maxima in the outbursts does not change with the wavelength of observation, so that each event is an independent outburst rather than the result of several expanding sources flying apart from a common initial generation, as proposed by Ozernoy and Sazonov (1969).

Very-long-baseline interferometry indicates that there is a core component ≥ 0.001 second of arc (Kellermann, et al., 1971) which may either be a circular ring or an equal point double separated by 0.00098 second of arc at a position angle $\phi = 95$ degrees (Cohen, et al., 1971). Current data suggest that 3C120 is expanding at suprarelativistic velocity (Kellermann, 1971b).

The 8 GHz data presented in Figure 3.3 has been averaged by calendar months in Figure 4.4 in order to more clearly display the long-term variations in the Stokes parameters. It is readily apparent that Q has remained

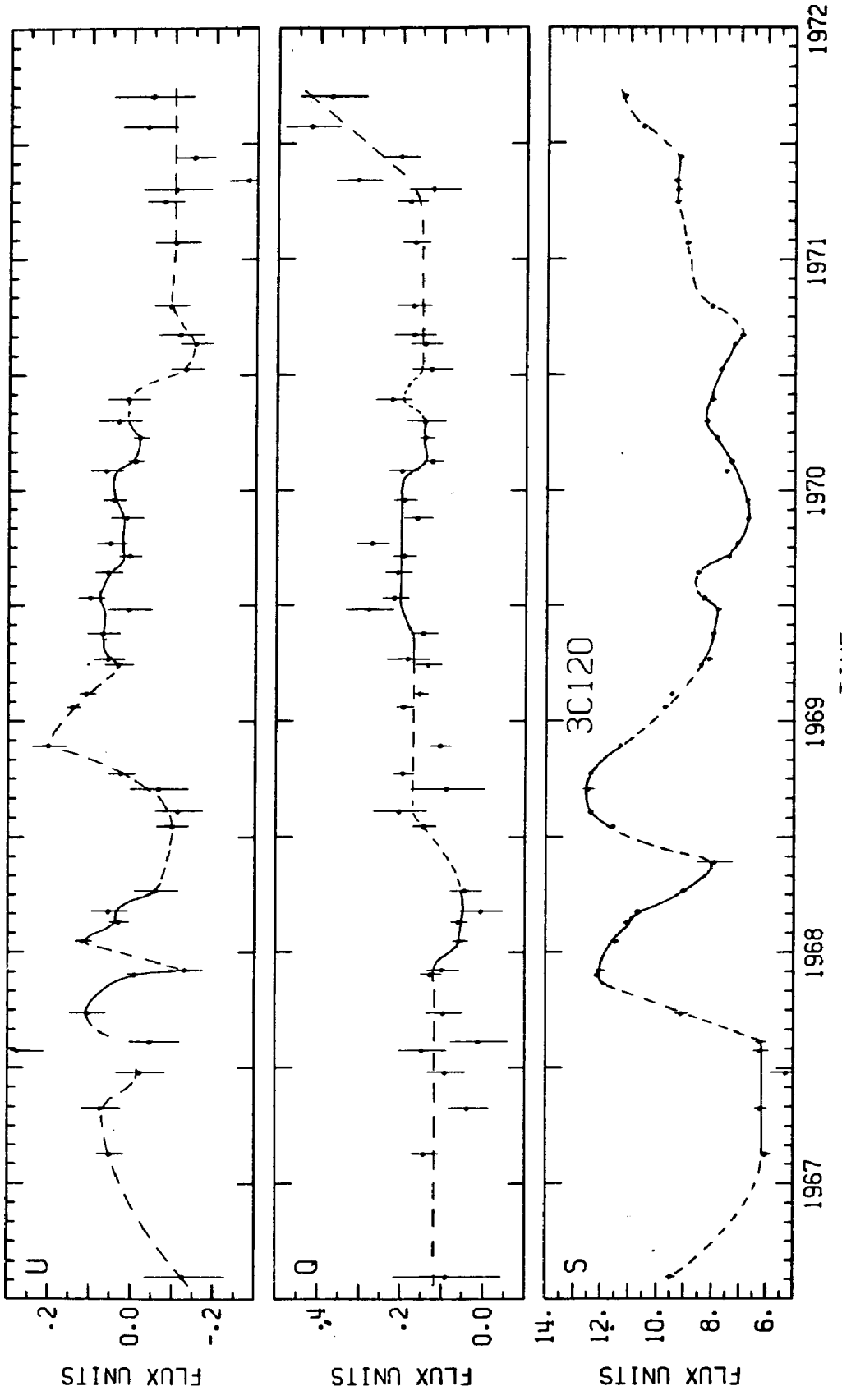


Figure 4.4: The Stokes parameters U and Q and the total flux density of 3C120 versus time. The data have been averaged over calendar-month intervals.

nearly constant until May 1971 when it increased sharply. The variations in the polarized emission have taken place for the most part in the Stokes parameter U . It is especially tempting to interpret the variations in the polarized emission in terms of the expanding double source as was done for 3C279. The Stokes parameter Q is the difference between the intensities observed perpendicular (within 5 degrees) to the line of separation and parallel to it, whereas the Stokes parameter U is the difference between the intensities observed at very nearly ± 45 degrees to the line of separation. If the magnetic lines of force are stretched between the two separating components and the region has low absorption depth as is the case with 3C279, we expect the plane of the polarized emission to be oriented perpendicular to the line of separation. This would result in a positive Q and a vanishingly small U .

There are at present only three observations of the polarization of 3C120 at frequencies low enough to be of use in determining the rotation measure and intrinsic position angle of the halo emission, and two of these are too near to each other in wavelength to resolve the inherent ambiguity in determining these quantities. At λ49.1 cm, the polarization position angle is 127 ± 12 degrees (Kronberg and Conway, 1970); at λ21.2 cm, it is 9 ± 4 degrees (Gardner, Morris, and Whiteoak, 1969); and

at λ18.1 cm, it is 174 ± 5 degrees (Gardner, Morris, and Whiteoak, 1969). Assuming that the difference in position angle is due to the Faraday rotation effect and no multiples of 180 degrees rotation are present,

$$\chi_\lambda = \chi_o + RM \cdot \lambda^2 , \qquad (10)$$

where χ_o is the intrinsic position angle, RM is the rotation measure, and χ_λ is the polarization position angle observed at wavelength λ.

The data are consistent with two different solutions to equation (10) :

$$RM = 10.8 \text{ rad m}^{-2} , \chi_o = 157 \text{ degrees}$$

and,

$$RM = -4.6 \text{ rad m}^{-2} , \chi_o = 12 \text{ degrees.}$$

Each of these solutions is consistant with that expected to result by interstellar electrons at the galactic coordinates of 3C120 ($|RM|<20$ rad m^{-2} , $\ell^{II} = 190^\circ$, $b^{II} = -27^\circ$). These values of the intrinsic position angle χ_o imply that the averaged magnetic field is oriented at a position angle of $\theta_B \approx$ 67 degrees or 102 degrees, respectively. Thus the compact double source is separating along a line which is at an angle of 28 degrees or 7 degrees to the averaged magnetic field.

Thus a possible model is that of a double source with magnetic lines of force stretched between components which are expanding outward into an ambient magnetic field.

The gross structure of this field is oriented at an angle $\lesssim$28 degrees with respect to the line of separation. The relatively steady polarized emission whose plane of polarization is $\sim$0 degree would arise in the region between the expanding components, as in 3C279; the fluctuating polarized emission is thought to arise in the leading edges of the expanding components. The sharp increase in Q in mid-1971 also fits this picture. The magnetic field in the volume between the expanding components has been stretched and become comparatively ordered, so that the next outburst which injected energetic particles into this region would greatly enhance the polarized emission oriented at $\sim$0 degree.

CHAPTER V

CONCLUSIONS

V-1. Summary of Results

Significant variations have been detected in the total flux density and linearly polarized emission of 4C39.25 and BL Lac, and continued polarizations variations have been observed in 3C120, 3C273, 3C279, 3C345, and 3C454.3. The time scale for these variations has ranged from less than one week in the case of BL Lac to more than four years for 4C39.25.

Comparison of the polarization observations with the results of very-long-baseline interferometry reveals that the variable polarization is intimately connected with the small-scale structure observed in compact objects. Table 6 compares the polarization position angle, χ , with the position angle of the line of separation of the compact double source, ϕ , and with the intrinsic position angle, χ_o , determined from low-frequency observations. Average values of χ are given, except for 3C279 and 4C39.25. These two sources have exhibited progressive changes in this quantity, and so the range of variation is indicated.

TABLE 6

Comparison of the Polarization Position Angle, Position Angle of the Line of Separation of the Compact Double Source, and Intrinsic Position Angle

Source	χ	ϕ	χ_o
3C120	5°	95°	--
4C39.25	141° —>50°	---	--
3C273	147°	60°	--
3C279(var. comp.)	116° —>43°	39°	116°
3C345	32°	103°	46°
BL Lacertae	61° *	174°	--
3C454.3	178°	---	13°

*This quantity has varied over 130°.

It is readily apparent that χ has been almost exactly orthogonal to ϕ in the case of 3C120 and 3C273. On the other hand, the polarization position angle of the variable component of 3C279 was equal at first to χ_o but then changed until it became equal to ϕ. Although the overall average χ of 3C345 is different from ϕ by nearly 70 degrees, there was a period of time (July 1969 through September 1970) during which χ was exceptionally stable at an average value of $\sim$ 20 degrees, which is very nearly orthogonal to ϕ. Thus, all sources for which χ and ϕ are known except for the exceptionally rapid variable BL Lac have exhibited the property that χ and ϕ are orthogonal. In the case of the variable component of 3C279, χ has changed from perpendicular to parallel to ϕ.

The simplest interpretation which is consistent with the observations is that the polarized emission associated with the variable components is generated in a region of low optical depth whose magnetic field is predominantly oriented parallel to the line of separation of the compact double source. The sources 3C279 and 4C39.25 have apparently exhibited a change in their magnetic field structure so that the polarization position angle has changed by 90 degrees. The model constructed for 3C279 involves the compression of the magnetic field along the leading surfaces of the two components which are separating

at relativistic speeds. This compression results in regions of enhanced emission wherein the magnetic fields are oriented perpendicular to the line of separation. If the same model can be applied to 4C39.25, very-long-baseline interferometry should in time reveal a double source whose line of separation is oriented at $\phi \approx 50$ degrees. 3C273 is an example of a source whose magnetic field must be regular and which must have controlled the direction in which the energetic particles have been expelled since the time of the formation of the optical jet.

V-2. Suggestions for Future Study.

Additional low-frequency polarization observations, particularly in the frequency interval 100 - 1000 MHz, are necessary in order to isolate the polarization of the variable components. It is important that these observations be as precise as possible, since the low-frequency polarization spectrum must be extrapolated to the centimeter wavelengths.

Simultaneous observations of the variable polarization in the frequency interval 3 - 10 GHz will give valuable data relevant to the source evolution. Regardless of opacity of the variable component, and the measure of the Faraday rotation produced by the thermal plasma within and/or surrounding the variable component. In

combination with the results of very-long-baseline interferometry and circular polarization data, these observations will be important in determining the density of the thermal plasma as well as the strength and structure of the magnetic fields in the sources.

A very important observational program to be undertaken is polarization measurements using very-long-baseline interferometers. Such a study can directly detect the changes in relative strengths of polarized emission in different regions of the variable components, and give further information concerning the dynamics of interaction of these components with the ambient material and magnetic fields. Further, small-scale structures in the magnetic fields should be detectable, so that such a study should, for example, be able to determine if polarized emission arises from the filaments of 3C84.

The observations proposed above will help to determine the magnetic field strength and initial energy distribution of the relativistic electrons responsible for the outbursts. Information will also become available as to the rates of change of particle energy and magnetic field strength and structure. By these means, it is hoped to better understand the source of energy for the outbursts and the means by which relativistic particles are generated.

APPENDIX I

EXPONENTIAL CORRECTION TO THE OBSERVED ANTENNA TEMPERATURE FOR A POINT SOURCE

AI-1. Observationally Determined Quantities

Prior to a series of off-on measurements, the apparent position of a radio source is determined by making scans in both right ascension and declination. A parabola is fit by means of least-squares analysis to each scan and the position of maximum response and its error are calculated ($\alpha_o \pm \sigma_{\alpha_o}$, $\delta_o \pm \sigma_{\delta_o}$). In the data analysis described below, this position is continuously corrected for changes in the position readout error with hour angle, as determined by M.J. Klein (private communication).

During each on-source measurement, the average position at which the antenna is pointing is calculated (α_{on}, δ_{on}). The differences between these positions and the position of the radio source

$$D_\alpha = \alpha_{on} - \alpha_o$$
$$D_\delta = \delta_{on} - \delta_o \qquad (1)$$

are averaged and their standard deviations determined

$$\begin{aligned} \bar{D}_\alpha &= \frac{1}{N} \Sigma \, (\alpha_{on} - \alpha_o) \\ \bar{D}_\delta &= \frac{1}{N} \Sigma \, (\delta_{on} - \delta_o) \\ \sigma_{D\alpha} &= \left[\frac{1}{N-1} \Sigma (D_\alpha - \bar{D}_\alpha)^2 \right]^{\frac{1}{2}} \\ \sigma_{D\delta} &= \left[\frac{1}{N-1} \Sigma (D_\delta - \bar{D}_\delta)^2 \right]^{\frac{1}{2}} \end{aligned} \tag{2}$$

for use in the analysis below. N is the number of on-off measurements performed in the series.

AI-2. Probable Observed Response

Assume that the antenna is pointing at the position (α_1 , δ_1). The response of the main beam may be represented by a gaussian with peak at (α_1 , δ_1) and standard deviations $(\sigma_\alpha , \sigma_\delta)$. Let us also represent the apparent position of the radio source by a gaussian probability function with peak at (α_o , δ_o) and standard deviations $(\sigma_{\alpha_o} , \sigma_{\delta_o})$. The normalized probable response is the convolution of these two gaussians over the main beam:

$$P \, (D_\alpha, D_\delta) = \frac{1}{(2\pi)^2 \sigma_\alpha \sigma_\delta \sigma_{\alpha_o} \sigma_{\delta_o}} \iint_{\text{main beam}} d\alpha \, d\delta \; e^{-(\alpha-\alpha_1)^2/2\sigma_\alpha^2} \tag{3}$$

$$e^{-(\alpha-\alpha_o)^2/2\sigma_{\alpha_o}^2} \; e^{-(\delta-\delta_1)^2/2\sigma_\delta^2} \; e^{-(\delta-\delta_o)^2/2\sigma_{\delta_o}^2} .$$

Since the response of the main beam falls to zero at large distances from its axis, we may extend the limits of

integration to infinity without introducing error. Let us also make the transformation

$$\begin{aligned} \alpha' &= \alpha - \alpha_1 = \alpha - \alpha_{on} \\ \delta' &= \delta - \delta_1 = \delta - \delta_{on} \end{aligned} \tag{4}$$

so that the equation (3) becomes

$$P(D_\alpha, D_\delta) = \frac{1}{(2\pi)^2 \sigma_\alpha \sigma_\delta \sigma_{\alpha_o} \sigma_{\delta_o}} \int_{-\infty}^{\infty}\int_{-\infty}^{\infty} d\alpha' d\delta' \; e^{-\alpha'^2/2\sigma_\alpha^2} \; e^{-(\alpha'-D_\alpha)^2/2\sigma_{\alpha_o}^2} \; e^{-\delta'^2/2\sigma_\delta^2} \; e^{-(\delta'-D_\delta)^2/2\sigma_{\delta_o}^2} . \tag{5}$$

It is well known that the convolution of two gaussians is itself a gaussian. Using this result and separating the two integrations, we have:

$$\int_{-\infty}^{\infty} d\alpha' \; e^{-\alpha'^2/2\sigma_\alpha^2} \; e^{-(\alpha'-D_\alpha)^2/2\sigma_{\alpha_o}^2} = \frac{\sqrt{2\pi}\,\sigma_\alpha\,\sigma_{\alpha_o}}{(\sigma_\alpha^2+\sigma_{\alpha_o}^2)^{\frac{1}{2}}} \; e^{-D_\alpha^2/2(\sigma_\alpha^2+\sigma_{\alpha_o}^2)} . \tag{6}$$

Performing the same calculation for the integration δ' and combining the two results, we have:

$$P(D_\alpha, D_\delta) = [2\pi(\sigma_\alpha^2+\sigma_{\alpha_o}^2)]^{-\frac{1}{2}} \; [2\pi(\sigma_\delta^2+\sigma_{\delta_o}^2)]^{-\frac{1}{2}} \; e^{-D_\alpha^2/2(\sigma_\alpha^2+\sigma_{\alpha_o}^2)} \; e^{-D_\delta^2/2(\sigma_\delta^2+\sigma_{\delta_o}^2)} . \tag{7}$$

Now, if we assume that the differences (D_α, D_δ) are normally distributed about their averages, we may

represent their distribution function by a gaussian centered upon $(\bar{D}_\alpha, \bar{D}_\delta)$ with standard deviations $(\sigma_{D\alpha}, \sigma_{D\delta})$. The most probable observed response of the antenna to the source is then just the convolution of $P (D_\alpha, D_\delta)$ with the distribution functions

$$P (\bar{D}_\alpha, \bar{D}_\delta) = \frac{1}{2\pi\sigma_{D\alpha}\sigma_{D\delta}} \int_{-\infty}^{\infty}\int_{-\infty}^{\infty} P(D_\alpha, D_\delta)\, e^{-(D_\alpha-\bar{D}_\alpha)^2/2\sigma_{D_\alpha}^2} e^{-(D_\delta-\bar{D}_\delta)^2/2\sigma_{D_\delta}^2}\, dD_\alpha\, dD_\delta \quad . \tag{8}$$

Once again, the two integrations may be separated and carried out in the same manner as before. The result is:

$$P (\bar{D}_\alpha, \bar{D}_\delta) = [2\pi(\sigma_\alpha^2+\sigma_{\alpha_o}^2+\sigma_{D_\alpha}^2)]^{-\frac{1}{2}}[2\pi(\sigma_\delta^2+\sigma_{\delta_o}^2+\sigma_{D_\delta}^2)]^{-\frac{1}{2}} e^{-\bar{D}_\alpha^2/2(\sigma_\alpha^2+\sigma_{\alpha_o}^2+\sigma_{D_\alpha}^2)} e^{-\bar{D}_\delta^2/2(\sigma_\delta^2+\sigma_{\delta_o}^2+\sigma_{D_\delta}^2)} \quad . \tag{9}$$

AI-3. The Exponential Correction Factor

Suppose that the apparent position of the radio source were known exactly. The probability distribution function for the source position would then be the delta function and equation (5) because

$$P\underset{\text{no error}}{(D_\alpha, D_\delta)} = \frac{1}{2\pi\sigma_\alpha\sigma_\delta}\int_{-\infty}^{\infty}\int_{-\infty}^{\infty} d\alpha' d\delta' \; e^{-\alpha'^2/2\sigma_\alpha^2} \; e^{-\delta'^2/2\sigma_\delta^2} \; \delta(\alpha'-D_\alpha)\,\delta(\delta'-D_\delta) \tag{10}$$

$$= \frac{1}{2\pi\sigma_\alpha\sigma_\delta} \; e^{-D_\alpha^2/2\sigma_\alpha^2} \; e^{-D_\delta^2/2\sigma_\delta^2} .$$

Let us suppose also that no errors were made in pointing the telescope, so that

$$\begin{aligned} \overline{D}_\alpha &= \overline{D}_\delta = 0 \\ \sigma_{D\alpha} &= \sigma_{D_\delta} = 0 \; . \end{aligned} \tag{11}$$

Equation (8) becomes:

$$P\underset{\text{no error}}{(\overline{D}_\alpha, \overline{D}_\delta)} = \int_{-\infty}^{\infty}\int_{-\infty}^{\infty} dD_\alpha dD_\delta \; \underset{\text{no error}}{P(D_\alpha, D_\delta)} \; \delta(D_\alpha) \; \delta(D_\delta)$$

$$= [2\pi\sigma_\alpha\sigma_\delta]^{-1} \tag{12}$$

The exponential correction factor which must be applied to the observed antenna temperature of a source is thus:

$$C_{EXP} = \underset{\text{no error}}{P(\overline{D}_\alpha, \overline{D}_\delta)} \; / \; P(\overline{D}_\alpha, \overline{D}_\delta)$$

$$= \left[1+\frac{\sigma_{\alpha_o}^2+\sigma_{D_\alpha}^2}{\sigma_\alpha^2}\right]^{\frac{1}{2}} \left[1+\frac{\sigma_{\delta_o}^2+\sigma_{D_\delta}^2}{\sigma_\delta^2}\right]^{\frac{1}{2}} \tag{13}$$

$$e^{+\overline{D}_\alpha^2/2(\sigma_\alpha^2+\sigma_{\alpha_o}^2+\sigma_{D_\alpha}^2)} \cdot e^{+\overline{D}_\delta^2/2(\sigma_\delta^2+\sigma_{\delta_o}^2+\sigma_{D_\delta}^2)}$$

SELECTED BIBLIOGRAPHY

ALLER, H.D. 1968, Ph.D. Thesis, University of Michigan, Ann Arbor, Michigan.

_____. 1970a, Nature, 225, 440.

_____. 1970b, Ap.J., 161, 1.

_____. 1970c, Ap.J., 161, 19.

_____, and HADDOCK, F.T. 1967, Ap.J., 147, 833.

_____, and OLSEN, E.T. 1971, A.J., 76, 671.

ANDREW, B.H., HARVEY, G.A., and MEDD, W.J. 1971, Astrophysical Letters, 9, 151.

_____, MacLEOD, J.M., LOCKE, J.L., MEDD, W.J., and PURTON, C.R. 1969, Nature, 223, 598.

ANGIONE, R.J. 1971, A.J., 76, 25.

APPENZELLER, I. 1968, Ap.J., 151, 769.

_____, and HILTNER, W.A. 1967, Ap.J. (Letters), 149, L17.

BASH, F.N. 1968, Ap.J., 152, 375.

BERGE, G.L., and SEIELSTAD, G.A. 1969, Ap.J., 157, 35.

BERTAUD, Ch., DUMORTIER, B., VERON, P., WLERICK, G., ADAM, G., BIGAY, J., GARNIER, R., and DURUY, M. 1969, Astron. and Astrophys., 3, 436.

BIRAUD, F. 1969, Astron. and Astrophys., 1, 156.

_____, and VERON, P. 1968, Nature, 219, 254.

BOLAND, J.W., HOLLINGER, J.P., MAYER, C.H., and McCULLOUGH, T.P. 1966, Ap.J., 144, 437.

BOLOGNA, J.M., McCLAIN, E.F., ROSE, W.K., and SLOANAKER, R.M. 1965, Ap.J., 142, 106.

BOWYER, C.S., LAMPTON, M., MACK, J., and de MENDONCA, F. 1970, Ap.J. (Letters), 161, L1.

BRANDIE, G. 1971, U.M.R.A.O. Instrumentation Memo No. 5.

BRODERICK, J.J., KELLERMANN, K.I., SHAFFER, D.B., and JAUNCEY, D.L. 1972, Ap.J., 172, 299.

_____, VITKEVICH, V.V., JAUNCEY, D.L., EFANOV, V.A., KELLERMANN, K.I., CLARK, B.G., KOGAN, L.R., KOSTENKO, V.I., COHEN, M.H., MATVEENKO, L.I., MOISEEV, I.G., PAYNE, J., and HANSSON, B. 1970, Astron. Zh., 47, 784.

BURBIDGE, E.M. 1967, Ann. Rev. Astron. and Astrophys., 5, 399.

_____, and BURBIDGE, G.R. 1967. Quasi-Stellar Objects. San Francisco: Freeman and Co.

BURBIDGE, G.R. 1970, Ann. Rev. Astron. and Astrophys., 8, 369, 1970.

_____, and STEIN, W. 1970, Ap.J., 160, 573.

CANNON, R.D., PENSTON, M.V., and BRETT, R.A. 1971, M.N.R.A.S., 152, 79.

CAVALIERE, A., MORRISON, P., and SARTORI, L. 1971, Science, 173, 525.

CHANDRASEKHAR, S. 1950. Radiative Transfer. London: Oxford University Press.

CLARK, B.G., KELLERMANN, K.I., BARE, C.C., COHEN, M.H., and JAUNCEY, D.L. 1968, Ap.J., 153, 795.

COHEN, M.H., CANNON, W., PURCELL, G.H., SHAFFER, D.B., BRODERICK, J.J., KELLERMANN, K.I., and JAUNCEY, D.L. 1971, Ap.J., 170, 207.

CONWAY, R.G., GILBERT, J.A., RAIMOND, E., and WEILER, K.W. 1971, M.N.R.A.S., 152, 1P.

DENT, W.A. 1965a, Science, 148, 1458.

_____. 1965b, Ph.D. Thesis, University of Michigan, Ann Arbor, Michigan.

_____. 1966, Ap.J., 144, 843.

_____. 1967 (Private Communication).

_____. 1968, Ap.J. (Letters), 153, L29.

_____. 1972, Science, 175, 1105.

DEROSSI, G. 1970, Ph.D. Thesis, Air Force Institute of Technology, Wright-Patterson Air Force Base, Ohio.

Du PUY, D., SCHMITT, J.L., MacCLURE, R., BERGH, S. van den, and RACINE, R. 1969, Ap.J. (Letters), 156, L135.

DYCK, H.M., KINMAN, T.D., LOCKWOOD, G.W., and LANDOLT, A.U. 1971, Nature Physical Sciences, 234, 71.

FOGARTY, W.G., EPSTEIN, E.E., MONTGOMERY, J.W., and DWORETSKY, M.M. 1971, A.J., 76, 537.

FOLSOM, G.H., SMITH, A.G., and HACKNEY, R.L. 1970, Astrophysical Letters, 7, 15.

FOMALONT, E.B. 1968, Ap.J., Supplement No. 138, 203.

GARDNER, F.F. and DAVIES, R.D. 1964, Nature, 201, 144.

_____. Aust. J. Phys., 19, 441.

GARDNER, F.F. and WHITEOAK, J.B. 1962, Phys. Rev. Letters, 9, 197.

_____. 1963, Nature, 197, 1162.

_____. 1966, Ann. Rev. Astron. Astrophys., 4, 245.

_____, and MORRIS, D. 1969, Aust. J. Phys., 22, 821.

GILBERT, J.A. and CONWAY, R.G. Nature, 227, 585.

GOL'NEV, V.Ya. and SOBOLEVA, N.S. 1965, Astron. Zh., 42, 694.

GUBBAY, J., LEGG, A.J., ROBERTSON, D.S., MOFFET, A.T., EKERS, R.D., and SEIDEL, B. 1969, Nature, 224, 1094.

GUBBAY, J., LEGG, A.J., ROBERTSON, D.S., MOFFET, A.T., and SEIDEL, B. 1969, Nature, 222, 730.

GURSKY, H., KELLOGG, E.M., LEONG, C., TANANBAUM, H., and GIACCONI, R. 1971, Ap.J. (Letters), 165, L43.

HARRIS, D.E. and HARDEBECK, E.G. 1970, Ap.J. (Supplement), 19, 115.

HOBBS, R.W., CORBETT, H.H., and SANTINI, N.J. 1969, Ap.J. (Letters), 156, L15.

HOBBS, R.W. and HADDOCK, F.T. 1967, Ap.J., 147, 908.

HOBBS, R.W., HOLLINGER, J.P., and MARANDINO, G.E. 1968. Ap.J. (Letters), 154, L49.

HOLLINGER, J.P., MAYER, C.H., and MENELLA, R.A. 1964, Ap.J., 140, 656.

KELLERMANN, K.I. 1971a, Survey Paper Presented at I.A.U. Symposium No. 144 (Unpublished).

_____. 1971b, Paper Presented at the A.A.S. Meeting, Arecibo, Puerto Rico (Unpublished).

_____, CLARK, B.G., JAUNCEY, D.L., COHEN, M.H., SHAFFER, D.B., MOFFET, A.T., and GULKIS, S. 1970, Ap.J., 161, 803.

_____, JAUNCEY, D.L., COHEN, M.H., SHAFFER, D.B., CLARK, B.G., BRODERICK, J., RÖNNÄNG, B., RYDBECK, D.E.H., MATVEYENKO, L, MOISEYEV, I., VITKEVITCH, V.V., COOPER, B.F.C., and BATCHELOR, R. 1971, Ap.J., 169, 1.

_____, and PAULINY-TOTH, I.I.K. 1968a, Ap.J., 152, 639.

_____, and PAULINY-TOTH, I.I.K. 1968b, Ann. Rev. Astron. Astrophys., 6, 417.

_____, and PAULINY-TOTH, I.I.K. 1971, Astrophysical Letters, 8, 153.

KELLOGG, E., GURSKY, H., LEONG, C., SCHREIER, E., TANANBAUM, H., and GIACCONI, R. 1971, Ap.J. (Letters), 165, L49.

KINMAN, T.D. 1967, Ap.J. (Letters), 148, L53.

_____. 1968, Science, 162, 1081.

_____, and CONKLIN, E.K. 1971, Astrophysical Letters, 9, 147.

_____, LAMLA, E., CIURIA, T., HARLAN, E., and WIRTANEN, C.A. 1968, Ap.J., 152, 357.

_____, LAMLA, E., and WIRTANEN, C.A. 1966, Ap.J., 146, 964.

KLEIN, M.J. 1968, PhD. Thesis, University of Michigan, Ann Arbor, Michigan.

KLEINMANN, D.E. and LOW, F.J. 1970, Ap.J. (Letters), 159, L165.

KNIGHT, C.A., ROBERTSON, D.S., ROGERS, A.E.E., SHAPIRO, I.I., WHITNEY, A.R., CLARK, T.A., GOLDSTEIN, R.M, MARANDINO, G.E., and VANDENBERG, N.R. 1971, Science, 172, 52.

KOMESAROFF, M.M., GARDNER, F.F., MORRIS, D., ROBERTS, J.A., and WHITEOAK, J.B. 1968, Nature, 218, 73.

KRISHNASWAMY, K.K. 1971, Ap.J., 167, 63.

KRONBERG, P.P. and CONWAY, R.G. 1970, M.N.R.A.S., 147, 149.

KRUSZEWSKI, A. 1971, Acta Astron., 21, 311.

KUZMIN, A.D. and DENT, W.A. 1966, Astron. Zh., 43, 692.

LAAN, H. van der. 1966, Nature, 211, 1131.

LEGG, M.P.C. and WESTFOLD, K.C. 1967, Proc. Astro. Soc. Aust., 1, 27.

_____. 1968, Ap.J., 154, 499.

LILLER, W. 1969, Ap.J., 155, 1113.

LIPOVKA, N.M. 1969, Astron. Zh., 46, 28.

LITTLE, L. and HEWISH, A. 1968, M.N.R.A.S., 138, 393.

LOW, F.J. 1965, Ap.J., 142, 1287.

_____, 1970, Ap.J. (Letters), 159, L173.

_____, and KLEINMANN, D.E. 1968, A.J., 73, 868.

LÜ, P.K. and HUNTER, J.H. 1969, Nature, 221, 755.

LYNDS, R. 1971, Ap.J. (Letters), 159, L151.

MacLEOD, J.M. 1971 (Private Communication).

_____, and ANDREW, B.H. 1968, Astrophysical Letters, 1, 243.

_____, ANDREW, B.H., MEDD, W.J., and OLSEN, E.T. 1971, Astrophysical Letters, 9, 19.

McCULLOUGH, T.P. and WAAK, J.A. 1969, Ap.J., 158, 849.

MALTBY, P. and MOFFET, A.T. 1965, Science, 150, 63.

MALTBY, P. and SEIELSTAD, G.A. 1966, Ap.J., 144, 216.

MATTHEWS, T.A. and SANDAGE, A.R. 1963, Ap.J., 138, 30.

MAYER, C.H., HOLLINGER, J.P., and ALLEN, P.J. 1963, Ap.J., 137, 1309.

MAYER, C.H., McCULLOUGH, T.P., and SLOANAKER, R.M. 1962, Ap.J., 135, 656.

_____. 1964, Ap.J., 139, 248.

MEDD, W.J., LOCKE, J.L., ANDREW, B.H., and BERGH, S. van den. 1968, A.J., 73, 293.

MELROSE, D.B. 1971, Astrophysics and Space Science, 12, 172.

MEZGER, P.G. and SCHRAMI, J. 1966, A.J., 71, 864.

MOFFET, A.T. 1966, Ann. Rev. Astron. Astrophys., 4, 145.

MORRIS, D. and BERGE, G.L. 1964, A.J., 69, 641.

MORRIS, D. and RADHAKRISHNAN, V. 1963, Ap.J., 137, 147.

MORRIS, D., RADHAKRISHNAN, V. and SEIELSTAD, G.A. 1964, Ap.J., 139, 758.

NIKULIN, N.S., KUVSHINOV, V.M., and SEVERNY, A.B. 1971, Ap.J. (Letters), 170, L53.

OKE, J.B., NEUGEBAUER, B., and BECKLIN, E.E. 1969, Ap.J. (Letters), 156, L41.

_____. 1970, Ap.J., 159, 341.

OLSEN, E.T. 1969, Nature, 224, 1008.

_____. 1970, Bull. Am. Ast. Soc., 2, 212.

_____, and ALLER, H.D. 1971, Bull. Am. Ast. Soc. (Part I), 3, 25.

OZERNOI, L.N. and SAZONOV, V.N. 1968, Nature, 219, 467.

_____. 1969, Astrophysics and Space Science, 3, 395.

PACHOLCZYK, A.G. and SWIHART, T.L. 1971a, Ap.J., 170, 495.

_____. 1971b, M.N.R.A.S., 153, 3P.

PACHOLCZYK, A.G. and WEYMANN, R.J. 1968, A.J., 73, 870.

PACHOLCZYK, A.G. and WISNIEWSKI, W.Z. 1967, Ap.J., 147, 394.

PAULINY-TOTH, I.I.K. and KELLERMANN, K.I. 1966, Ap.J., 146, 634.

_____. 1968, Ap.J. (Letters), 152, L169.

PENSTON, M.V. and CANNON, R.D. 1970, Radio Obs. Bull., 159.

RACINE, R. 1970, Ap.J. (Letters), 159, L99.

REES, M.J. 1966, Nature, 211, 468.

_____. 1967, M.N.R.A.S., 135, 345.

_____, and SIMON, M. 1968, Ap.J. (Letters), 152, L145.

ROBERTS, J.A., RIBES, J.C., MURRAY, J.D., and COOKE, D.J. 1972, Nature Physical Sciences, 236, 3.

SASTRY, C.V., PAULINY-TOTH, I.I.K., and KELLERMANN, K.I. 1966, A.J., 19, 441.

SCHEUER, P.A.G. and WILLIAMS, P.J.S. 1968, Ann. Rev. Astron. Astrophys., 6, 321.

SCHMITT, J.L. 1968, Nature, 218, 663.

SCIAMA, D.W. and REES, M.J. 1967, Nature, 216, 147.

SEAQUIST, E.R. 1970, Astrophysical Letters, 5, 111.

_____. 1971, Nature Physical Sciences, 231, 93.

SEIELSTAD, G.A. 1967, Ap.J. (Letters), 150, L147.

_____. 1969, Astron. and Astrophys., 2, 372.

_____, MORRIS, D. and RADHAKRISHNAN, C.V. 1963, Ap.J., 138, 602.

_____, MORRIS, D. and RADHAKRISHNAN, C.V. 1964, Ap.J., 140, 53.

_____, and WEILER, K.W. 1968, A.J., 73, 1.

_____, and WEILER, K.W. 1971, A.J., 76, 211.

_____, and YIP, K.B. 1969, Nature, 222, 967.

SHKLOVSKII, I.S. 1960, Astron. Zh., 37, 256.

_____. 1965a, Astron. Zh., 42, 30.

_____. 1965b, Nature, 206, 1976.

STEIN, W.A. and GILLETT, F.C. 1969, Nature, 224, 675.

STULL, M.A. 1971, A.J., 76, 1.

TAKARADA, K. 1970a, Pub. Ast. Soc. Japan, 22, 551.

_____. 1970b, Prog. Theoretical Phys., 43, 303.

TRITTON, K.P. and BRETT, A. 1970, Observatory, 90, 110.

TRITTON, K.P. and SELMES, R.A. 1971, M.N.R.A.S., 153, 453.

VISVANATHAN, N. 1968, Ap.J. (Letters), 153, L19.

_____. 1969, Ap.J. (Letters), 155, L133.

WARDLE, J.F.C. 1971, Astrophysical Letters, 8, 183.

WESTFOLD, K.C. 1959, Ap.J., 130, 250.

WHITNEY, A.R., SHAPIRO, I.I., ROGERS, A.E.E., ROBERTSON, D.S., KNIGHT, C.A., CLARK, T.A., GOLDSTEIN, R.M., MARANDINO, G.E., and VANDENBERG, N.R. 1971, Science, 173, 225.

WILLS, D. 1971, Ap.J., 169, 221.

WITZEL, A. and VERON, P. 1971, Astrophysical Letters, 7, 22.